Модели ядра

Р.В.Джолос, ОИЯИ, Дубна

Февраль , 2024

Содержание

- Введение
- Оболочечная модель ядра
- Коллективная модель ядра
- Микроскопические модели ядра

- Creation of Nuclear Physics

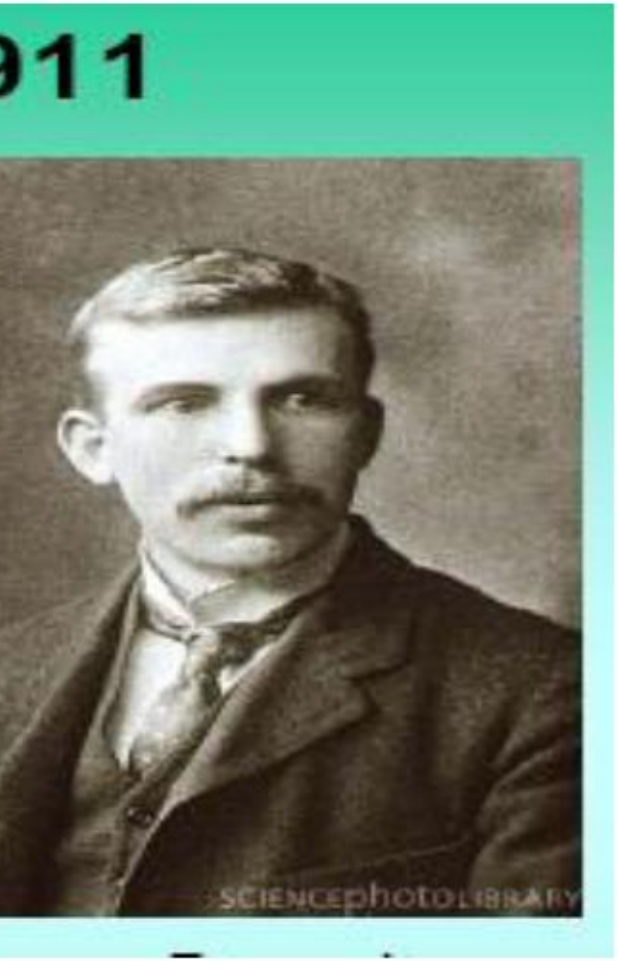

- Saturday, March 11, 1911
- Session of the Manchester Philisophical Society.
- E.Ruserford : Scattering of alpha- and beta- rays and the structure of atom.

Phyl.Mag.1911, May, ser.6, 21, 669-698

LXXIX. *The Scattering of α and β Particles by Matter and the Structure of the Atom.*

By Professor E. RUTHERFORD, *F.R.S., University of Manchester* *.

§ 1. It is well known that the α and β particles suffer deflexions from their rectilinear paths by encounters with atoms of matter. This scattering is far more marked for the β than for the α particle on account of the much smaller momentum and energy of the former particle. There seems to be no doubt that such swiftly moving particles pass through the atoms in their path, and that the deflexions observed are due to the strong electric field traversed within the atomic system. It has generally been supposed that the scattering of a pencil of α or β rays in passing through a thin plate of matter is the result of a multitude of small scatterings by the atoms of matter traversed. The observations, however, of Geiger and Marsden † on the scattering of α rays indicate that some of the α particles must suffer a deflexion of more than a right angle at a single encounter. They found, for example, that a small fraction of the incident α particles, about 1 in 20,000, were turned through an average angle of 90° in passing through a layer of gold-foil about ·00004 cm. thick, which was equivalent in stopping-power of the α particle to 1·6 millimetres of air. Geiger ‡ showed later that the most probable angle of deflexion for a pencil of α particles traversing a gold-foil of this thickness was about 0°·87. A simple calculation based on the theory of probability shows that the chance of an α particle being deflected through 90° is vanishingly small. In addition, it will be seen later that the distribution of the α particles for various angles of large deflexion does not follow the probability law to be expected if such large deflexions are made up of a large number of small deviations. It seems reasonable to suppose that the deflexion through a large angle is due to a single atomic encounter, for the chance of a second encounter of a kind to produce a large deflexion must in most cases be exceedingly small. A simple calculation shows that the atom must be a seat of an intense electric field in order to produce such a large deflexion at a single encounter.

Recently Sir J. J. Thomson § has put forward a theory to

* Communicated by the Author. A brief account of this paper was communicated to the Manchester Literary and Philosophical Society in February, 1911.

† Proc. Roy. Soc. lxxxii. p. 495 (1909).

‡ Proc. Roy. Soc. lxxxiii. p. 492 (1910).

§ Camb. Lit. & Phil. Soc. xv. pt. 5 (1910).

the central charge, that the field due to the uniform distribution of negative electricity may be neglected. In general, a simple calculation shows that for all deflexions greater than a degree, we may without sensible error suppose the deflexion due to the field of the central charge alone. Possible single deviations due to the negative electricity, if distributed in the form of corpuscles, are not taken into account at this stage of the theory. It will be shown later that its effect is in general small compared with that due to the central field.

Consider the passage of a positive electrified particle close to the centre of an atom. Supposing that the velocity of the particle is not appreciably changed by its passage through the atom, the path of the particle under the influence of a repulsive force varying inversely as the square of the distance will be an hyperbola with the centre of the atom S as the external focus. Suppose the particle to enter the atom in the direction PO (fig. 1), and that the direction of motion

Fig. 1.

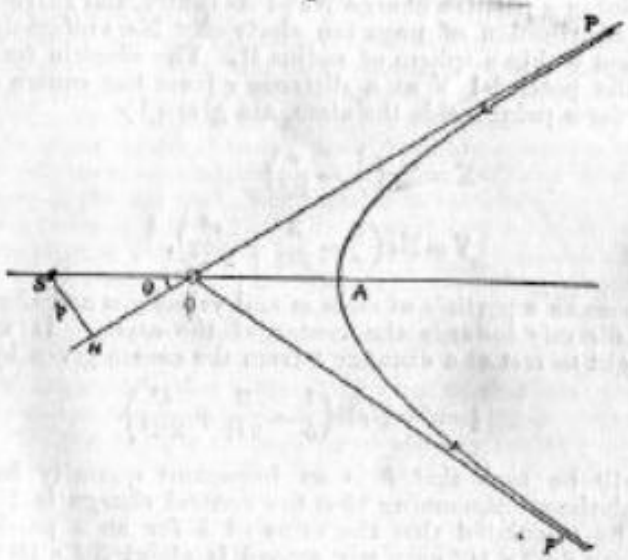

on escaping the atom is OP'. OP and OP' make equal angles with the line SA, where A is the apse of the hyperbola. $p = SN$ = perpendicular distance from centre on direction of initial motion of particle.

F.Soddi (1877-1956)

1913

Изотопы

$${}^{Z+N}_{Z}X$$

$${}^{1}_{1}H,\ {}^{2}_{1}D,\ {}^{4}_{2}He,\ {}^{226}_{88}Ra,\ {}^{235}_{92}U,$$

Фредерик Содди

Изучая радиоактивный распад Ra Содди смог показать, что при распаде образуется гелий. Так было впервые показано, счто один химический элемент может превратиться в другой.

В 1904 г. Содди сумел показать, что Ra получается при распаде U «через промежуточный элемент». Постепенно количество промежуточных элементов накапливалось, и они совсем не укладывались в таблицу Менделеева. Более того, некоторые из них невозможно было различить химически.

В 1913 г. Содди формулирует: существуют элементы с разными атомными массами, которые занимают одно и то же место в таблице Менделеева. «Одинаковое место» по-гречески – «изотоп». Так в химии и физике появились изотопы. (Нобелевская премия 1921 г.)

Nuclear binding energy

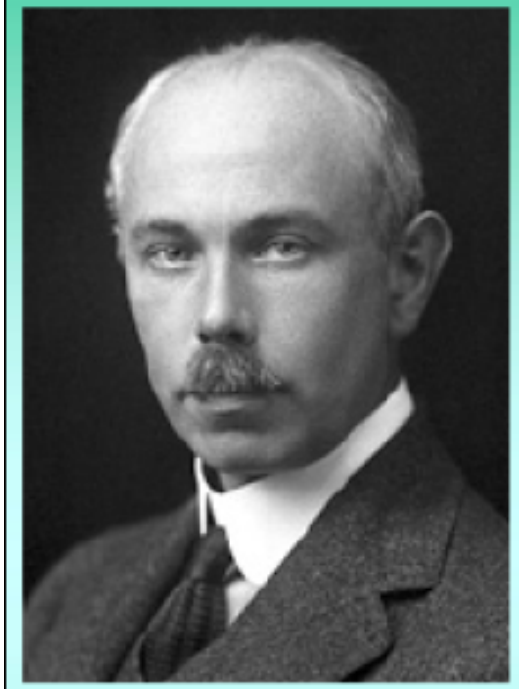

Френсис Астон
(1877 – 1945)

$$\Delta E = \Delta m \cdot c^2$$

дефект массы

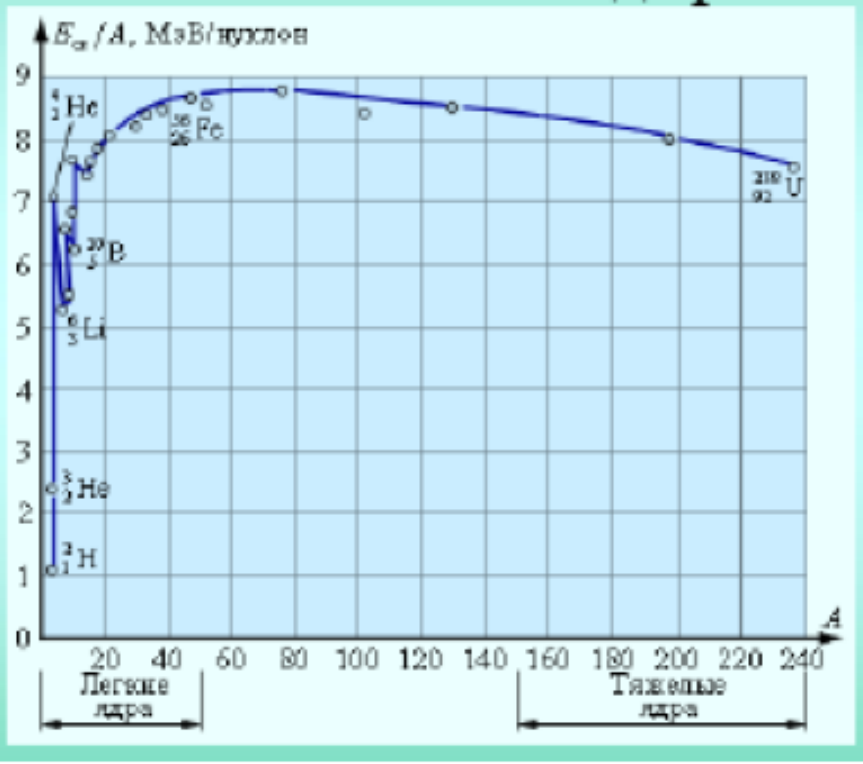

Фрэнсис Астон

В 1913 г. Дж.Томсон поставил перед Астоном задачу усовершенствовать аппарат, который измеряет соотношение между зарядом и массой для пучка положительно заряженных частиц. Для разделения Ne и немного более тяжелого компонента, который Томсон назвал мета-неоном. Астон изобрел метод газовой диффузии, который основан на различии скорости диффузии частиц, отличающихся по массе. Чтобы измерять массу продуктов диффузии, Астон сконструировал кварцевые микровесы, чувствительностью 10^{-9} г. С помощью масс-спектрографа Астон обнаружил, что почти все элементы имеют несколько изотопов.

В ходе исследований Астон сформулировал правило целых чисел, согласно которому массы атомов всегда выражаются целыми числами, кратными кислородной единице.

С помощью более мощных спектрографов Астон смог измерить малые отклонения от целых чисел и объяснил их потерей атомной массы из-за энергии связи. (Нобелевская премия 1922г.)

1928 Theory of alpha-decay
G.Gamov (1904-1968)

Георгий Гамов

$$N = N_o \cdot e^{-t/\tau},$$

$$\tau = \hbar/\Gamma$$

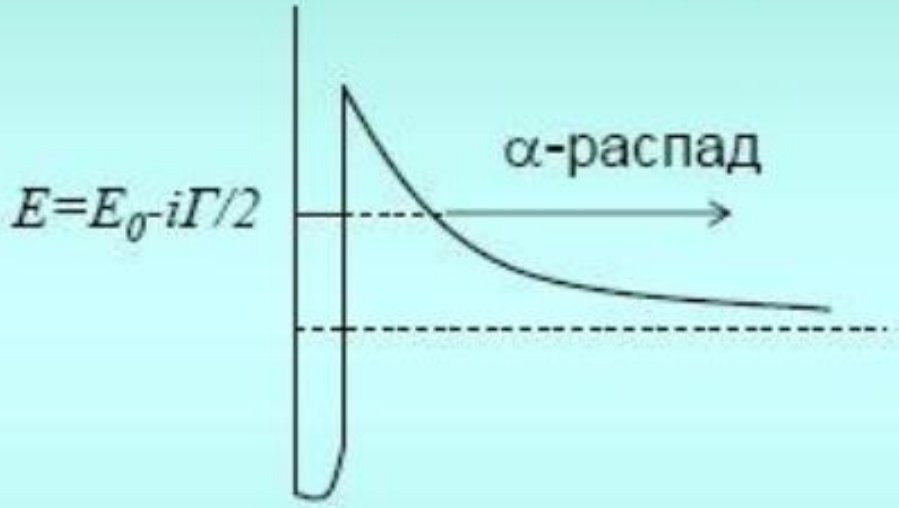

Discovery of neutron
J.Chadwick (1891-1974)

1932

Analyzing the scattering data of of Bothe and Becker and I. and F. Joliot-Curie Chadwick has discovered neutron

$$\alpha + {}^{9}_{4}Be \rightarrow {}^{12}_{6}C + n$$

Proton-neutron model of a nucleus

D.Ivanenko (1904-1994) and
W.Heisenberg (1901-1978)

Nuclear Fission

O.Hahn (1879-1968)

L.Meitner (1878-1968)

F.Schtrassman (1902-1980)

1938

Отто Ган
(1879 – 1968)
Лизе Майтнер
(1878 – 1968)

Отто Ган
Фриц Штрассман
(1902 - 1980)

$$n + {}^{235}_{92}U \rightarrow {}^{236}_{92}U^{*} \rightarrow 2n +$$

$$+ \begin{cases} {}^{93}_{38}Sr \xrightarrow[7,9\ \text{мин}]{\beta} {}^{93}_{39}Y \xrightarrow[10,3\ \text{ч}]{\beta} {}^{93}_{40}Zr \xrightarrow[1,1\cdot 10^{6}\ \text{лет}]{\beta} {}^{93}_{41}Nb^{*} \xrightarrow[12\ \text{лет}]{\gamma} {}^{93}_{41}Nb \\ {}^{141}_{54}Xe \xrightarrow[1,7\ \text{с}]{\beta} {}^{141}_{55}Cs \xrightarrow[25\ \text{с}]{\beta} {}^{141}_{56}Ba \xrightarrow[18\ \text{мин}]{\beta} {}^{141}_{57}La \xrightarrow[3,7\ \text{ч}]{\beta} {}^{141}_{58}Ce \xrightarrow[33\ \text{дня}]{\beta} {}^{141}_{59}Pr \end{cases}$$

или

$$n + {}^{235}_{92}U \rightarrow {}^{236}_{92}U^{*} \rightarrow 3n +$$

$$+ \begin{cases} {}^{93}_{38}Sr \xrightarrow[7,9\ \text{мин}]{\beta} {}^{93}_{39}Y \xrightarrow[10,3\ \text{ч}]{\beta} {}^{93}_{40}Zr \xrightarrow[1,1\cdot 10^{6}\ \text{лет}]{\beta} {}^{93}_{41}Nb^{*} \xrightarrow[12\ \text{лет}]{\gamma} {}^{93}_{41}Nb \\ {}^{140}_{54}Xe \xrightarrow[16\text{с}]{\beta} {}^{140}_{55}Cs \xrightarrow[66\text{с}]{\beta} {}^{140}_{56}Ba \xrightarrow[12,8\ \text{дня}]{\beta} {}^{140}_{57}La \xrightarrow[40,2\ \text{ч}]{\beta} {}^{140}_{58}Ce \end{cases}$$

Interpretation

O.Frish (1902-1980)

1939

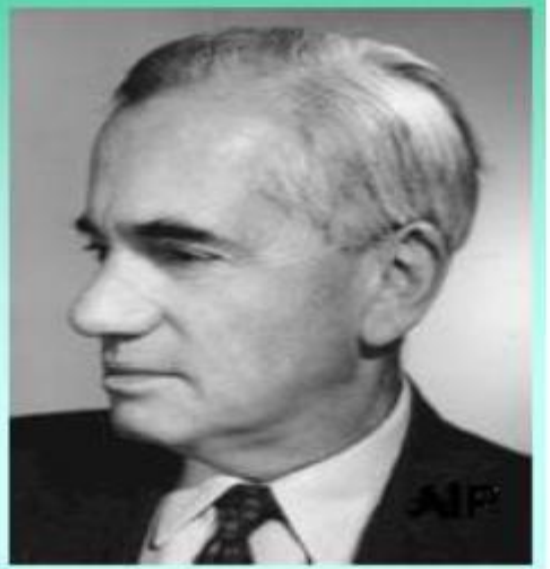

$$n + {}^{235}_{92}U \rightarrow \text{осколки} + \Delta E$$

Liquid drop model

1936

Нильс Бор
(1885 – 1962)

Фридрих Вайцзеккер
(1912 – 2007)

$$E = \alpha A - \beta A^{2/3} - \gamma Z^2 A^{-1/3} - \varepsilon\left(\frac{A}{2} - Z\right)A^{-1} + \chi A^{-3/4}$$

Neutrino

W.Pauli (1900-1958)

1930

In 1914 J,Chadwick has found that in beta-decay energy of the electron is not constant.

N.Bohr assumed that energy is not conserved in a microworld. However, Pauli suggest the other solution

$$^{210}_{83}Bi \rightarrow ^{210}_{83}Po + e^{-} + \nu$$

1933 Elsasser "On the Pauli principle in nuclei"

"The field due to N-1 nucleons acting on the Nth nucleon has probably spherical symmetry leading to the analogy with electron shells in atoms".

- 1934-1935 Elsasser
- Magic numbers: Z=50, 82; N=126

1936 Bethe and Bacher

"The opposite extreme to the assumption of alpha-particle as nuclear subunits is that of independent motion of individual protons and neutrons"

-- There are magic numbersof protons and neutrons.

-- The potential which reproduces these magic numbers is not found.

-- We should not forget about residual interaction of protons and neutrons.

1936 N.Bohr

"Energy of the incident neutron will be rapidly divided among all nuclear particles with the result that for some time afterwords no single particle will posess sufficient kinetic energy to leave the nucleus"

" In the atom and in the nucleus we have indeed to do with two extreme cases of mechanical many-body problem"

1948 Rosenfeld

"Quasi-atomic model plays a minor role"

Nuclear Shell Model

1948

Мария Гепперт-Майер
(1906 – 1972)

Ханс Йенсен
(1907 -1973)

?

n: 2, 8, 20, 28, 50, 82, 126, 184,

p: 2, 8, 20, 28, 50, 82, 114, 126

Самосогласованный потенциал ядра

Оболочечная модель ядра в ее простейшей форме – это описание независимого движения протонов и нейтронов в потенциале, который является результатом усредненного воздействия всех нуклонов ядра на один. Этот потенциал получил название среднего поля ядра. Ясно, что такой потенциал должен определяться самосогласованно.

In the history of the nuclear shell model there was period of the initial intensive development and then the period when the majority of nuclear physicists thought that the shell model has no relation to nuclear structure.

The renaissance of the nuclear shell model began by the paper of Maria Göppert-Mayer (1948). She presented strong experiment evidence for the reality of magic numbers 20, 50, 82 and 126 (for neutrons). She based her conclusion not only on binding energies but also on isotopic abundance. Her paper drew attention of nuclear physicists to existence of magic numbers in heavy nuclei. Some of them tried to obtain shell closures at 50, 82 and 126.

The paper of M.Göppert-Mayer was published in August 1948. On December of 1948 already two manuscripts were received in Physical Review. Both presented level schemes which reproduce the magic numbers 50 and 82. However, their schemes suggest also shell closure at 18, 32, 60 or have other problems. Thus, the problem of the construction of the mean field potential describing correctly all magic numbers was not solved.

Up to this moment people believe in LS-coupling, i.e. in the scheme where L, L_z S, S_z are good (conserving) quantum numbers. With this assumption it was difficult to find a level scheme with shell closure at 50, 82 and 126.

In the papers of M.Göppert-Mayer and J.H.D.Jensen et al. (1949) the strong spin-orbit interaction has been introduced

$$-v_{ls}\,\bar{l}\cdot\bar{s}$$

$$\bar{l}\cdot\bar{s} = \frac{1}{2}\left[j(j+1) - l(l+1) - \frac{3}{4}\right]$$

$$= \begin{cases} l, & j = l + \frac{1}{2} \\ -l-1, & j = l - \frac{1}{2} \end{cases}$$

Splitting : $\sim(2l+1)$

Среднее поле ядра

- Простейший потенциал, который можно использовать как образ среднего поля ядра – это потенциал гармонического осциллятора

Гармонический осциллятор

$$H = -\frac{\hbar^2}{2}\Delta + \frac{1}{2}m\omega^2 r^2 + C\vec{l}\cdot\vec{s} + D\vec{l}^2$$

$$\vec{l}\cdot\vec{s} = \frac{1}{2}\left(\vec{j}^2 - \vec{l}^2 - \vec{s}^2\right)$$

$$< jl|\vec{l}\cdot\vec{s}|jl >= \frac{1}{2}\left(j(j+1) - l(l+1) - \frac{1}{2}(\frac{1}{2}+1)\right)$$

$$E_{Nlj} = \hbar\omega\left(N + \frac{3}{2}\right) + \frac{1}{2}C\left(j(j+1) - l(l+1) - \frac{3}{4}\right) + Dl(l+1)$$

$$V^{(WS)}(r) = -V_0 \frac{1}{1+\exp(\frac{r-R_0}{a})},$$

$$\lambda \frac{1}{r}\frac{dV}{dr}\vec{l}\cdot\vec{s}, \quad \lambda = -0.5 \text{ фм}^2.$$

$$\vec{l}\cdot\vec{s} = \frac{1}{2}\left(\vec{j}^2 - \vec{l}^2 - \vec{s}^2\right),$$

$$< jl|\vec{l}\cdot\vec{s}|jl > = \frac{1}{2}\left(j(j+1) - l(l+1) - \frac{1}{2}(\frac{1}{2}+1)\right).$$

$$H_{SM} = \sum_{k=1}^{A} \left(\frac{p_k^2}{2m} + \frac{1}{2} m \omega^2 r_k^2 + v_{ls} \bar{l}_k \cdot \bar{s}_k \right)$$

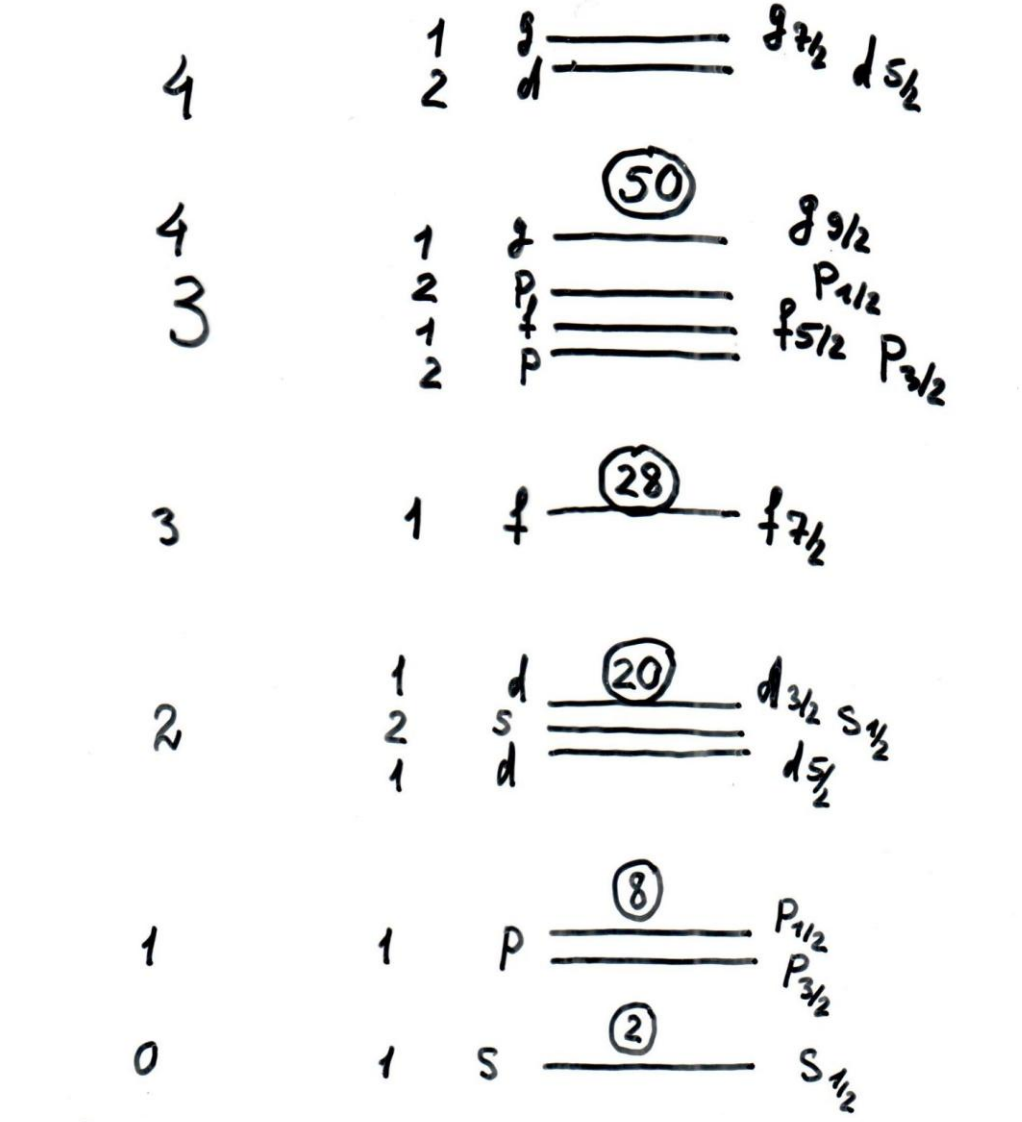

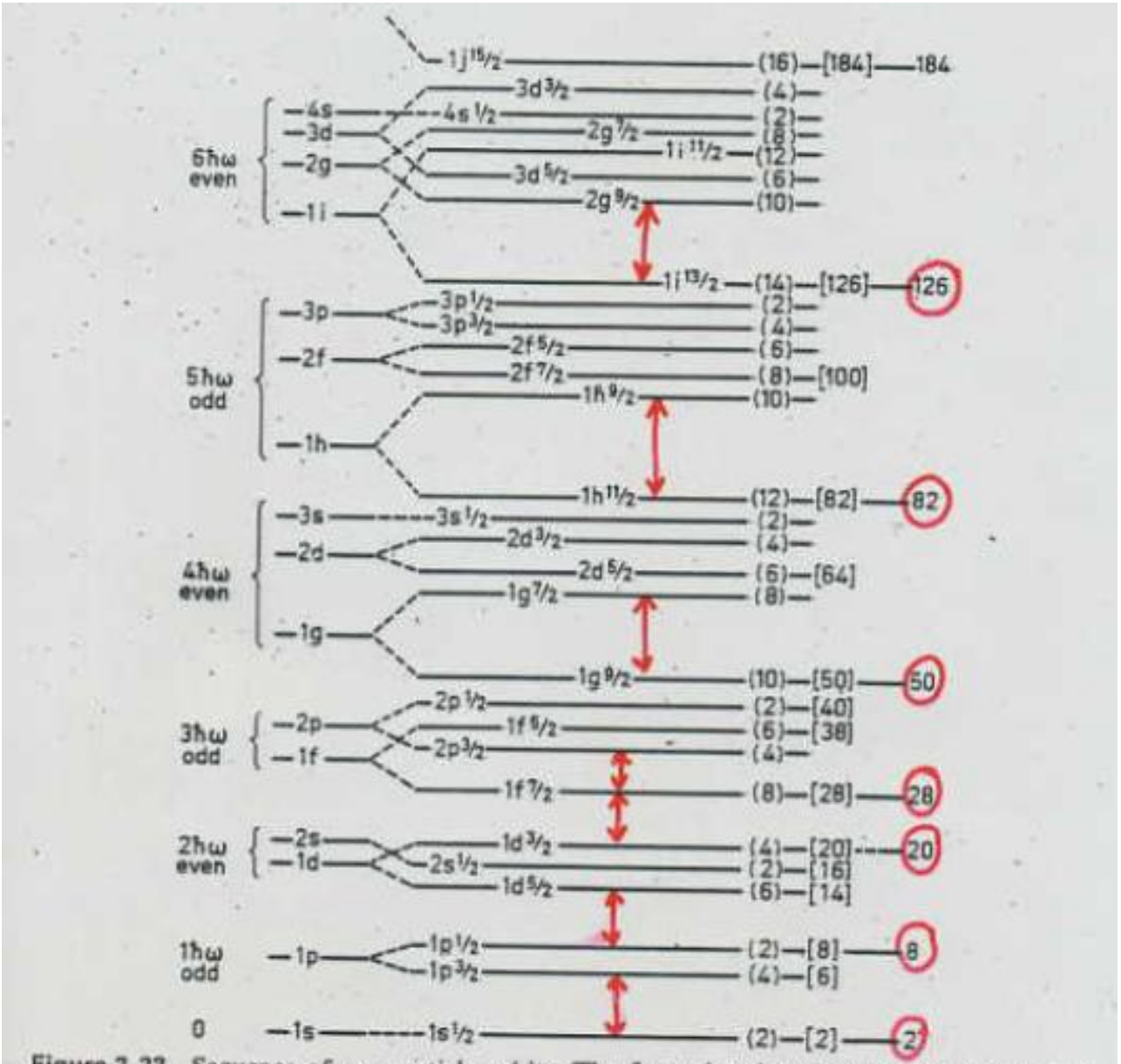

Figure 2-23 Sequence of one-particle orbits. The figure is taken from M. G. Mayer and J. H. D. Jensen, *Elementary Theory of Nuclear Shell Structure*, p. 58, Wiley, New York, 1955.

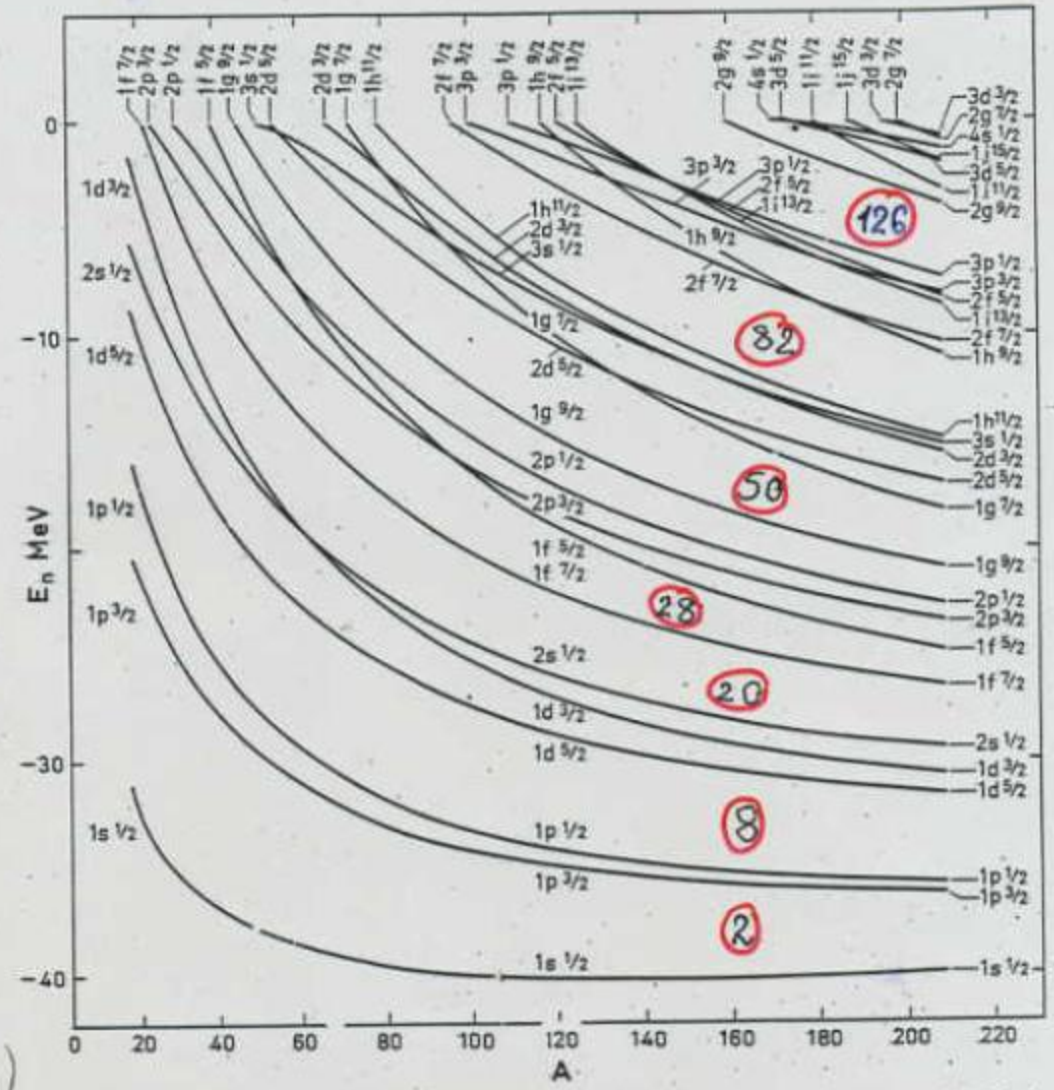

Figure 2-30 Energies of neutron orbits calculated by C. J. Veje (private communication).

Periodic orbits

$$\varepsilon(n,l) = \varepsilon(n_0,l_0) + (n-n_0)\left(\frac{\partial\varepsilon}{\partial n}\right)_0 + (l-l_0)\left(\frac{\partial\varepsilon}{\partial l}\right)_0 +$$
$$+\frac{1}{2}(n-n_0)^2\left(\frac{\partial^2\varepsilon}{\partial n^2}\right)_0 + (n-n_0)(l-l_0)\left(\frac{\partial^2\varepsilon}{\partial n\partial l}\right)_0 +$$
$$+\frac{1}{2}(l-l_0)^2\left(\frac{\partial^2\varepsilon}{\partial l^2}\right)_0 + \dots$$

$$b\left(\frac{\partial\varepsilon}{\partial n}\right)_0 = a\left(\frac{\partial\varepsilon}{\partial l}\right)_0 ,$$

$$(n-n_0)(\frac{\partial\varepsilon}{\partial n})_0+(l-l_0)(\frac{\partial\varepsilon}{\partial l})_0=\left((n-n_0)+\frac{b}{a}(l-l_0)\right)(\frac{\partial\varepsilon}{\partial n})_0=$$

$$=(a(n-n_0)+b(l-l_0))\,\frac{1}{a}(\frac{\partial\varepsilon}{\partial n})_0.$$

$$N\equiv a(n-n_0)+b(l-l_0)$$

Dirac equation

$$\left(\gamma^{\mu}(cp_{\mu}+V_{\mu})+Mc^{2}+V_{s}\right)\psi=0$$

$$V_{\mu}=(V_{0},\vec{V})$$

In the stationary case

$$H=\alpha(c\vec{p}+\vec{V})+V_{0}+\beta(Mc^{2}+V_{s})$$

$$\psi = \begin{pmatrix} g \\ f \end{pmatrix}$$

$$\begin{pmatrix} M + V_0 + V_S & \bar{\sigma} \cdot \bar{p} \\ \bar{\sigma} \cdot \bar{p} & -M + V_0 - V_S \end{pmatrix} \begin{pmatrix} g \\ f \end{pmatrix}$$

$$= E \begin{pmatrix} g \\ f \end{pmatrix}$$

$$E = M + \epsilon$$

Assuming $|\epsilon| \ll 2\tilde{M}$

$$\tilde{M} = M - \frac{1}{2}(V_0 - V_s)/c^2$$

we obtain

$$\left(\bar{p}\frac{1}{2\tilde{M}}\bar{p} + \frac{\hbar^2}{4\tilde{M}^2c^2}\frac{1}{2}\frac{\partial(V_0-V_s)}{\partial z}\bar{\ell}\cdot\bar{s} + (V_s+V_0)\right)g = \epsilon g$$

$$V_0 + V_s \approx -50 \text{ MeV}$$

$$V_0 - V_s \approx 700 - 800 \text{ MeV}$$

From QCD sum rules with 20% accuracy

$$V_s / V_0 \approx -1.1$$

Formally, pseudospin symmetry takes place if $V_0 + V_s = 0$

Changings of magic numbers

In 70^{th} in the neutron rich isotopes of Na were found anomously large values of binding energies. It was explained by disappearance of the magic number N=20 for Z=11. Recent investigations of the neutron rich isotopes of Ne, Mg and Si support the conclusion that the magic numbers can changes. This happens because the configuration of the ground state is changed.

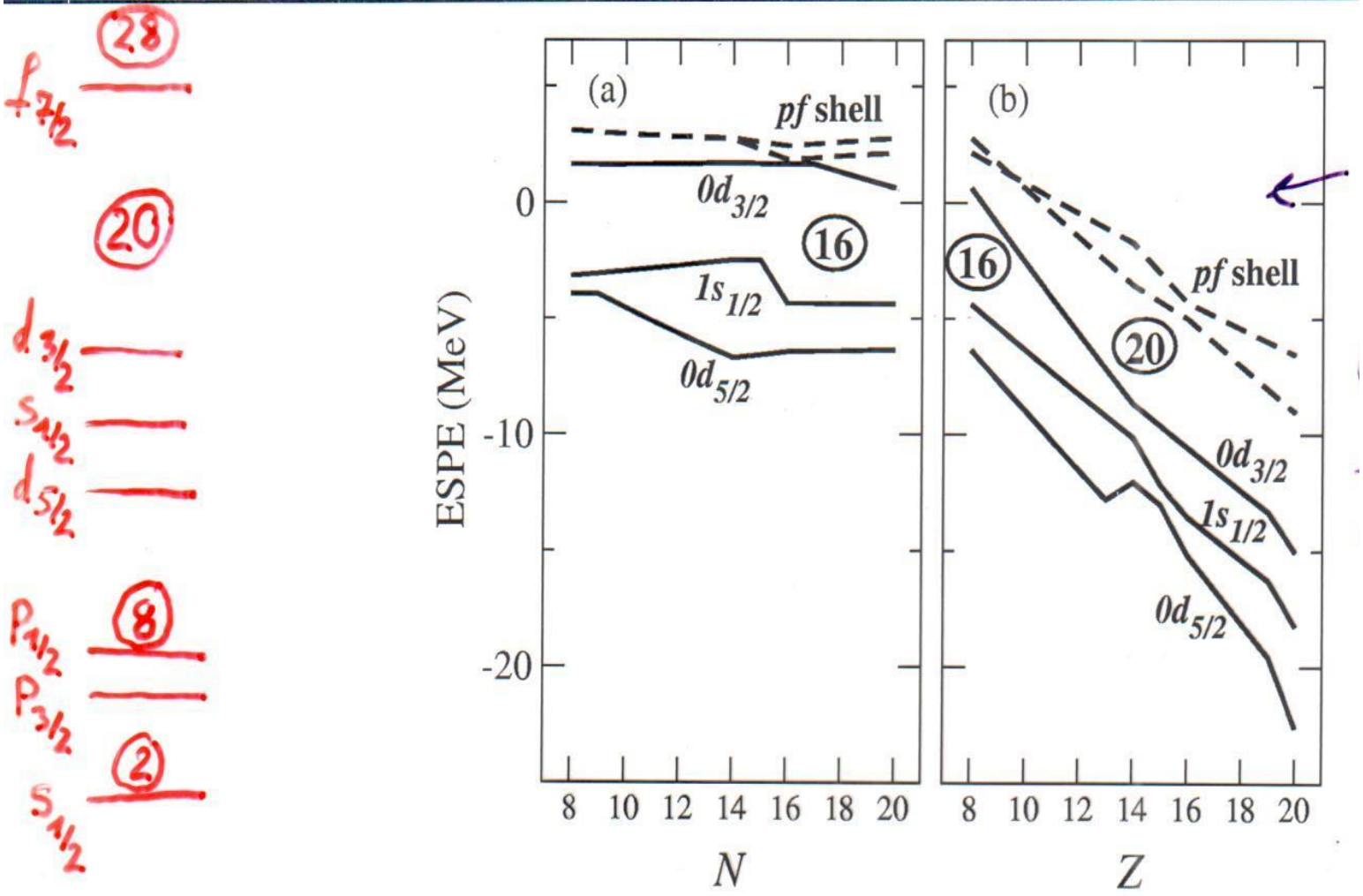
28
$f_{7/2}$
20
$d_{3/2}$
$s_{1/2}$
$d_{5/2}$
8
$p_{1/2}$
$p_{3/2}$
2
$s_{1/2}$
(a)
pf shell
$0d_{3/2}$
16
$1s_{1/2}$
$0d_{5/2}$
0
-10
-20
ESPE (MeV)
8 10 12 14 16 18 20
N
(b)
16
pf shell
20
$0d_{3/2}$
$1s_{1/2}$
$0d_{5/2}$
8 10 12 14 16 18 20
Z

Signatures of the shell closeness

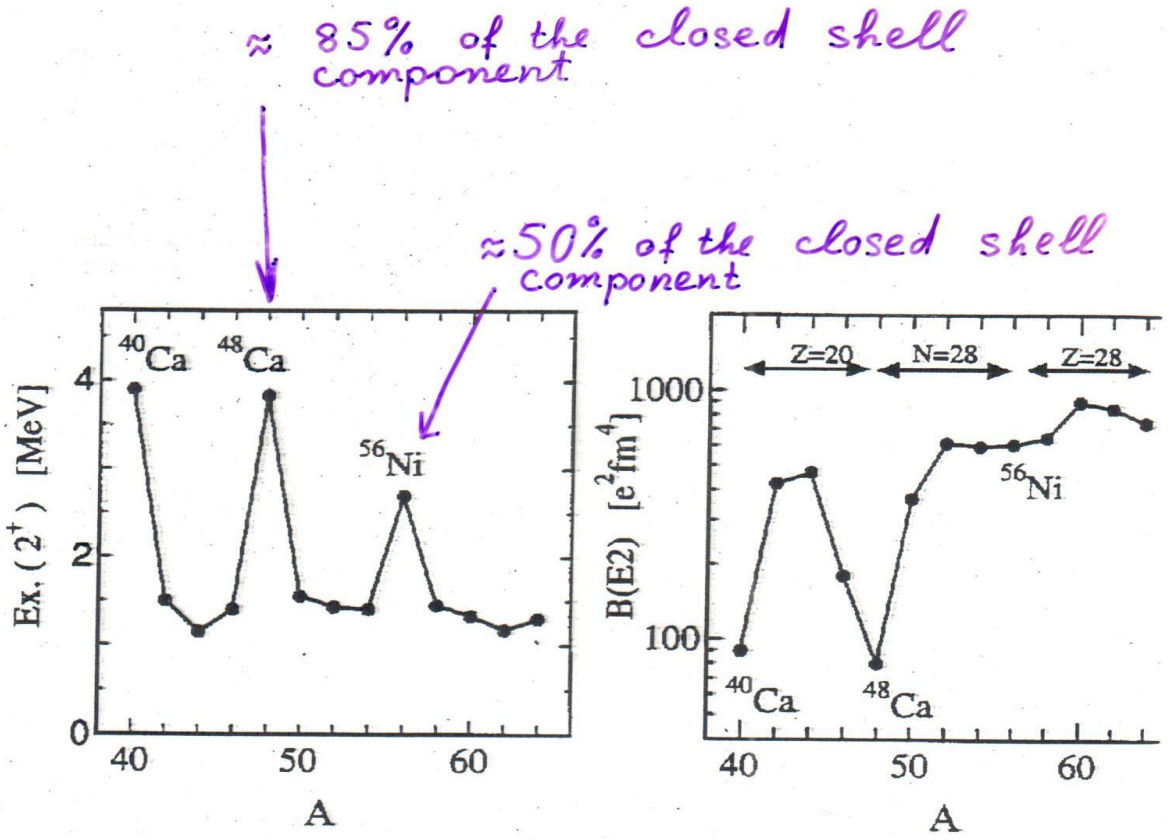

Одночастичные уровни в деформированных ядрах

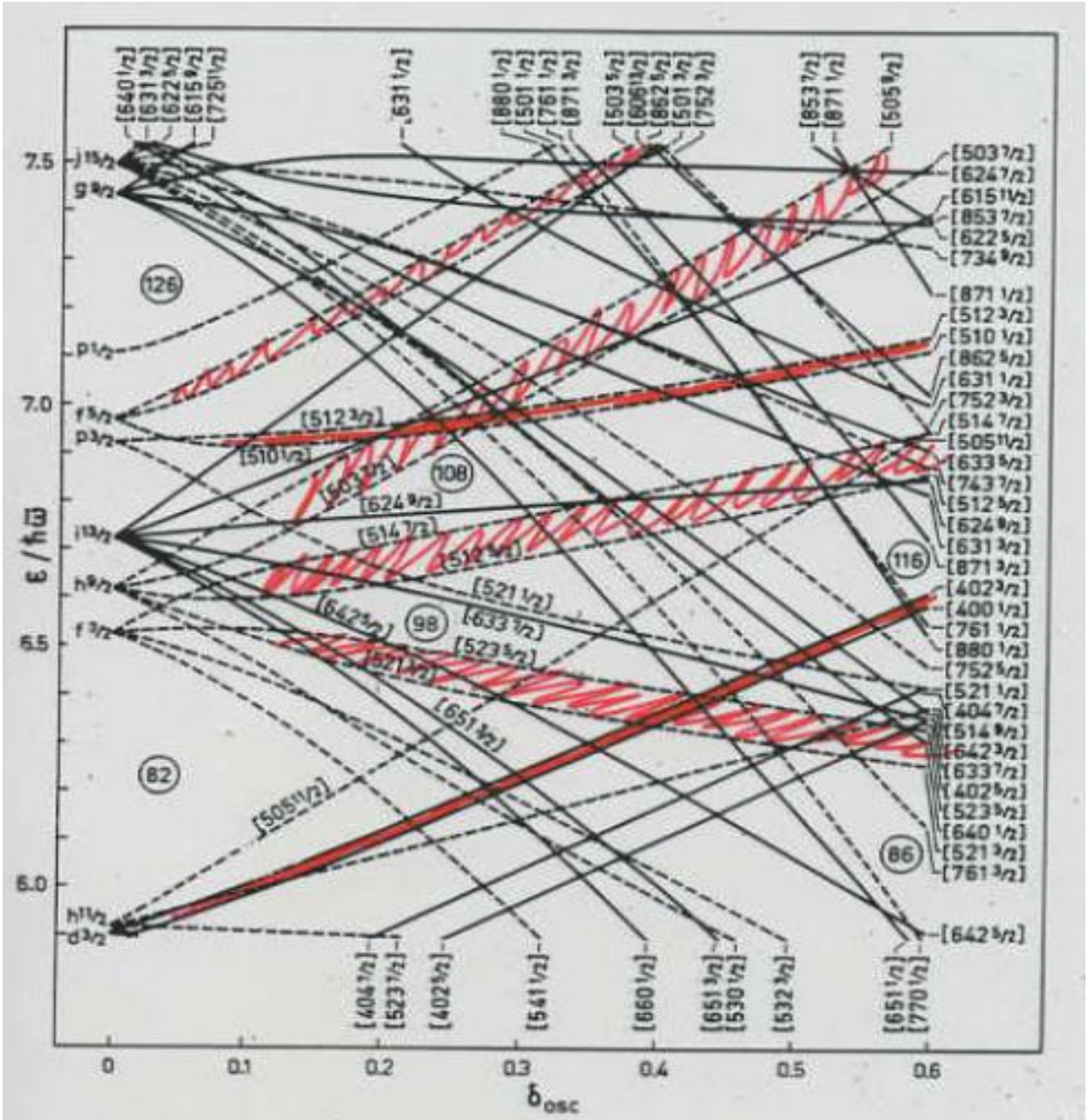

Figure 5-3 Neutron orbits in prolate potential ($82 < N < 126$). See caption to Fig. 5-2.

- Since the first paper s of M.G-Mayer and Jensen et al. the shell model made enormous impact on almost all aspects of nuclear physics.
- The shell model is marvelous creation, especially when one realizes it exists in spite of relatively strong nucleon-nucleon forces.
- We now realize that the mean field feature is characteristic of complex systems and relatively independent of the character of the interparticle forces.
- The theoretical foundation of the shell model is a problem. We can say that the shell model is an energy average of the many-body Hamiltonian (H.Feshbach)

Generalized nuclear model

$$R(\vartheta,\varphi) = R_0\left(1+\alpha_{00}+\sum_{\lambda=1}^{\infty}\sum_{\mu=-\lambda}^{\lambda}\alpha^{*}_{\lambda,\mu}Y_{\lambda,\mu}(\vartheta,\varphi)\right)$$

$$\alpha_{2\mu} = D^2_{\mu 0}(\theta_1,\theta_2,\theta_3)a_{20} + \frac{1}{\sqrt{2}}\left(D^2_{\mu 2}(\theta_1,\theta_2,\theta_3)+D^2_{\mu -2}(\theta_1,\theta_2,\theta_3)\right)a_{22}.$$

$$a_{20} = \beta\cos\gamma,$$

$$a_{22} = \beta\sin\gamma.$$

$$\delta R_1 \equiv R(\frac{\pi}{2}, 0) - R_0 = R_0 \beta \cos(\gamma - \frac{2\pi}{3}),$$
$$\delta R_2 \equiv R(\frac{\pi}{2}, \frac{\pi}{2}) - R_0 = R_0 \beta \cos(\gamma + \frac{2\pi}{3}),$$
$$\delta R_3 \equiv R(0, 0) - R_0 = R_0 \beta \cos(\gamma).$$

Spherical nuclei

$$T = \frac{1}{2}\sum_{\lambda,\mu} B_\lambda |\dot{\alpha}_{\lambda\mu}|^2.$$

$$\pi_{\lambda\mu} = B_\lambda \dot{\alpha}^*_{\lambda\mu}.$$

$$V = \frac{1}{2}\sum_{\lambda,\mu} C_\lambda |\alpha_{\lambda\mu}|^2.$$

$$H = \frac{1}{2}\sum_{\lambda,\mu} B_\lambda |\dot{\alpha}_{\lambda\mu}|^2 + \frac{1}{2}\sum_{\lambda,\mu} C_\lambda |\alpha_{\lambda\mu}|^2.$$

$$H = \frac{1}{2}\sum_{\lambda,\mu}\frac{1}{B_\lambda}\pi^+_{\lambda\mu}\pi_{\lambda\mu} + \frac{1}{2}\sum_{\lambda,\mu} C_\lambda \alpha^+_{\lambda\mu}\alpha_{\lambda\mu}.$$

$$\left[\pi_{\lambda\mu}, \alpha_{\lambda'\mu'}\right] = -i\hbar\delta_{\lambda\lambda'}\delta_{\mu\mu'}, \quad \left[\alpha_{\lambda\mu}, \alpha_{\lambda',\mu'}\right] = \left[\pi_{\lambda\mu}, \pi_{\lambda',\mu'}\right] = 0.$$

$$\alpha_{\lambda\mu} = \sqrt{\frac{\hbar}{2B_\lambda\omega_\lambda}}(b^+_{\lambda\mu} + (-1)^\mu b_{\lambda-\mu}),$$

$$\pi^+_{\lambda\mu} = i\sqrt{\frac{\hbar B_\lambda\omega_\lambda}{2}}((-1)^\mu b^+_{\lambda-\mu} - b_{\lambda\mu}).$$

$$H = \frac{5}{2}\sum_{\lambda}\hbar\omega_{\lambda} + \sum_{\lambda,\mu}\hbar\omega_{\lambda}\, b^{+}_{\lambda\mu} b_{\lambda\mu}.$$

$$|0> : \quad b^{+}_{\lambda\mu}|0> \; b^{+}_{\lambda\mu} b^{+}_{\lambda'\mu'}|0>$$

ров гармонических квадрупольного ($\lambda = 2$) и октупольного ($\lambda = 3$)

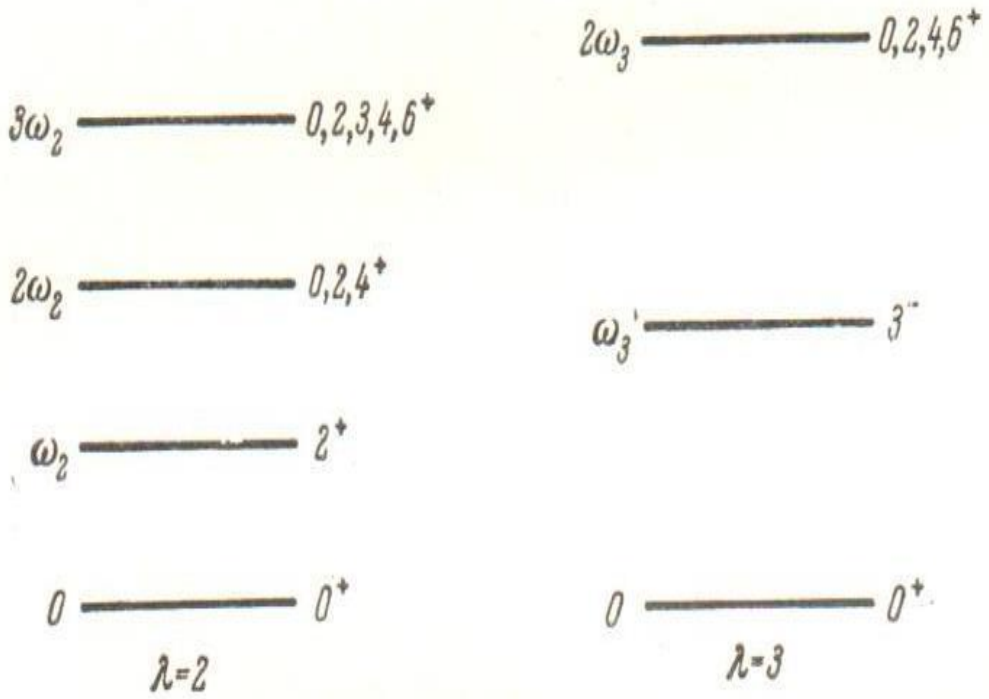

Рис. 2.9. Энергетический спектр гармонических колебаний.

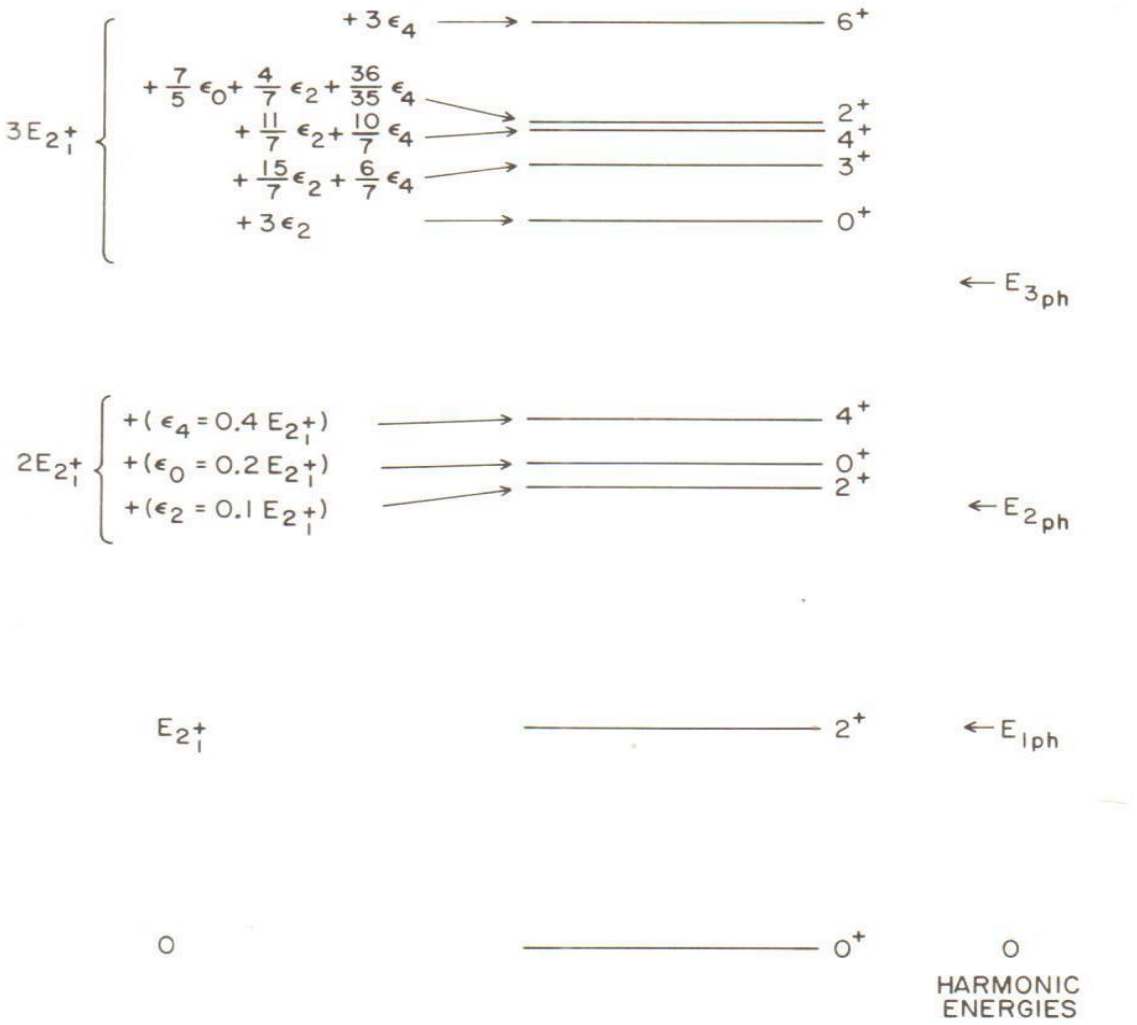

Fig. 6.5. Energy anharmonicities in the vibrator model assuming arbitrary two-body residual interactions.

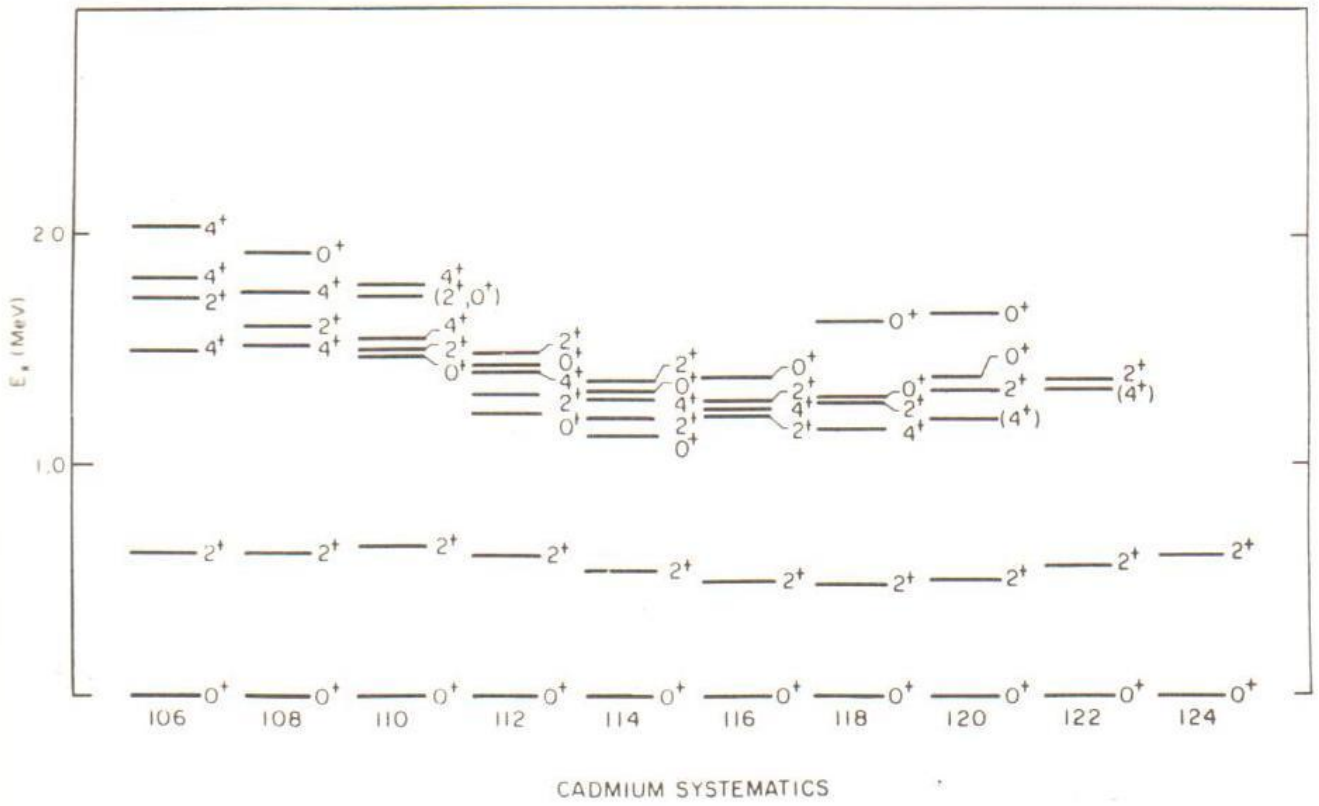

Fig. 6.6. Energy systematics in the Cd isotopes. Note the intermingling of two-phonon triplet states with extra levels (Aprahamian, 1984).

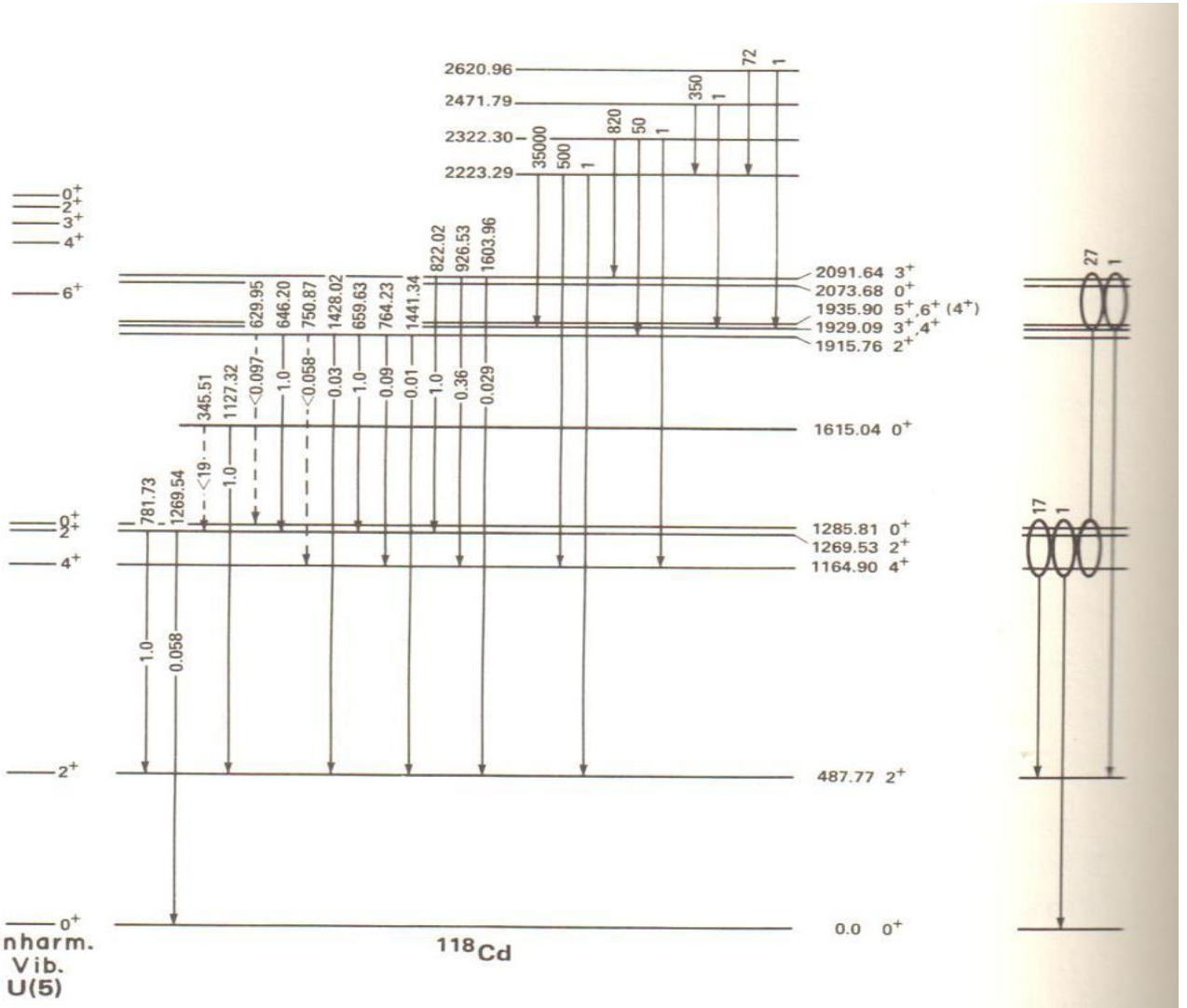

Fig. 6.9. Level scheme of ^{118}Cd showing the one-, two-, and three-phonon states as well as an intruder 0^+ level at 1615 keV and possible candidates for four-phonon excitations above 2.2 MeV. On the right are shown the average $(\Delta N_{ph} = 1)/(\Delta N_{ph} = 2)$ branching ratios. On the left are the predictions for the three-phonon states assuming the empirically observed anharmonicities in the two-phonon states. These are the same predictions one would obtain in the U(5) limit of the IBA (Arahamian, 1987).

- Harmonic oscillations of quadrupole degree of freedom:

$$V = \frac{1}{2} C_2 \sum_{\mu} |\alpha_{2\mu}|^2$$

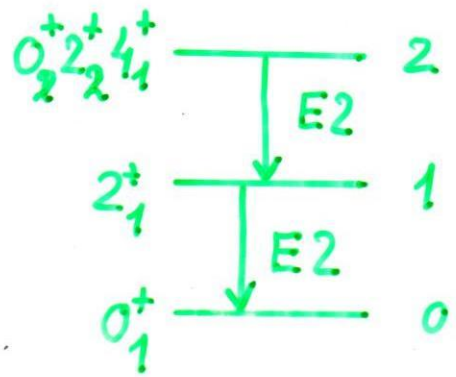

$$\frac{E(0_2^+, 2_2^+, 4_1^+)}{E(2_1^+)} = 2$$

$$\frac{B(E2; 0_2^+, 2_2^+, 4_1^+ \rightarrow 2_1^+)}{B(E2; 2_1^+ \rightarrow 0_1^+)} = 2$$

Deformed nuclei

$$H = -\frac{\hbar^2}{2B_2}\left(\frac{1}{\beta^4}\frac{\partial}{\partial\beta}\beta^4\frac{\partial}{\partial\beta} + \frac{1}{\sin 3\gamma}\frac{\partial}{\partial\gamma}\sin 3\gamma\frac{\partial}{\partial\gamma} - \sum_{k=1}^{3}\frac{\hat{I}_k^2}{4\beta^2\sin^2(\gamma - \frac{2\pi}{3}k)}\right) + V(\beta,\gamma).$$

$$[\hat{I}_1, \hat{I}_2] = -\imath\hat{I}_3, [\hat{I}_2, \hat{I}_3] = -\imath\hat{I}_1, [\hat{I}_3, \hat{I}_1] = -\imath\hat{I}_2.$$

$$\Im_k \equiv 4B_2\beta^2\sin^2(\gamma - \frac{2\pi}{3}k)$$

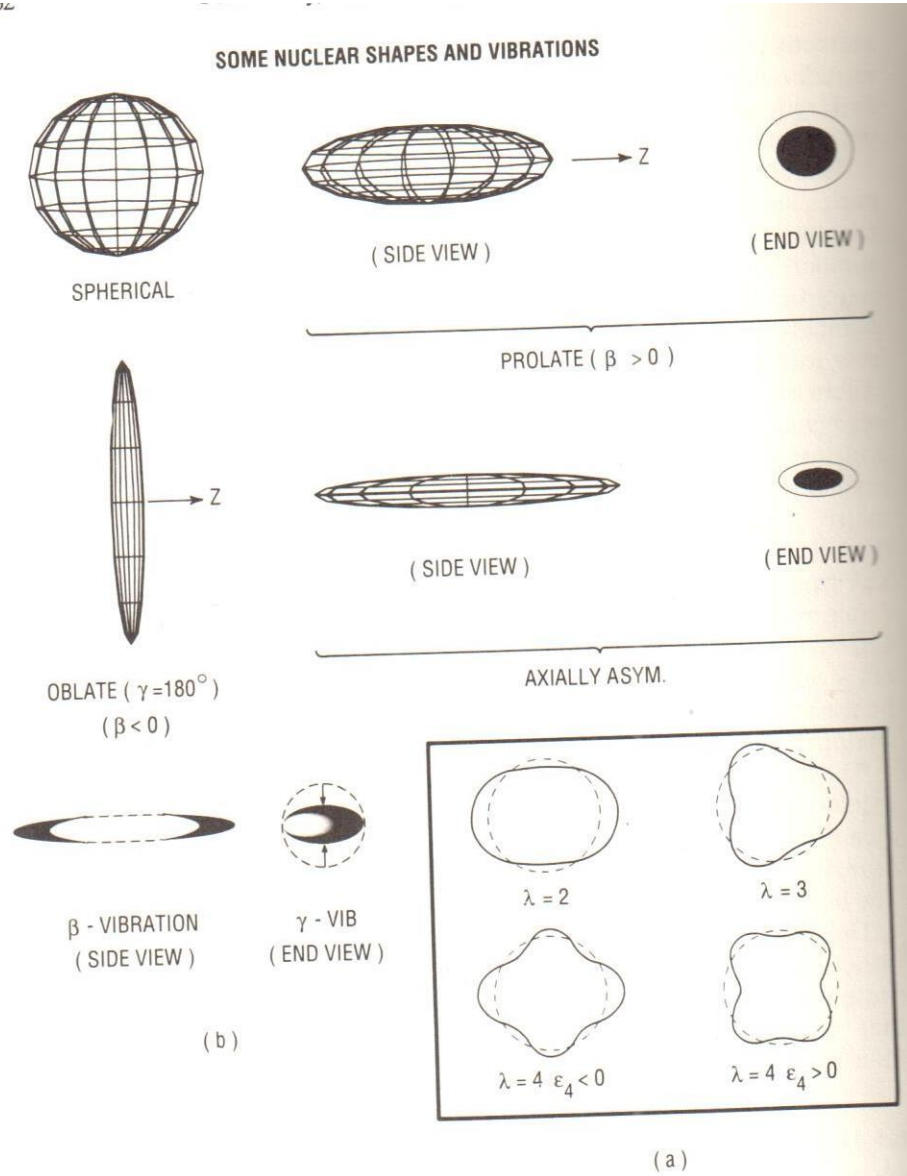

Fig. 6.10. (a) Equal potential surfaces for different multipole distortions. (b) Schematic illustrations of various quadrupole shapes (prolate, oblate, axially asymmetric) as well as of γ and β vibrational motions.

$\beta = \beta_0$ и $\gamma = 0$. В этом случае $\Im_1 = \Im_2 = 3B_2\beta_0^2 \equiv \Im$ и $\Im_3 = 4B_2\beta_0^2\gamma^2$

$$H_{\rm rot} = \sum_{k=1}^{3} \frac{\hbar^2 \hat{I}_k^2}{2\Im_k} = \frac{\hbar^2(\hat{I}_1^2 + \hat{I}_2^2)}{2\Im} = \frac{\hbar^2}{2\Im}(I(I+1) - \hat{I}_3^2).$$

$$E^*(I) = \frac{\hbar^2}{2\Im} I(I+1).$$

$$E^*(I, K, n_\beta, n_\gamma) = \frac{\hbar^2}{2\Im}(I(I+1) - K^2) + \hbar\omega_\beta n_\beta + \hbar\omega_\gamma n_\gamma.$$

$$\Psi_{IMK}(\beta, \gamma, \vec{\theta}) = \sqrt{\frac{2I+1}{16\pi^2(1+\delta_{K0})}} \left(D^I_{MK}(\vec{\theta}) + (-1)^I D^I_{M-K}(\vec{\theta})\right) \varphi_{n_\beta, n_\gamma}(\beta, \gamma).$$

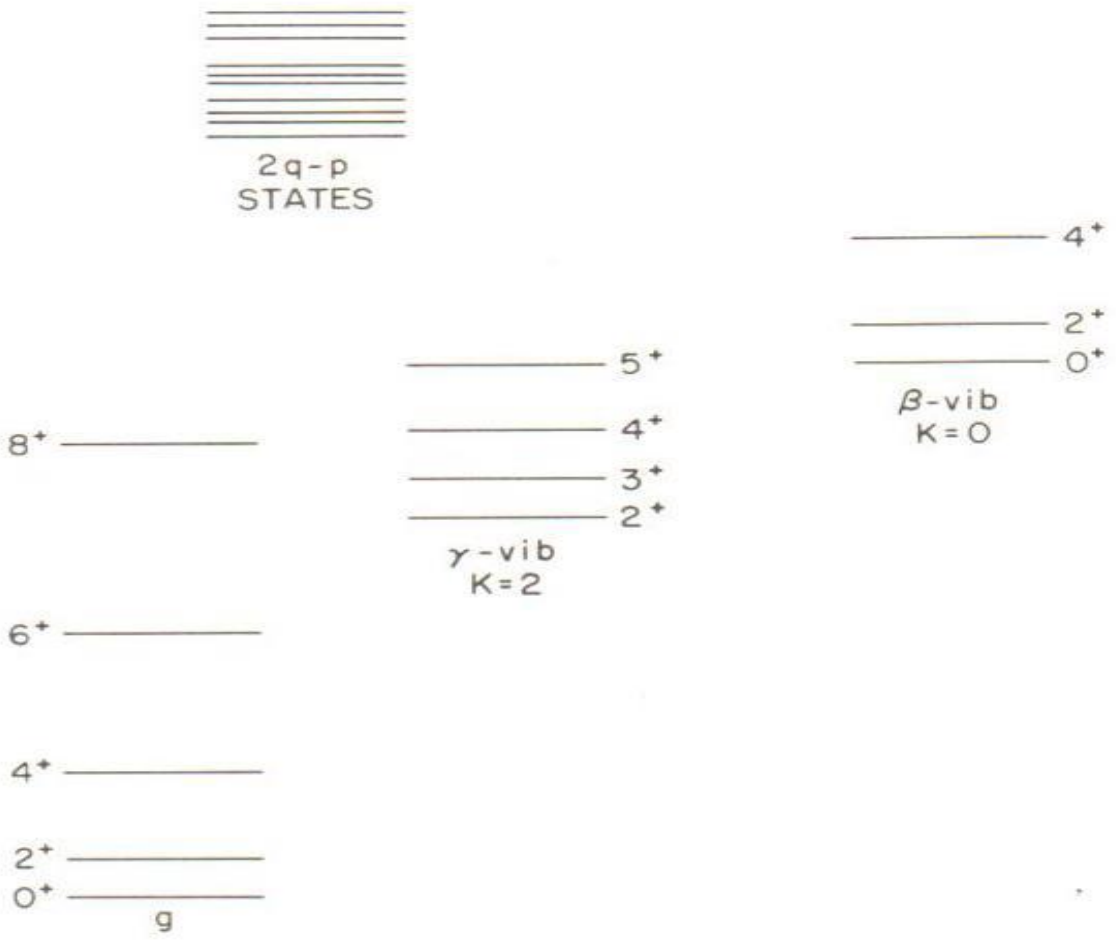

Fig. 6.13. Positive parity levels of a typical deformed nucleus.

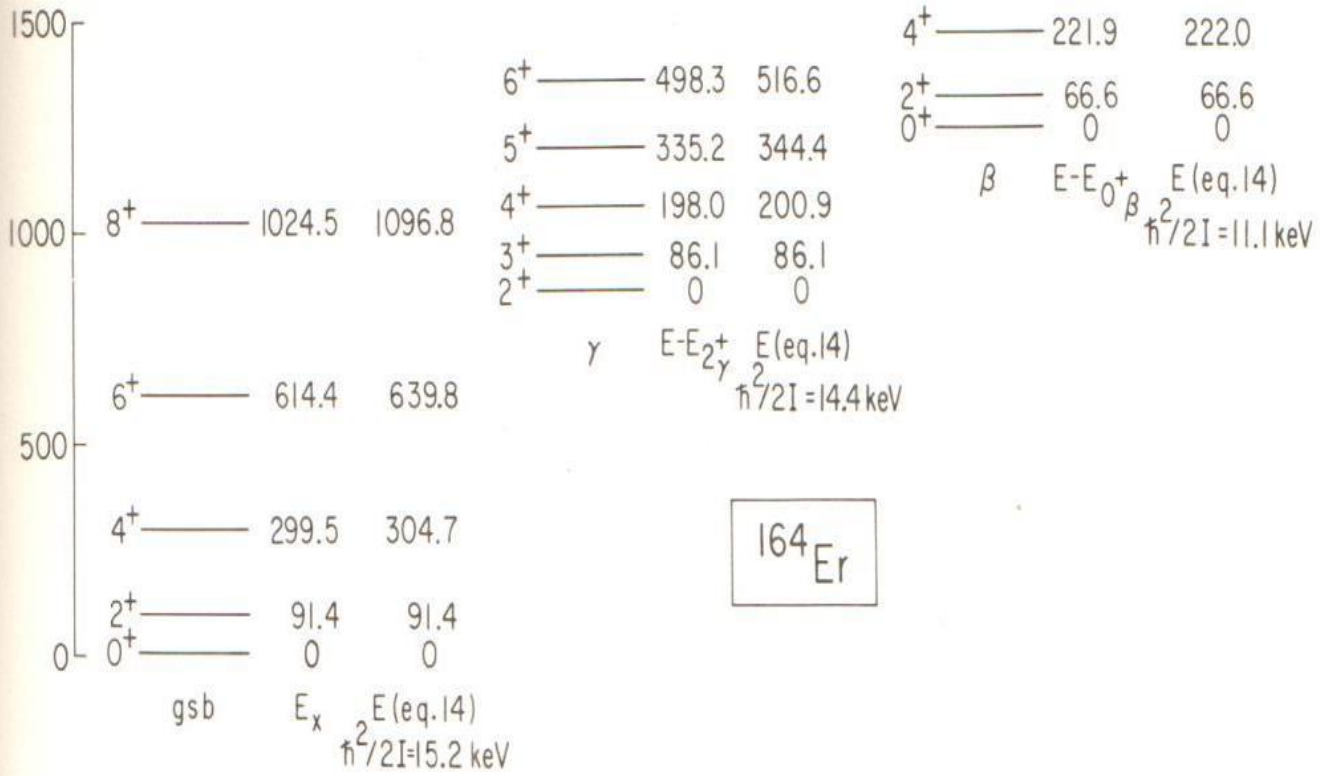

Fig. 6.12. Ground, γ, and β band levels of a typical deformed nucleus ^{164}Er. For each band the symmetric top rotational energy predictions (Eq. 6.14) are shown.

Superdeformation

$$H_{\text{osc}} = -\frac{\hbar^2}{2m}\left(\frac{\partial^2}{\partial x^2}+\frac{\partial^2}{\partial y^2}+\frac{\partial^2}{\partial z^2}\right)+\frac{m}{2}\left(\omega_\perp^2(x^2+y^2)+\omega_z^2 z^2\right)$$

$$E = \left(n_z+\frac{1}{2}\right)\hbar\omega_z + (n_\perp+1)\,\hbar\omega_\perp$$

$$\omega_\perp = 1.2\omega_0(\delta),$$

$$\omega_z = 0.6\omega_0(\delta)$$

$$E = \hbar\omega_z \left(n_z + 2n_\perp + 5/2\right)$$

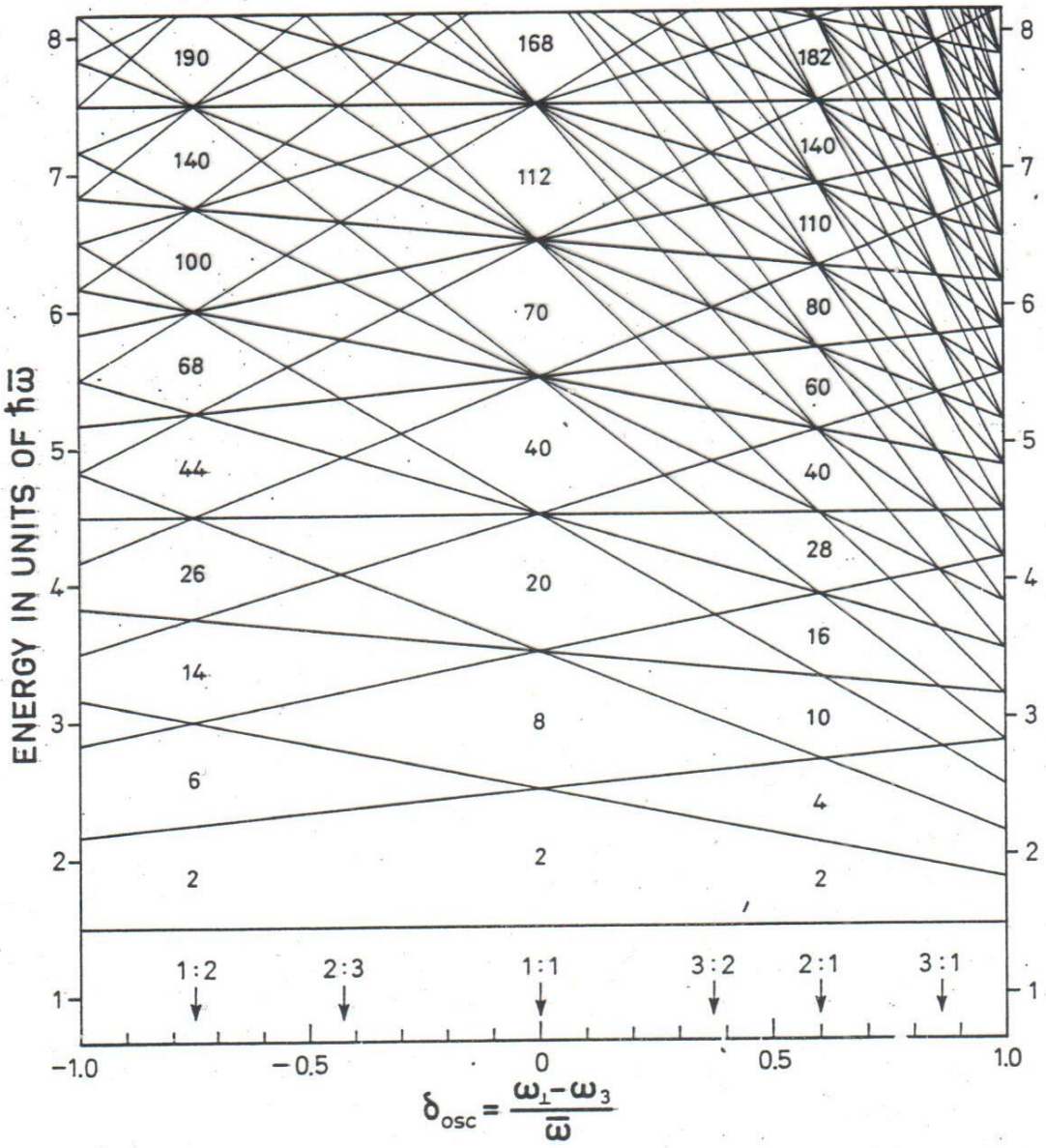

Figure 6-48 Single-particle spectrum for axially symmetric harmonic oscillator potentials. The eigenvalues are measured in units of $\overline{\omega} = (2\omega_\perp + \omega_3)/3$, and the deformation parameter δ_{osc} is that defined by Eq. (5-11). The arrows mark the deformations corresponding to the indicated rational ratios of frequencies $\omega_\perp : \omega_3$.

H 7346.5+w 6, (48⁻) γ_{6269+w} 1077.3 2 $I^{(1)}$=87.3, $I^{(2)}$=88.1, ħω=0.550
H 8469.2+w 6, (50⁻) γ_{7347+w} 1122.7 2 $I^{(1)}$=87.3, $I^{(2)}$=90.1, ħω=0.572
H 9636.3+w 6, (52⁻) γ_{8469+w} 1167.1 2 $I^{(1)}$=87.4, $I^{(2)}$=89.9, ħω=0.595
H 10847.9+w 7, (54⁻) γ_{9636+w} 1211.6 2 $I^{(1)}$=87.5, $I^{(2)}$=88.7, ħω=0.617
H 12104.6+w 7, (56⁻) $\gamma_{10848+w}$ 1256.7 2 $I^{(1)}$=87.6, $I^{(2)}$=92.6, ħω=0.639
H 13404.5+w 7, (58⁻) $\gamma_{12105+w}$ 1299.9 2 $I^{(1)}$=87.7, $I^{(2)}$=90.1, ħω=0.661
H 14748.8+w 7, (60⁻) $\gamma_{13405+w}$ 1344.3 2 $I^{(1)}$=87.8, $I^{(2)}$=90.7, ħω=0.683
H 16137.2+w 9, (62⁻) $\gamma_{14749+w}$ 1388.4 5 $I^{(1)}$=87.9, $I^{(2)}$=88.7, ħω=0.705
H 17570.7+w 13, (64⁻) $\gamma_{16137+w}$ 1433.5 10

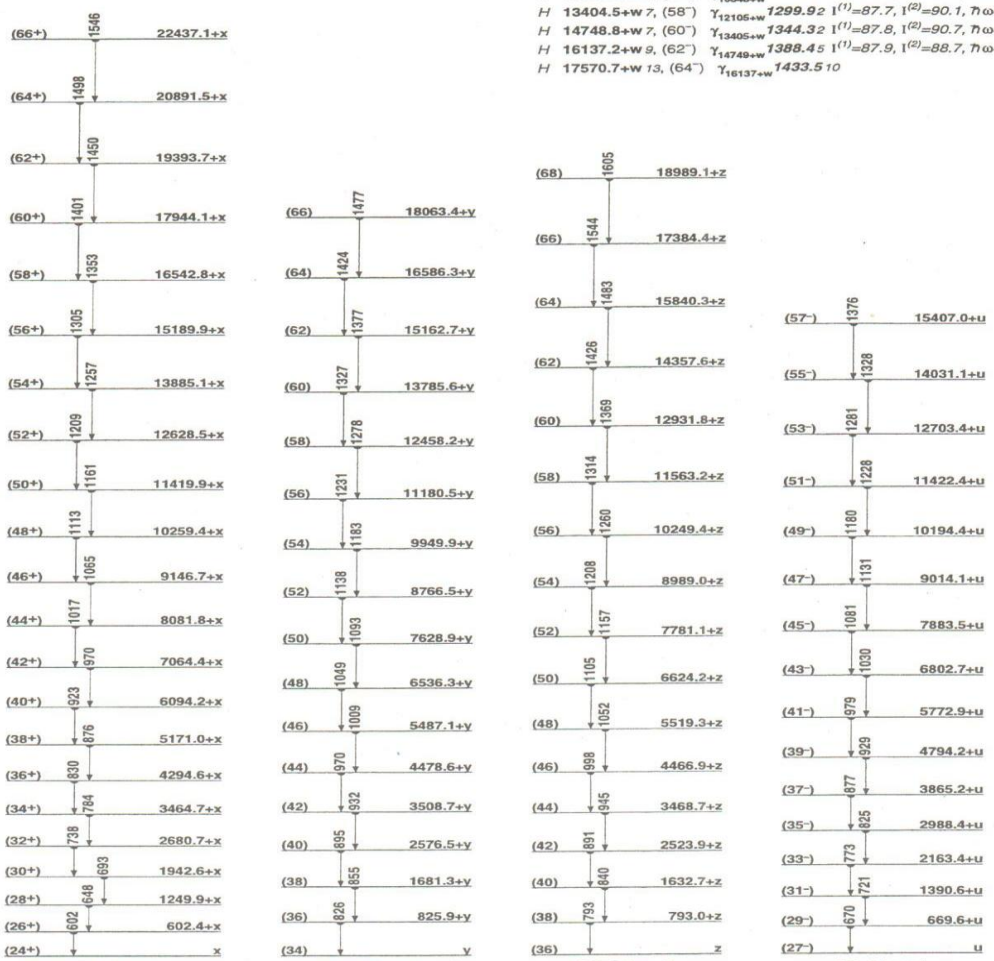

$^{152}_{66}Dy$

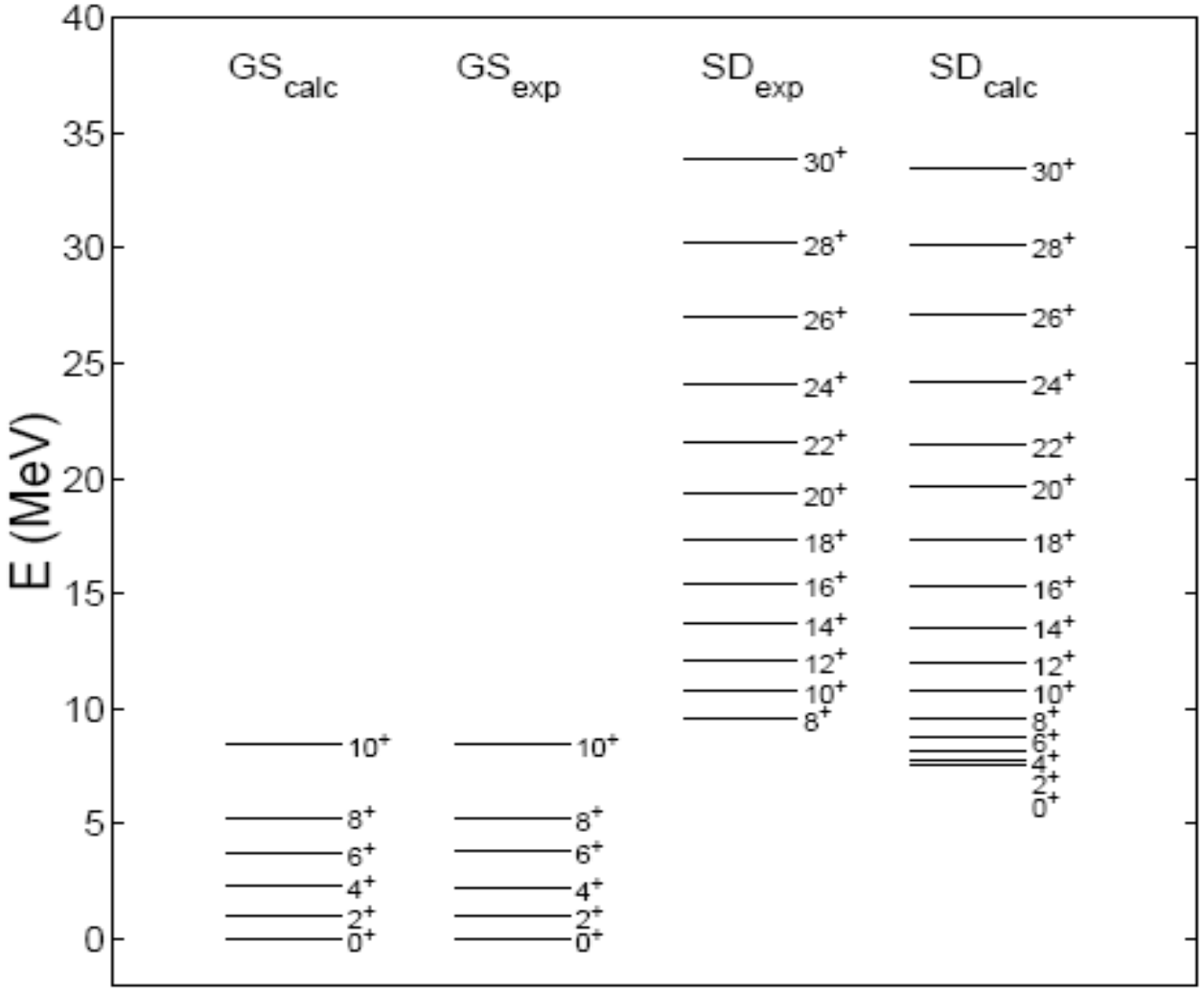

FIG. 2. Experimental and calculated energies of the states of the ground state (GS) and superdeformed (SD) bands in ^{60}Zn. Experimental data are taken from Ref. [7].

Identical bands

Owing to the rapid accumulation of the experimental data with the new gamma-balls it became possible to compare excitation energies of the neighboring even-even and odd-A nuclei. Such corresponding pair has been observed, for instance, in $^{152}_{66}Dy_{86}$ and $^{151}_{65}Tb_{86}$. It has been found that within experimental errors the transition energies of two corresponding SD bands of these two nuclei are equal to an accuracy of the order $3 \cdot 10^{-2}$.

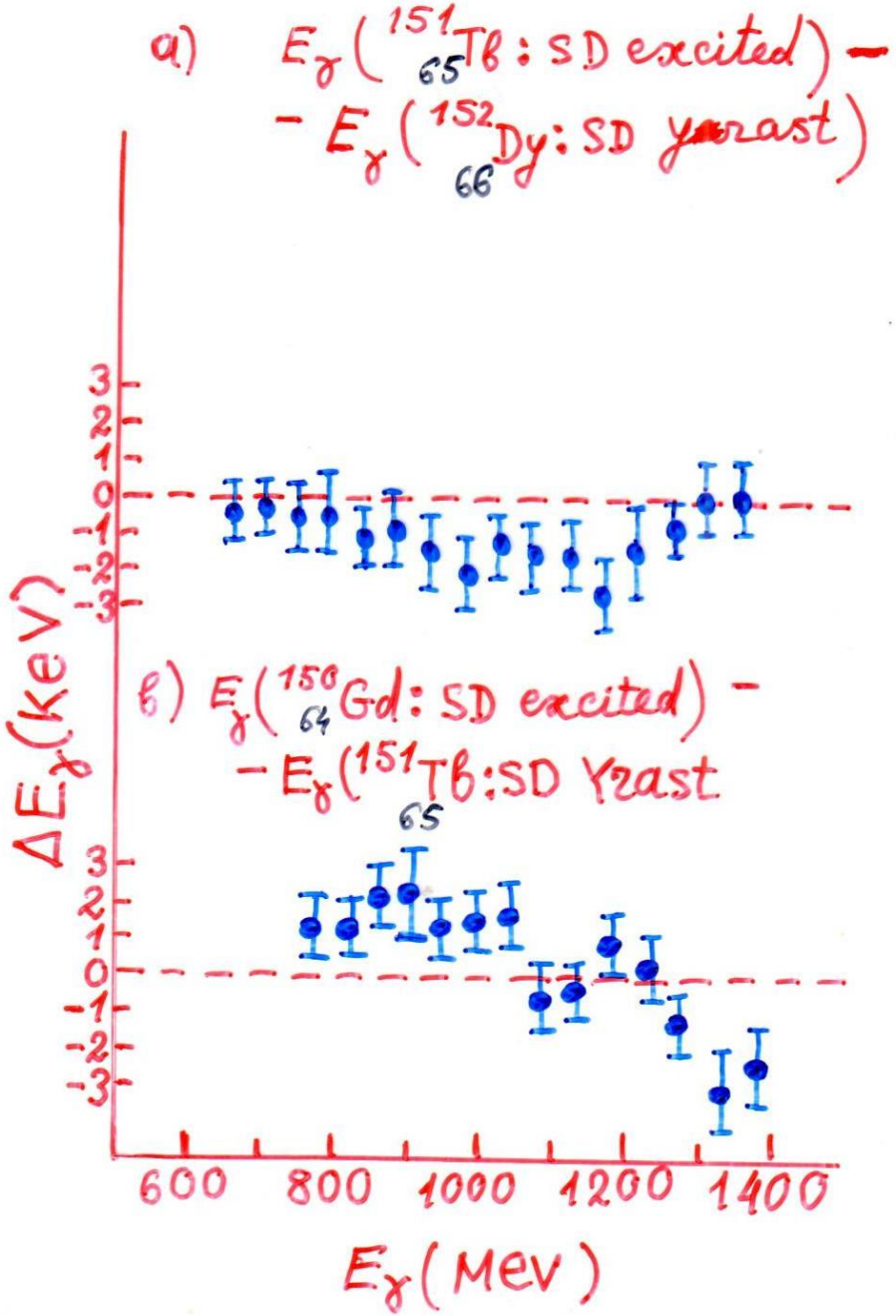
a) $E_\gamma(^{151}_{65}Tb$: SD excited) −
− $E_\gamma(^{152}_{66}Dy$: SD yrast)
b) $E_\gamma(^{150}_{64}Gd$: SD excited) −
− $E_\gamma(^{151}_{65}Tb$: SD Yrast
ΔE_γ (keV)
3
2
1
0
-1
-2
-3
600
800
1000
1200
1400
E_γ (MeV)

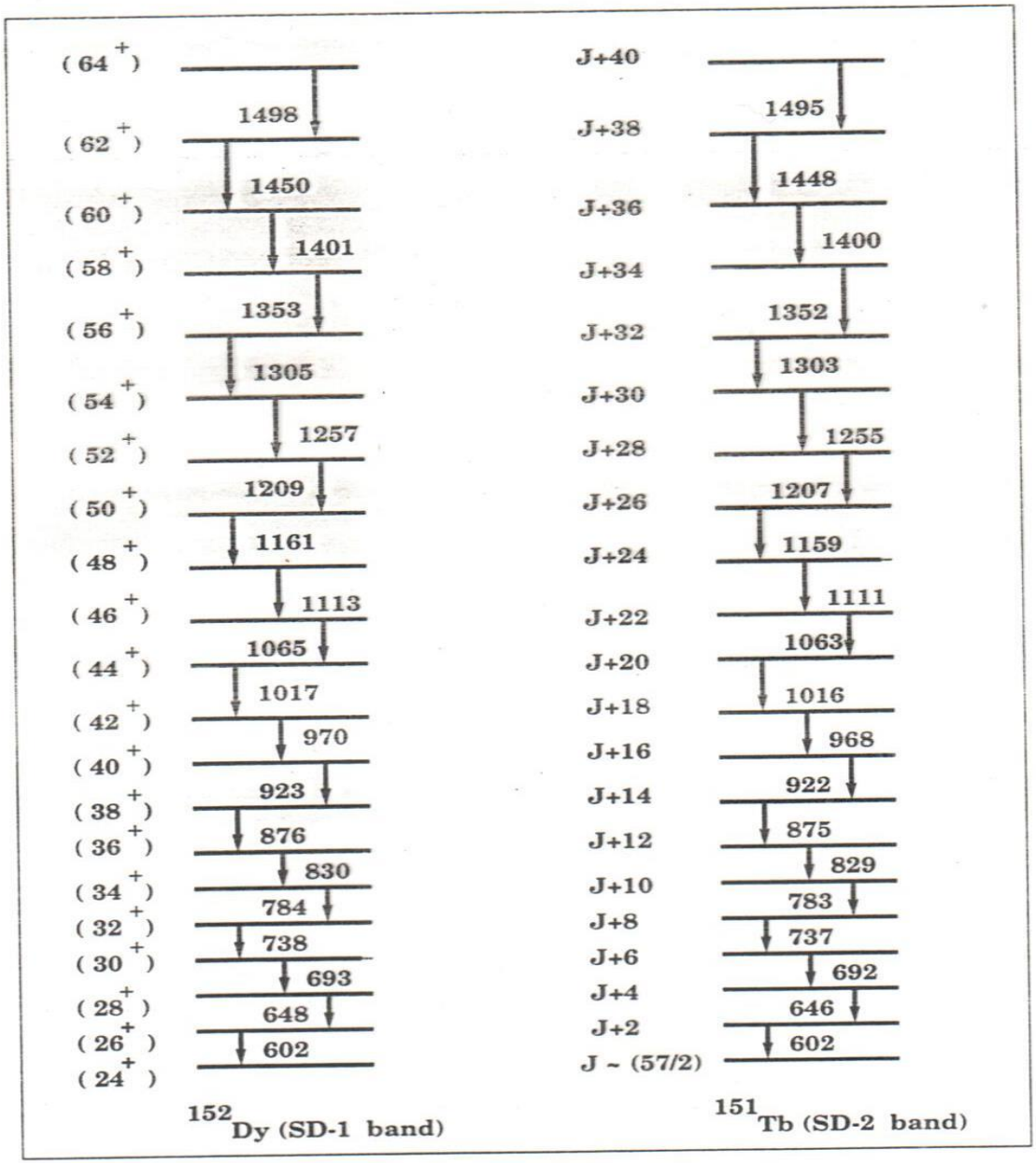
(64+)
1498
(62+)
1450
(60+)
1401
(58+)
1353
(56+)
1305
(54+)
1257
(52+)
1209
(50+)
1161
(48+)
1113
(46+)
1065
(44+)
1017
(42+)
970
(40+)
923
(38+)
876
(36+)
830
(34+)
784
(32+)
738
(30+)
693
(28+)
648
(26+)
602
(24+)
152Dy (SD-1 band)
J+40
1495
J+38
1448
J+36
1400
J+34
1352
J+32
1303
J+30
1255
J+28
1207
J+26
1159
J+24
1111
J+22
1063
J+20
1016
J+18
968
J+16
922
J+14
875
J+12
829
J+10
783
J+8
737
J+6
692
J+4
646
J+2
602
J ~ (57/2)
151Tb (SD-2 band)

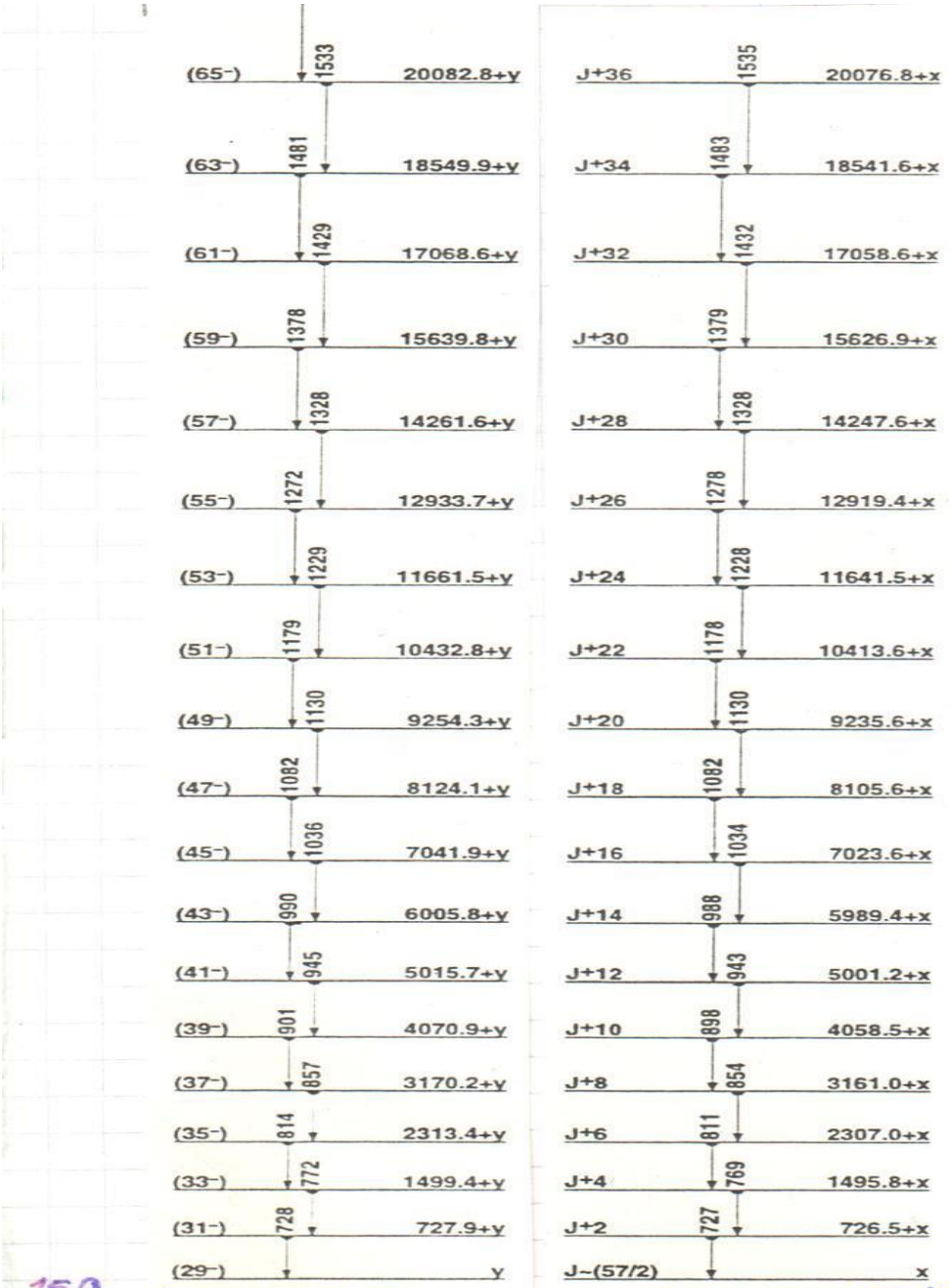
(65⁻)
1533
20082.8+y
(63⁻)
1481
18549.9+y
(61⁻)
1429
17068.6+y
(59⁻)
1378
15639.8+y
(57⁻)
1328
14261.6+y
(55⁻)
1272
12933.7+y
(53⁻)
1229
11661.5+y
(51⁻)
1179
10432.8+y
(49⁻)
1130
9254.3+y
(47⁻)
1082
8124.1+y
(45⁻)
1036
7041.9+y
(43⁻)
990
6005.8+y
(41⁻)
945
5015.7+y
(39⁻)
901
4070.9+y
(37⁻)
857
3170.2+y
(35⁻)
814
2313.4+y
(33⁻)
772
1499.4+y
(31⁻)
728
727.9+y
(29⁻)
y
SD-2 band
J+36
1535
20076.8+x
J+34
1483
18541.6+x
J+32
1432
17058.6+x
J+30
1379
15626.9+x
J+28
1328
14247.6+x
J+26
1278
12919.4+x
J+24
1228
11641.5+x
J+22
1178
10413.6+x
J+20
1130
9235.6+x
J+18
1082
8105.6+x
J+16
1034
7023.6+x
J+14
988
5989.4+x
J+12
943
5001.2+x
J+10
898
4058.5+x
J+8
854
3161.0+x
J+6
811
2307.0+x
J+4
769
1495.8+x
J+2
727
726.5+x
J~(57/2)
x
SD-1 band

Table. Comparison of the identical bands in ^{151}Tb (yrast) and ^{152}Gd* (excited).

I	^{151}Tb	I	^{152}Gd
133/2	1380.7	66	1378.0
129/2	1330.0	64	1337.0
125/2	1278.5	62	1277.0
121/2	1228.5	60	1229.0
117/2	1178.9	58	1180.0
113/2	1130.2	56	1130.0
109/2	1082.5	54	1082.0
105/2	1034.9	52	1036.0
101/2	988.7	50	990.0
97/2	942.8	48	944.0
93/2	898.0	46	900.0
89/2	854.0	44	856.0
85/2	811.3	42	813.0
81/2	769.2	40	770.0

Table. Comparison of the identical superdeformed bands in ^{152}Dy (yrast) and ^{151}Tb (excited).

I	^{152}Dy	I	^{151}Tb
59	1353.0	119/2	1353.0
57	1304.7	115/2	1305.0
55	1256.6	111/2	1256.0
53	1208.7	107/2	1207.0
51	1160.8	103/2	1158.0
49	1112.7	99/2	1112.0
47	1064.8	95/2	1063.0
45	1017.0	91/2	1016.0
43	970.0	87/2	970.0
41	923.1	83/2	922.0
39	876.1	79/2	976.0
37	829.2	75/2	828.0
35	783.5	71/2	783.0
33	737.5	67/2	738.0
31	692.2	63/2	692.0
29	647.2	59/2	647.0

Pseudospin symmetry

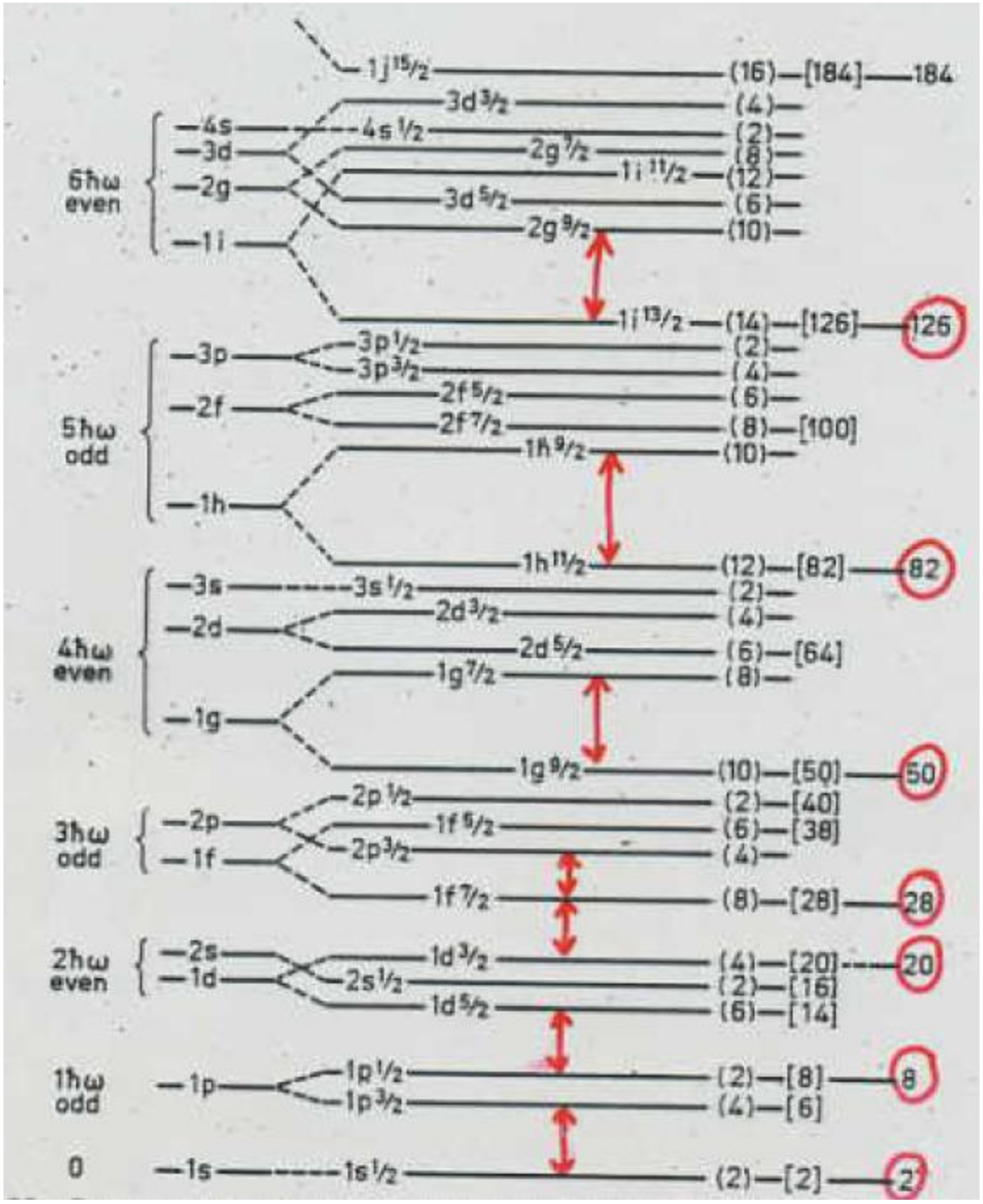
1j15/2 (16) [184] 184
3d3/2 (4)
4s 4s1/2 (2)
3d 2g7/2 (8)
6ħω 2g 1i11/2 (12)
even 3d5/2 (6)
1i 2g9/2 (10)
1i13/2 (14) [126] 126
3p 3p1/2 (2)
3p3/2 (4)
5ħω 2f 2f5/2 (6)
odd 2f7/2 (8) [100]
1h 1h9/2 (10)
1h11/2 (12) [82] 82
3s 3s1/2 (2)
2d 2d3/2 (4)
4ħω 2d5/2 (6) [64]
even 1g 1g7/2 (8)
1g9/2 (10) [50] 50
2p 2p1/2 (2) [40]
3ħω 1f 1f5/2 (6) [38]
odd 2p3/2 (4)
1f7/2 (8) [28] 28
2s 1d3/2 (4) [20] 20
2ħω 1d 2s1/2 (2) [16]
even 1d5/2 (6) [14]
1p 1p1/2 (2) [8] 8
1ħω 1p3/2 (4) [6]
odd
0 1s 1s1/2 (2) [2] 2

Twenty years later, i.e. 35 years ago a quasidegeneracy was observed , at first for spherical nuclei, (Arima, Harvey,… and Hecht , Adler – 1969):

Single-particle states with $J=l+\frac{1}{2}$ and $J=(l+2)-\frac{1}{2}$ lie very close in energy.

It is convenient to label them as pseudospin doublets with the following quantum numbers

$$\tilde{N} = N-1$$

$$\tilde{\ell} = \begin{cases} \ell_1 - 1 & : \; j_1 = \ell_1 - \frac{1}{2} \\ \ell_2 + 1 & : \; j_2 = \ell_2 + \frac{1}{2} \end{cases}$$

$$\tilde{S} = 1/2$$

Examples of Pseudospin Doublets

$$(n_r\ \ell\ j;\ (n_r-1)\ \ell+2,\ j+1)$$

$$j = \tilde{\ell} \pm \tilde{s}\ ,\ \tilde{s} = 1/2\ ;$$

$\tilde{\ell}$ pseudo-orbital angular momentum, $\tilde{s}$ pseudo-spin

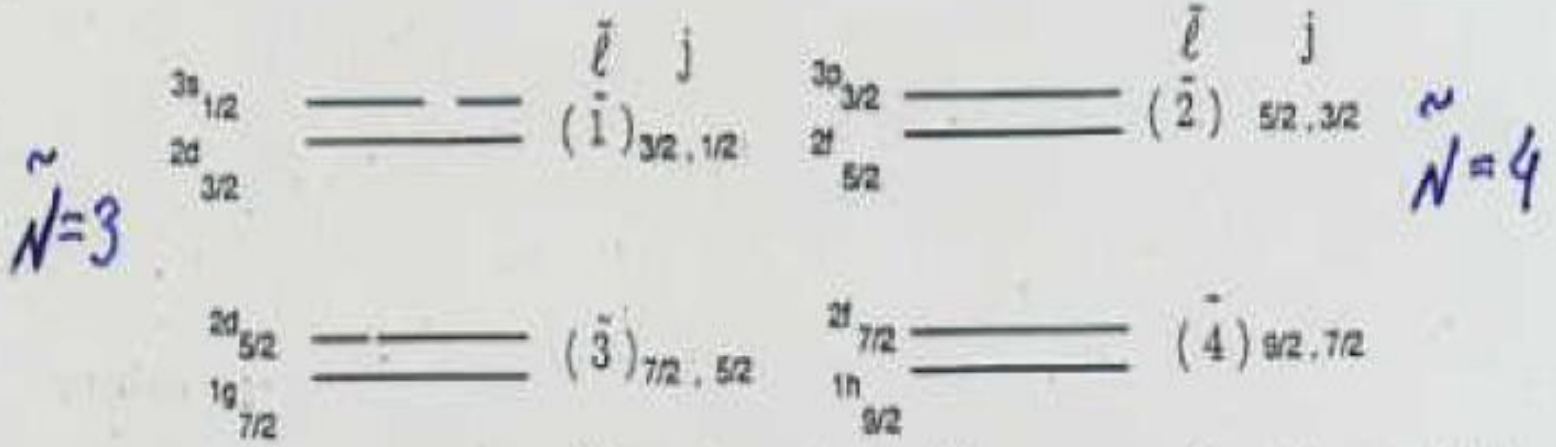

Fig. 1. Examples of pseudospin doublets in the ^{208}Pb region. n_r is the radial quantum number of the state, ℓ is the orbital angular momentum, j the total angular momentum.

This introduction of the pseudospin and pseudoorbital momenta is always possible mathematically

$$a^{+}_{N\ell jm} = \sum_{\tilde{m},\tilde{\sigma}} C^{jm}_{\tilde{\ell}\tilde{m}\,\frac{1}{2}\tilde{\sigma}}\, a^{+}_{\tilde{N}\tilde{\ell}\tilde{m},\frac{1}{2}\tilde{\sigma}}$$

$$a^{+}_{\tilde{N}\tilde{\ell}\tilde{m},\frac{1}{2}\tilde{\sigma}} = \sum_{jm} C^{jm}_{\tilde{\ell}\tilde{m}\,\frac{1}{2}\tilde{\sigma}}\, a^{+}_{N\ell jm}$$

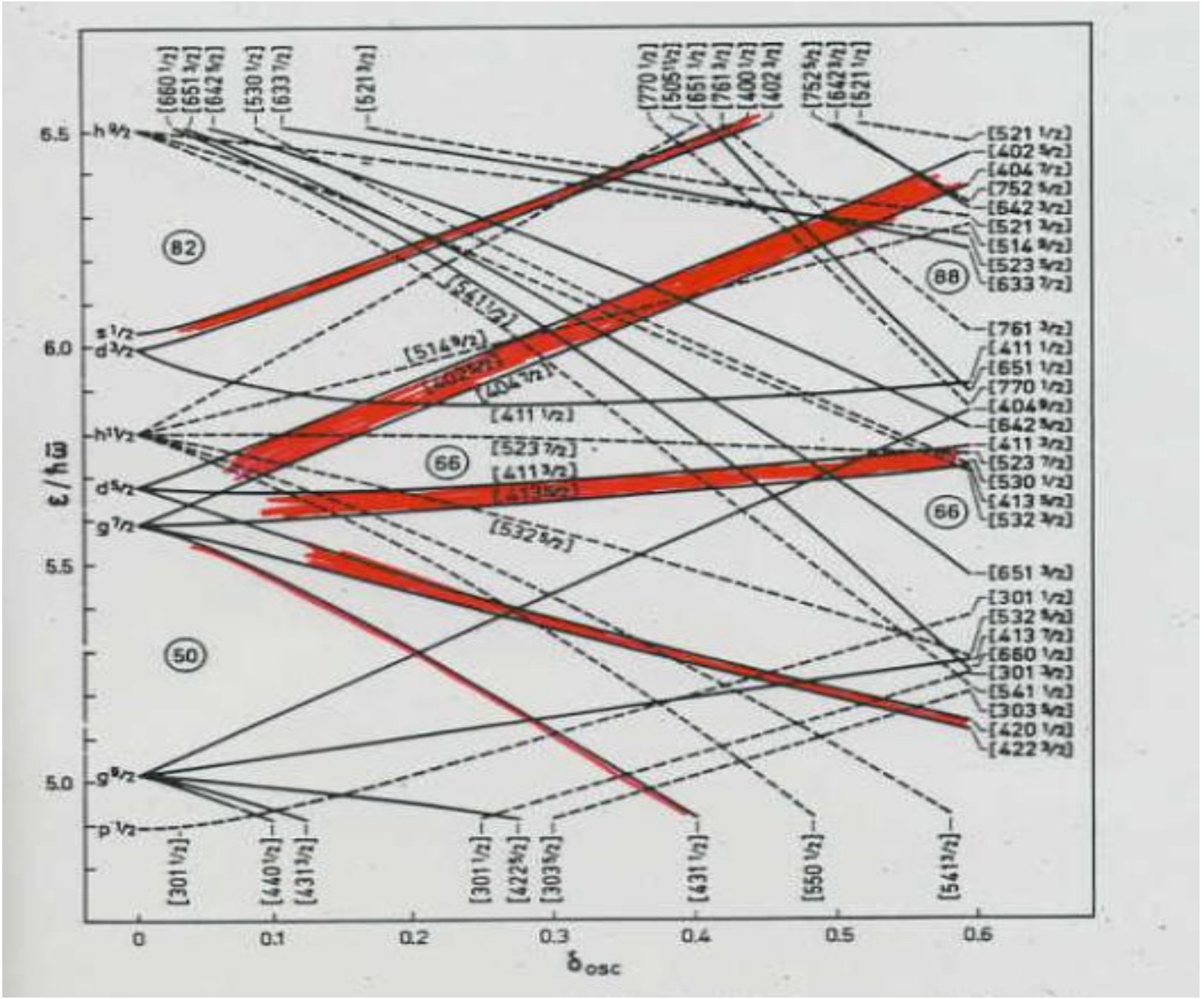
ε / ħω
δ osc
6.5
6.0
5.5
5.0
0
0.1
0.2
0.3
0.4
0.5
0.6
82
66
50
88
66
h 9/2
s 1/2
d 3/2
h 11/2
d 5/2
g 7/2
g 9/2
p 1/2
[660 1/2]
[651 3/2]
[642 5/2]
[530 1/2]
[633 7/2]
[521 1/2]
[770 1/2]
[505 11/2]
[651 1/2]
[761 3/2]
[400 1/2]
[402 3/2]
[752 5/2]
[642 3/2]
[521 1/2]
[541 1/2]
[514 9/2]
[402 5/2]
[404 7/2]
[411 1/2]
[523 7/2]
[411 3/2]
[532 5/2]
[301 1/2]
[440 1/2]
[431 3/2]
[301 1/2]
[422 5/2]
[303 5/2]
[431 1/2]
[550 1/2]
[541 3/2]
[521 1/2]
[402 5/2]
[404 7/2]
[752 5/2]
[642 3/2]
[521 3/2]
[514 9/2]
[523 5/2]
[633 7/2]
[761 3/2]
[411 1/2]
[651 1/2]
[770 1/2]
[404 9/2]
[642 5/2]
[411 3/2]
[523 7/2]
[530 1/2]
[413 5/2]
[532 3/2]
[651 3/2]
[301 1/2]
[532 5/2]
[413 7/2]
[660 1/2]
[301 3/2]
[541 1/2]
[303 5/2]
[420 1/2]
[422 3/2]

Later J.Ginocchio has shown that pseudo-spin symmetry in nuclei arise from nucleons moving in a relativistic mean field which has an attractive scalar and a repulsive vector potentials nearly equal in magnitude.

Уравнение для малой компоненты спинора Дирака

$$g(\vec{r}) = \frac{1}{\varepsilon - V_0 + S}(\vec{\sigma}\cdot\vec{p})f(\vec{r}).$$

Подставляя этот результат в уравнение для $f(\vec{r})$, получаем

$$\left(\vec{\sigma}\cdot\vec{p}\frac{1}{\varepsilon - V_0 + S}\vec{\sigma}\cdot\vec{p} + (V_0 + S) - 2Mc^2\right) f(\vec{r}) = \varepsilon f(\vec{r})$$

или

$$\left(\vec{p}\frac{1}{\varepsilon - V_0 + S}\vec{p} + \frac{1}{(\varepsilon - V_0 + S)^2}\frac{1}{r}\frac{\partial(V_0 - S)}{\partial r}\vec{l}\cdot\vec{s} + (V_0 + S - 2Mc^2)\right) f(\vec{r}) \approx \varepsilon f(\vec{r})$$

In the limit of the equality of the magnitude of the vector and scalar potentials the pseudospin symmetry is exactly conserved

Such a near equality of the scalar and vector mean fields has been obtained
-in relativistic field theories with interacting nucleons and mesons;
-in relativistic field theories with nucleons interacting via Skyrme-type interactions.
Probably this result is a general feature of any relativistic model which fits nuclear binding energies.

Applying QCD sum rules in nuclear matter, the ratio of the scalar and vector selfenergies were determined to be

$$\frac{V_s}{V_v} \approx -\frac{\sigma_N}{8 m_q}, \quad m_q \equiv \tfrac{1}{2}(m_u + m_d)$$

$$\sigma_N = 45 \pm 10 \text{ MeV}$$

where σ_N is the sigma term which arises from the spontaneous breaking of chiral symmetry. For reasonable values of σ_N and quark masses, this ratio is close to -1. The implication of these results is that chiral symmetry breaking is responsible for a scalar field being approximately equal in magnitude to the vector field, thereby producing pseudo-spin symmetry.

The relative weakness of the pseudo-spin-orbit coupling implies that pseudo-orbital angular momenta of the quasiparticles are strongly coupled to the deformation forming, together with the core, a rotating system with angular momentum

$$\tilde{\tilde{L}} = \bar{R} + \tilde{\tilde{l}}$$

The pseudo-spins are then added to form the total angular momentum

$$\hat{J} = \tilde{\tilde{L}} + \tilde{s}.$$

Identical bands

The consequence of the pseudo-spin symmetry: the appearance of identical bands. Strong deformation in the pseudo-space part of the many-particle basis gives rise to $\tilde{L}\,(\tilde{L}+1)$ rotational sequences for each of the $(2\tilde{S}+1)$ orientations of the pseudo-spin. A prediction of the theory is that additional, strongly deformed bands should be found.

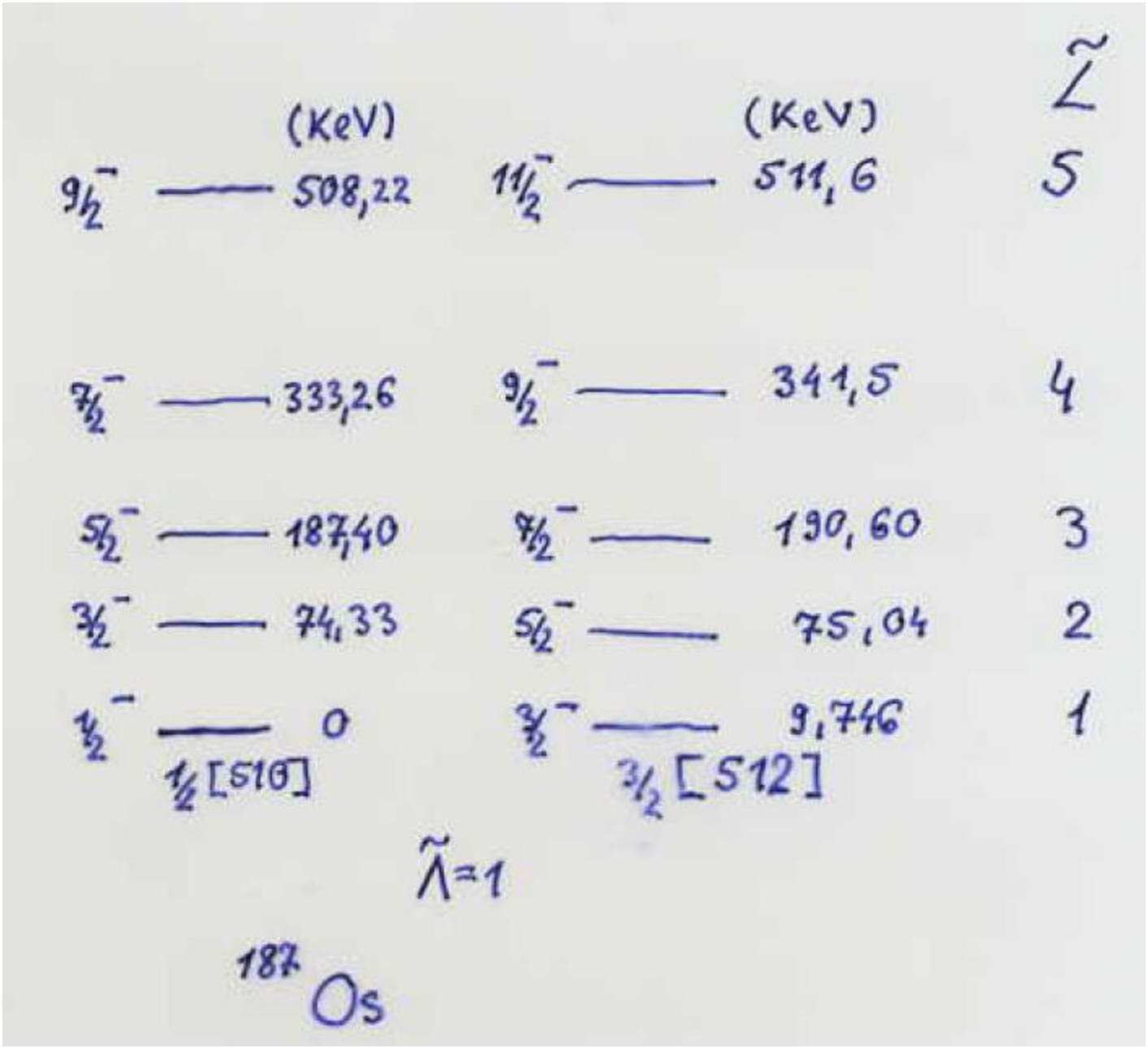
(KeV)
(KeV)
$\tilde{\Sigma}$
$9/2^-$ 508,22
$11/2^-$ 511,6
5
$7/2^-$ 333,26
$9/2^-$ 341,5
4
$5/2^-$ 187,40
$7/2^-$ 190,60
3
$3/2^-$ 74,33
$5/2^-$ 75,04
2
$1/2^-$ 0
$3/2^-$ 9,746
1
$1/2[510]$
$3/2[512]$
$\tilde{\Lambda}=1$
^{187}Os

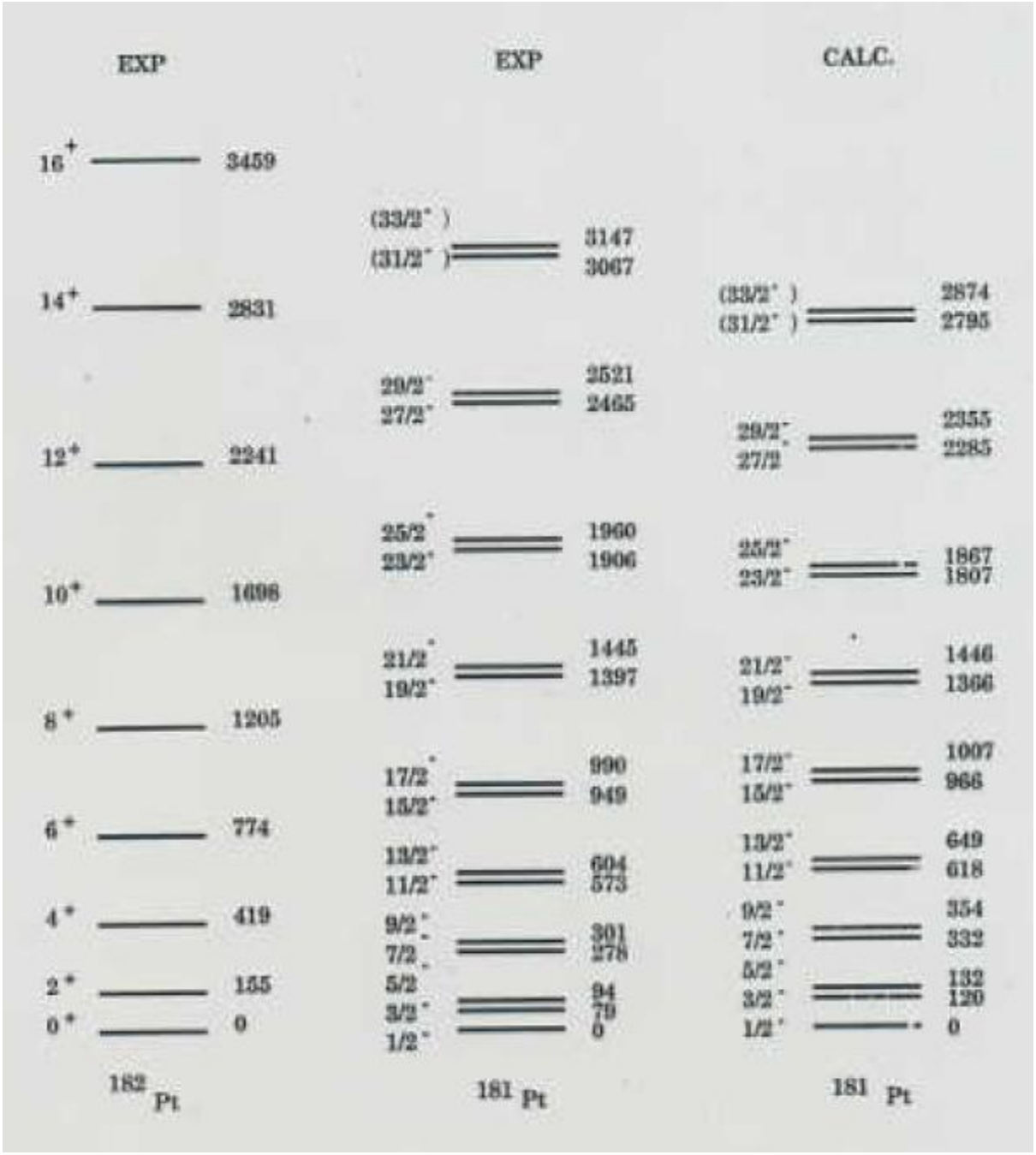
EXP
EXP
CALC.
16+ 3459
14+ 2831
12+ 2241
10+ 1698
8+ 1205
6+ 774
4+ 419
2+ 155
0+ 0
182 Pt
(33/2-) 3147
(31/2-) 3067
29/2- 2521
27/2- 2465
25/2- 1960
23/2- 1906
21/2- 1445
19/2- 1397
17/2- 990
15/2- 949
13/2- 604
11/2- 573
9/2- 301
7/2- 278
5/2- 94
3/2- 79
1/2- 0
181 Pt
(33/2-) 2874
(31/2-) 2795
29/2- 2355
27/2- 2285
25/2- 1867
23/2- 1807
21/2- 1446
19/2- 1366
17/2- 1007
15/2- 966
13/2- 649
11/2- 618
9/2- 354
7/2- 332
5/2- 132
3/2- 120
1/2- 0
181 Pt

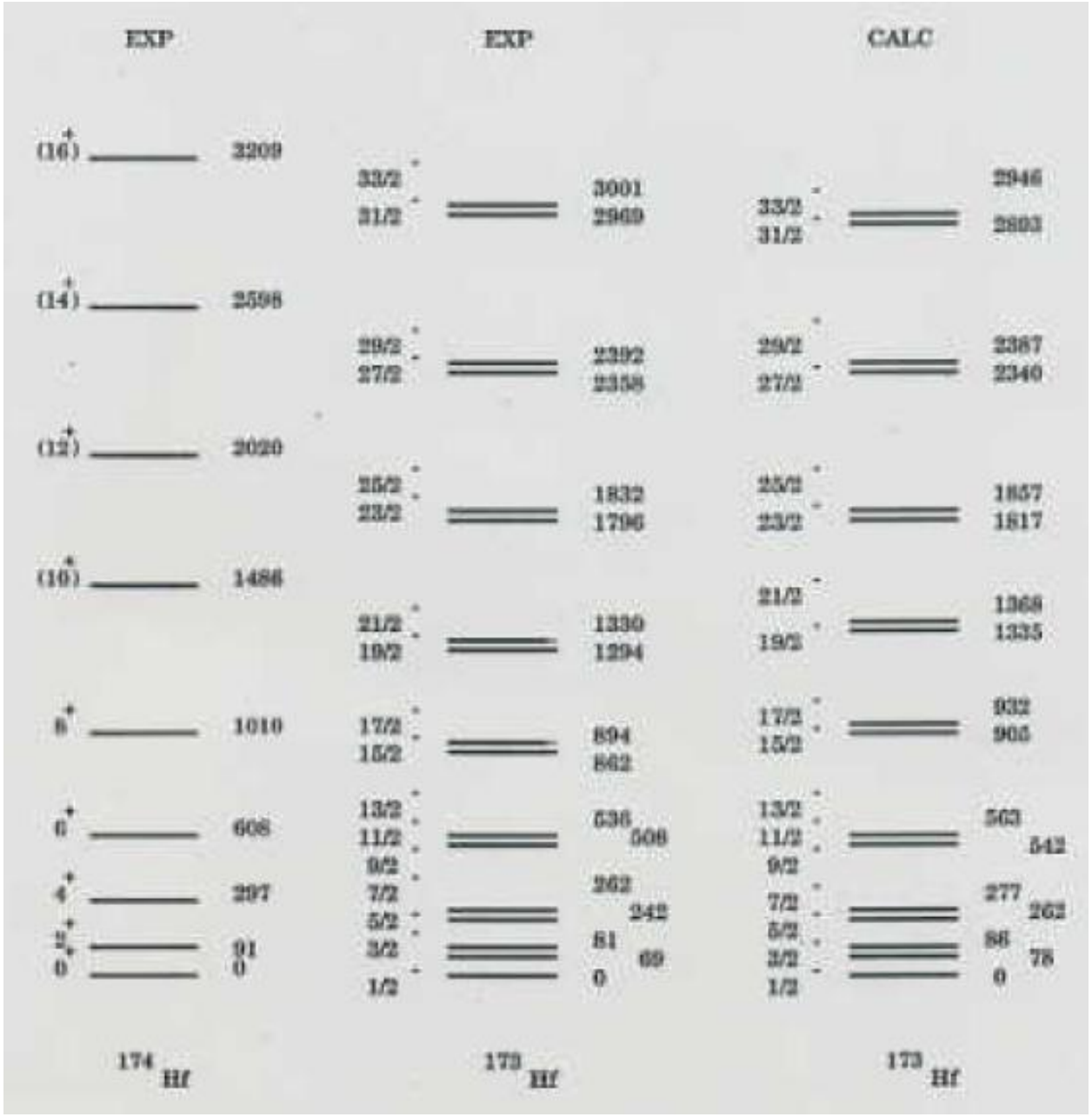
EXP
EXP
CALC
(16+) 3209
33/2- 3001
31/2- 2969
33/2- 2946
31/2- 2893
(14+) 2598
29/2- 2392
27/2- 2358
29/2- 2367
27/2- 2340
(12+) 2020
25/2- 1832
23/2- 1796
25/2- 1857
23/2- 1817
(10+) 1486
21/2- 1330
19/2- 1294
21/2- 1368
19/2- 1335
8+ 1010
17/2- 894
15/2- 862
17/2- 932
15/2- 905
6+ 608
13/2- 636
11/2- 608
9/2- 562
13/2- 563
11/2- 542
4+ 397
7/2- 262
5/2- 242
7/2- 277
5/2- 262
2+ 91
3/2- 61
1/2- 69
3/2- 86
1/2- 78
0+ 0
1/2- 0
0
174 Hf
173 Hf
173 Hf

Microscopical nuclear models

- Pair correlations. u-v Bogoliubov transformation.
- Random phase approximation. (RPA)
- Nuclear mean field. Hartree-Fock-Bogoliubov method.

Pairing (Pair correlations of nucleons)

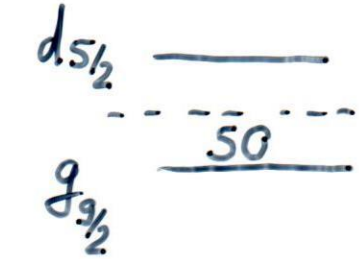

$(d_{5/2})^2$: $0^+, 2^+, 4^+$

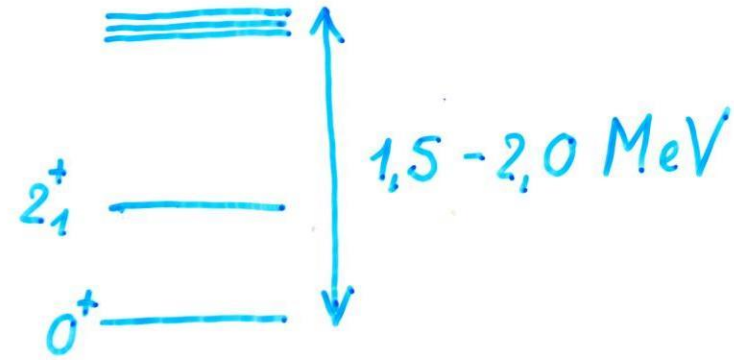

Independent Particle model

Exp.

Energy gap like in a superconductor!

Pair correlations. u-v Bogoliubov transformation.

$$\left(-\frac{\hbar^2}{2m}\triangle + V(r) + \lambda\frac{1}{r}\frac{dV}{dr}\vec{l}\cdot\vec{s}\right)\psi_{nljm}(\vec{r}) = E_{nljm}\psi_{nljm}(\vec{r}).$$

$$\psi(\vec{r}) = \sum_{nljm}\psi_{nljm}(\vec{r})a_{nljm}.$$

$$\{\psi(x),\psi^+(y)\} \equiv \psi(x)\psi^+(y) + \psi^+(y)\psi(x) = \delta(\vec{x}-\vec{y}).$$

$$\left\{a_{nljm}, a^+_{n'l'j'm'}\right\} = \delta_{nn'}\delta_{ll'}\delta_{jj'}\delta_{mm'}.$$

$$H_{sp} = \sum_{nljm} E_{nljm} a^{+}_{nljm} a_{nljm}.$$

$$|0>,$$

$$a^{+}_{nljm}|0>,$$

$$(a^{+}_{nlj} a^{+}_{n'l'j'})_{JM}|0> \ \ldots$$

$$a^{+}_{nljm} = \alpha^{+}_{nljm}, \quad E_{nlj} > E_F \equiv \lambda,$$

$$a^{+}_{nljm} = (-1)^{j-m} \alpha_{nlj-m}, \quad E_{nlj} < E_F \equiv \lambda.$$

$$\alpha_s^+ = u_s a_s^+ + v_s \sigma_s a_{\bar{s}},$$

u_s=1, а $v_s = 0$, если $E_s > \lambda$, и u_s=0, а $v_s = 1$, если $E_s < \lambda$.

$$u_s^2 + v_s^2 = 1$$

$$N = 2 \sum_{s>} v_s^2.$$

Particles and Holes

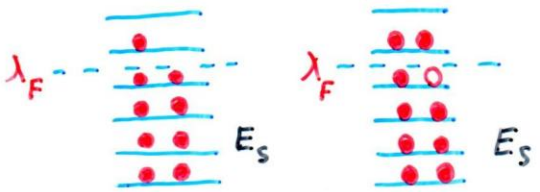

Quasiparticles are introduced to describe excitations

$$\alpha_s^+ = u_s a_s^+ - v_s a_{\bar{s}}$$

$$u_s = \begin{cases} 0 , & E_s < \lambda_F \\ 1 , & E_s > \lambda_F \end{cases}$$

$$v_s = \begin{cases} 1 , & E_s < \lambda_F \\ 0 , & E_s > \lambda_F \end{cases}$$

$$u_s^2 + v_s^2 = 1$$

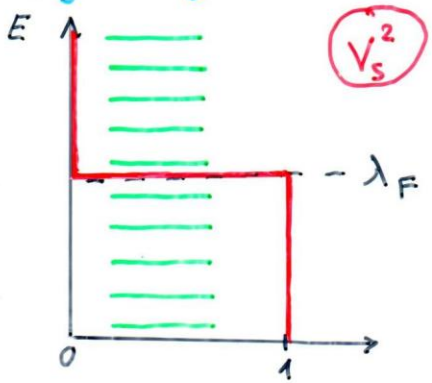

$$\alpha_s |gs>= 0.$$

$$|gs>= \Pi_{t>}(u_t - \sigma_t v_t a_t^+ a_{\bar{t}}^+)|0>$$

Generalization:

u_s^2, v_s^2 can take any values between zero and one

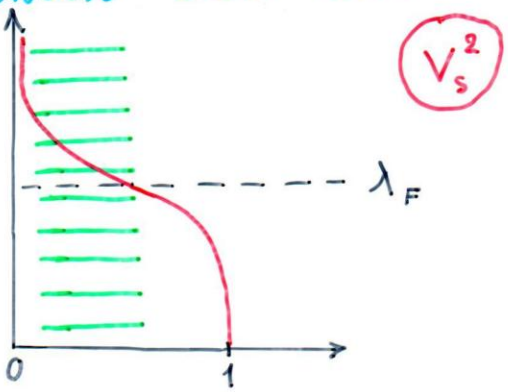

Let us find the wave function of the ground state which must satisfy to the following condition

$$\alpha_s |g.s.\rangle = 0$$

$$|g.s.\rangle = \prod_s (u_s + v_s a_s^+ a_{\bar{s}}^+) |0\rangle$$

$$\alpha_t |g.s.\rangle = (u_t a_t - v_t a_{\bar{t}}^+) \prod_s (u_s + v_s a_s^+ a_{\bar{s}}^+) |0\rangle$$

$$= (u_t v_t a_{\bar{t}}^+ - u_t v_t a_{\bar{t}}^+) \prod_{s \neq t} (u_s + v_s a_s^+ a_{\bar{s}}^+) |0\rangle$$

$$= 0$$

$$|g.s.\rangle \equiv |BCS\rangle$$

$$\hat{H} = \sum_{s} (E_s - \lambda) a_s^+ a_s - G \sum_{s,s'>} a_s^+ a_{\bar{s}}^+ a_{\bar{s}'} a_{s'}.$$

$$a_s^+ = u_s \alpha_s^+ - \sigma_s v_s \alpha_{\bar{s}},$$

$$a_s = u_s \alpha_s - \sigma_s v_s \alpha_{\bar{s}}^+,$$

$$\sigma_s^2 = 1, \quad \sigma_s \sigma_{\bar{s}} = -1,$$

$$u_s^2 = \frac{1}{2}\left(1 + \frac{(E_s - \lambda)}{\sqrt{(E_s - \lambda)^2 + \Delta^2}}\right),$$

$$v_s^2 = \frac{1}{2}\left(1 - \frac{(E_s - \lambda)}{\sqrt{(E_s - \lambda)^2 + \Delta^2}}\right).$$

$$\Delta = \frac{G}{2}\sum_{s>} \frac{\Delta}{\sqrt{(E_s - \lambda)^2 + \Delta^2}}.$$

1) $\Delta = 0,$

2) $$1 = \frac{G}{2}\sum_{s>} \frac{1}{\sqrt{(E_s - \lambda)^2 + \Delta^2}}.$$

$$\frac{G}{2}\sum_{s>} \frac{1}{|E_s - \lambda|} > 1$$

$$H = 2\sum_{s>}(E_s - \lambda)v_s^2 - \frac{\Delta^2}{G} + \sum_{s>}\sqrt{(E_s - \lambda)^2 + \Delta^2}(\alpha_s^+\alpha_s + \alpha_{\bar{s}}^+\alpha_{\bar{s}}).$$

$$H = \sum_s \varepsilon_s \alpha_s^+ \alpha_s.$$

$$\alpha_s^+\alpha_{s'}^+|gs>$$

$$\sqrt{(E_s - \lambda)^2 + \Delta^2} + \sqrt{(E_s' - \lambda)^2 + \Delta^2} \geq 2\Delta.$$

RPA

$$H = \sum_s \varepsilon_s \alpha_s^+ \alpha_s - \kappa F F,$$

$$F = \sum_{s,s'} f_{ss'}(u_s v_{s'} + v_s u_{s'})(\alpha_s^+ \alpha_{s'}^+ + \alpha_{s'} \alpha_s),$$

$$[H, B^+] = \omega B^+ \qquad\qquad B^+|gs>$$

$$H|gs> = 0.$$

$$HB^+|gs> = (HB^+ - B^+H)|gs> = [H, B^+]|gs> = \omega B^+|gs> .$$

$$B^{+} = \sum_{s.t} \left(\psi_{st} \alpha_s^{+} \alpha_t^{+} - \varphi_{st} \alpha_t \alpha_s \right).$$

$$B|gs> = -\sum_{s,t} \varphi_{st} \alpha_s^{+} \alpha_t^{+}) |gs>$$

$$|gs_{RPA}> = -\sum_{s,t} \varphi_{st} \alpha_s^{+} \alpha_t^{+}) |gs> + 12 \sum \psi_{st} \xi_{stkl} \alpha_k^{+} \alpha_l^{+} |gs> -$$

$$- \sum \varphi_{st} \xi_{ijkl} \alpha_s^{+} \alpha_t^{+} \alpha_i^{+} \alpha_j^{+} \alpha_k^{+} \alpha_l^{+} |gs> .$$

Boson type approximation

$$[\alpha_j\alpha_i, \alpha_s^+\alpha_t^+] = \delta_{is}\delta_{jt} - \delta_{it}\delta_{js} -$$

$$-\delta_{is}\alpha_t^+\alpha_j + \delta_{it}\alpha_s^+\alpha_j + \delta_{js}\alpha_t^+\alpha_i - \delta_{jt}\alpha_s^+\alpha_i.$$

$$< gs|[\alpha_j\alpha_i, \alpha_s^+\alpha_t^+]|gs >= \delta_{is}\delta_{jt} - \delta_{it}\delta_{js}.$$

$$\left[H, B^{+}\right] = \omega B^{+}$$

$$\sum_{s,t}(E_s + E_t)\psi_{st}\alpha_s^{+}\alpha_t^{+} + \sum_{s,t}(E_s + E_t)\varphi_{st}\alpha_t\alpha_s -$$

$$-2\kappa\Gamma_{RPA}\sum_{s,t} f_{st}(u_s v_t + u_t v_s)(\alpha_s^{+}\alpha_t^{+} + \alpha_t\alpha_s) =$$

$$= \omega\sum_{s,t}(\psi_{st}\alpha_s^{+}\alpha_t^{+} - \varphi_{st}\alpha_t\alpha_s),$$

$$\psi_{st} = 2\kappa\Gamma_{RPA}\frac{f_{st}(u_s v_t + u_t v_s)}{E_s + E_t - \omega},$$

$$\varphi_{st} = 2\kappa\Gamma_{RPA}\frac{f_{st}(u_s v_t + u_t v_s)}{E_s + E_t + \omega}.$$

$$\frac{1}{4\kappa} = \sum_{s,t}\frac{(E_s + E_t)f_{st}^2(u_s v_t + u_t v_s)^2}{(E_s + E_t)^2 - \omega^2}.$$

$$1 = 2(\kappa\Gamma_{RPA})^2\sum_{s,t}\frac{4\omega(E_s + E_t)f_{st}^2(u_s v_t + u_t v_s)^2}{\left((E_s + E_t)^2 - \omega^2\right)^2}.$$

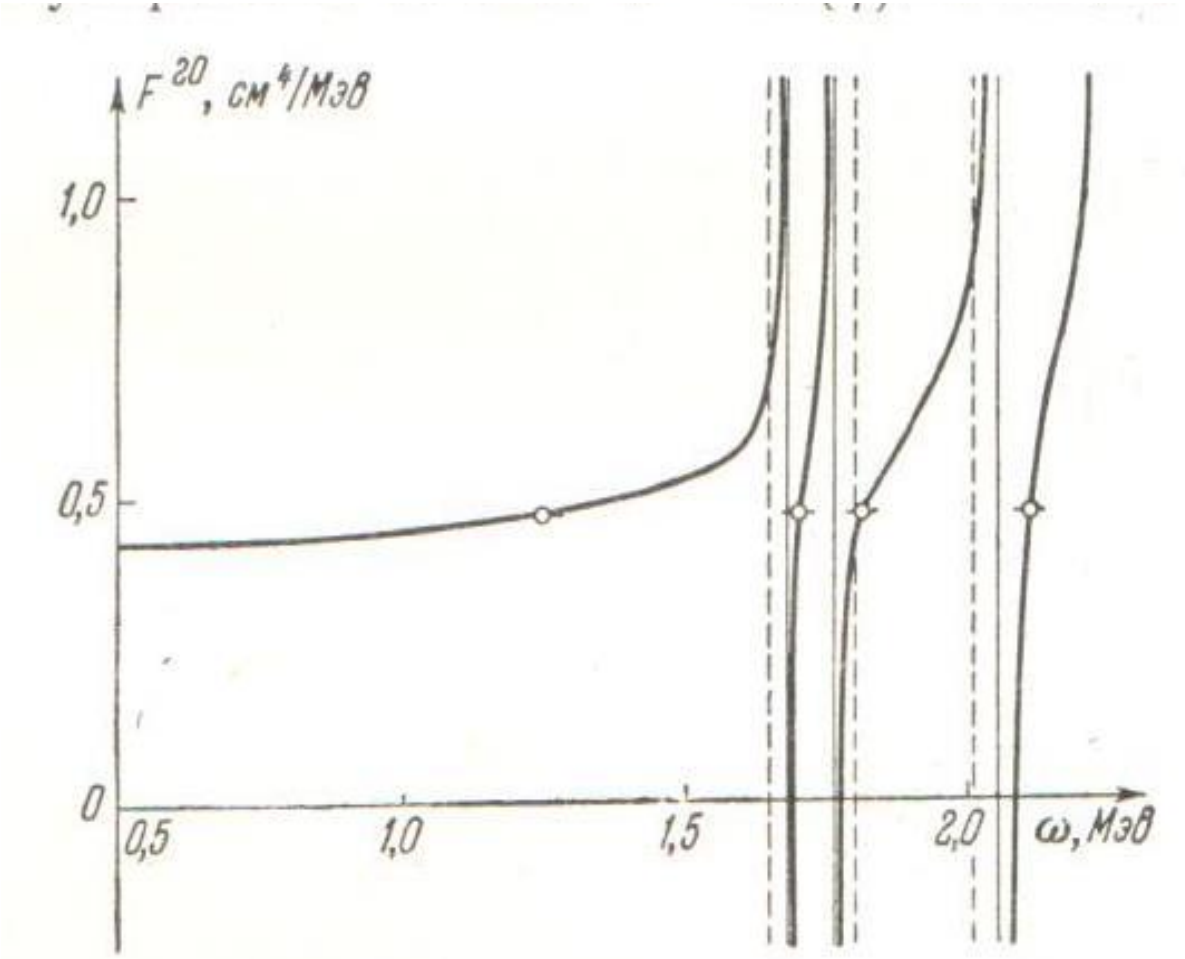
F^{20}, см⁴/МэВ
1,0
0,5
0
0,5
1,0
1,5
2,0
ω, МэВ

Nuclear mean field

$$\hat{H} = T + V_{\rm int},$$

$$T = -\frac{\hbar^2}{2m}\int d^3r \psi^+(\vec{r})\nabla^2\psi(\vec{r}),$$

$$V_{\rm int} = \frac{1}{2}\int d^3r d^3r' \rho(\vec{r})V(\vec{r}-\vec{r'})\rho(\vec{r'}),$$

$$H = \sum_{k,k'} t_{kk'} a_k^+ a_{k'} + \frac{1}{2} \sum_{i,j,k,l} v_{ijkl} a_i^+ a_j^+ a_l a_k,$$

$$t_{kk'} = \int d^3r \varphi_k^*(\vec{r}) \hat{t} \varphi_{k'}(\vec{r}),$$

$$v_{ijkl} = \int d^3r \int d^3r' \varphi_i^*(\vec{r}) \varphi_j^*(\vec{r}') v(\vec{r}, \vec{r}') \varphi_l(\vec{r}') \varphi_k(\vec{r}).$$

$$H = \sum_{k,k'} t_{kk'} < \Phi | a_k^+ a_{k'} | \Phi > + \frac{1}{2} \sum_{i,j,k,l} v_{ijkl} < \Phi | a_i^+ a_j^+ a_l a_k | \Phi >$$

$$< \Phi | a_k^+ a_{k'} | \Phi > \equiv \rho_{kk'}.$$

$$< \Phi | a_i^+ a_j^+ a_l a_k | \Phi > := $$

$$= \rho_{ik}\rho_{jl} - \rho_{il}\rho_{jk} =$$

$$< \Phi | a_i^+ a_k | \Phi >< \Phi | a_j^+ a_l | \Phi > -$$

$$- < \Phi | a_i^+ a_l | \Phi >< \Phi | a_j^+ a_k | \Phi > .$$

$$< \Phi \big| H \big| \Phi >= \sum_{k,k'} t_{kk'} \rho_{kk'} + \frac{1}{2} \sum_{i,j,k,l} v_{ijkl} (\rho_{ik} \rho_{jl} - \rho_{jk} \rho_{il}) =$$

$$= \sum_{k,k'} \left(t_{kk'} + \frac{1}{2} \sum_{j,l} (v_{kjk'l} - v_{jkk'l}) \rho_{jl} \right) \rho_{kk'}.$$

$$U_{kk'} = \frac{1}{2} \sum_{j,l} (v_{kjk'l} - v_{jkk'l}) \rho_{jl}.$$

$$< \Phi \big| H \big| \Phi >= \sum_{k,k'} (t_{kk'} + U_{kk'}) \rho_{kk'}.$$

$$H_{sp} = \sum_{k,k'} (t_{kk'} + U_{kk'}) a_k^+ a_{k'},$$

$$U_{kk'} = \frac{1}{2} \sum_{j,l} (v_{kjk'l} - v_{jkk'l}) < \Phi | a_j^+ a_l | \Phi >$$

Hartree-Fock-Bogoliubov

$$< \Phi|a_i^+ a_j^+ a_l a_k|\Phi >=< \Phi|a_i^+ a_k|\Phi >< \Phi|a_j^+ a_l|\Phi > -$$
$$- < \Phi|a_i^+ a_l|\Phi >< \Phi|a_j^+ a_k|\Phi > .$$

$$< \Phi|a_i^+ a_j^+ a_l a_k|\Phi >=< \Phi|a_i^+ a_k|\Phi >< \Phi|a_j^+ a_l|\Phi > -$$
$$- < \Phi|a_i^+ a_l|\Phi >< \Phi|a_j^+ a_k|\Phi > +$$
$$+ < \Phi|a_i^+ a_j^+|\Phi >< \Phi|a_l a_k|\Phi > .$$

$$H_{sqp} = \sum_{k,k'} (t_{kk'} + U_{kk'}) a_k^+ a_{k'} +$$

$$+\frac{1}{4} \sum_{i,j,k,l} v_{ijkl} (< \Phi|a_l a_k|\Phi > a_i^+ a_j^+ + < \Phi|a_i^+ a_j^+|\Phi > a_l a_k),$$

$$H = \Sigma\, t\, a^{+}a + \Sigma\, V\, a^{+}a\, a^{+}a$$

$$\langle H \rangle = \Sigma\, t \langle a^{+}a \rangle + \Sigma\, V \langle a^{+}a \rangle \langle a^{+}a \rangle$$

$$= \Sigma (T + \Sigma\, V \langle a^{+}a \rangle) \langle a^{+}a \rangle$$

$$H \rightarrow H_{sp} = \Sigma (T + \Sigma\, V \langle a^{+}a \rangle)\, a^{+}a$$

SU(6) symmetry in the nuclear structure model. Interacting boson model

From the shell model point of view collective vibrational states are superpositions of the large number of the particle-hole excitations

To treat them in the harmonic approximation RPA has been invented. Inclusion of the anharmonic effects or, especially, treatment of the transitional nuclei nrequires shell model consideration in a very large configurational space which is cumbersome. This creates a need in a simplified model which, however, should take into account Pauli principle, in some way.

Application of the Bohr-Mottelson model to consideration of the transitional nuclei requires too many parameters.

We know, however, that usually introduction of symmetry into consideration reduces the number of parameters in the models!

What was known at the beginning of 70^{th}?

- Quasirotational bands in nuclei from vibrational to rotational limits:

  ^{166}Er – rotor

  118Cd – vibrator

  Large variety of transitional nuclei.

  $R_{4/2}=E(4^+_1)/E(2^+_1)$:

^{146}Gd	^{148}Gd	^{150}Gd	^{152}Gd	^{154}Gd	^{156}Gd	^{158}Gd	^{160}Gd
1.33	1.81	2.02	2.19	3.02	3.24	3.29	3.30

$$B^{+(i)}_{2\mu} = \sum_{st} \left(\psi^{(i)}_{st} (\alpha^{+}_{s} \alpha^{+}_{t})_{2\mu} - (-1)^{\mu} \varphi^{(i)}_{st} (\alpha_{s} \alpha_{t})_{2-\mu} \right)$$

$$\left[B^{(1)}_{2\mu} , B^{+(1)}_{2\nu} \right]$$

$$\left[\left[B^{(1)}_{2\mu} , B^{+(1)}_{2\nu} \right], B^{+(1)}_{2\lambda} \right] =$$

$$= \sum_{K} C^{(K)}_{\mu\nu\lambda\eta} \, B^{+(K)}_{2\eta}$$

$$\approx C^{(1)}_{\mu\nu\lambda\eta} \, B^{+(1)}_{2\eta}$$

$$B^{(1)}_{2\mu} \rightarrow 5 \quad , \quad B^{+(1)}_{2\mu} \rightarrow 5$$

$$\left[B^{(1)}_{2\mu} , B^{+(1)}_{2\nu} \right] \rightarrow 25$$

$$5 + 5 + 25 = 35$$

$$SU(6) \quad !$$

Representation

$$B^{+(1)}_{2\mu} \to d^{+}_{2\mu} \sqrt{N - \sum_{\nu} d^{+}_{2\nu} d_{2\nu}}$$

$$[B^{(1)}_{2\mu}, B^{+(1)}_{2\nu}] \to d^{+}_{2\nu} d_{2\mu}$$

or

$$B^{+(1)}_{2\mu} \to d^{+}_{2\mu} S$$

$$[B^{+(1)}_{2\mu}, B^{+(1)}_{2\nu}] \to d^{+}_{2\nu} d_{2\mu}$$

$$S^{+} S + \sum_{\nu} d^{+}_{2\nu} d_{2\nu} = N$$

$$[S, S^{+}] = 1 \quad , \quad [d_{2\nu}, d^{+}_{2\mu}] = \delta_{\mu\nu}$$

$$[d_{2\mu}, d_{2\nu}] = 0$$

$$H^B = E_0^{(N)} + \varepsilon \hat{N}_d + V$$

$$V = \frac{1}{2} \sum_{L=0,2,4} c_L([d^\dagger d^\dagger]^{(L)} \cdot [\tilde{d}\tilde{d}]^{(L)})$$
$$+ \frac{1}{\sqrt{2}} y\{([d^\dagger d^\dagger]^{(2)} \cdot [s\tilde{d}]^{(2)}) + \text{h.c.}\}$$
$$+ \frac{1}{2} w\{([d^\dagger d^\dagger]^{(0)}[ss]^{(0)}) + \text{h.c.}\},$$

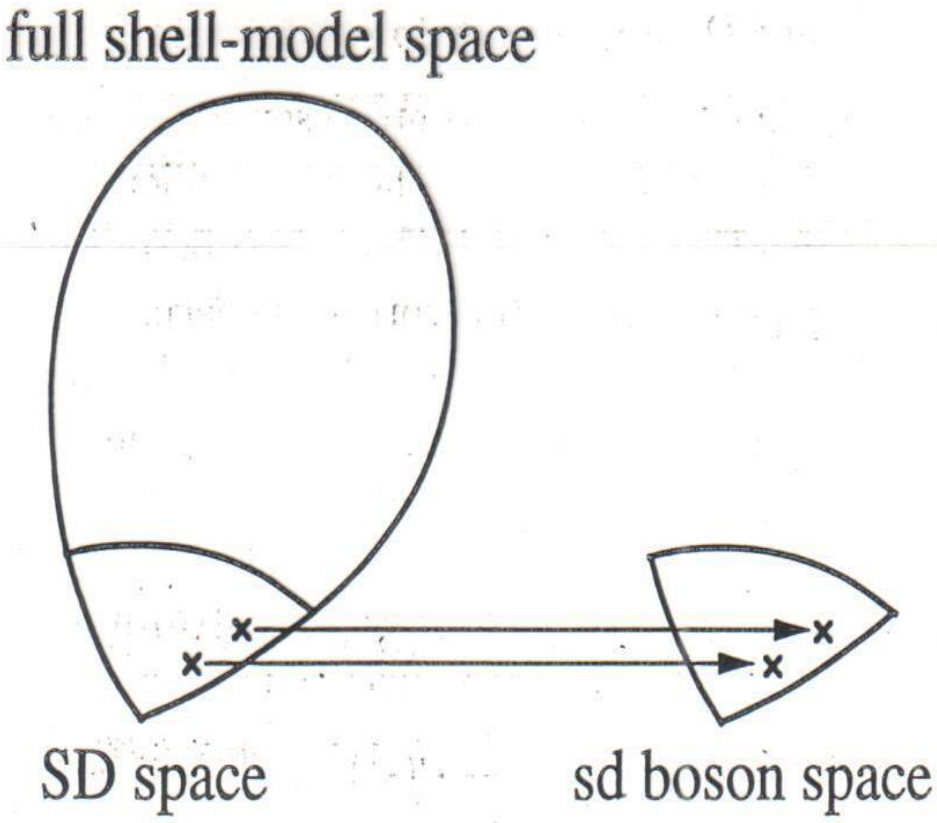

Fig. 2. Mapping from the SD subspace of the full shell-model space onto the sd boson space.

This algebra has subgroups

1. $SU(5)$

$d_\mu^+ d_{\mu'}$ (25)

harmonic vibrator

$n_d \equiv \sum_\mu d_\mu^+ d_\mu = \text{const}$

2. $SU(3)$, $\overline{SU(3)}$

rotor

$I_\mu \sim (d^+ d)_{1\mu}$

$Q_{2\mu} = d_\mu^+ s + s^+ d_{-\mu}(-)^\mu \pm \frac{\sqrt{7}}{2}(d^+ d)_{2\mu}$ (8)

3. $O(6)$

$(d^+ d)_{1\mu}$, $(d^+ d)_{3\mu}$, $d_\mu^+ s + s^+ (-)^\mu d_{-\mu}$ (15)

γ-unstable nucleus

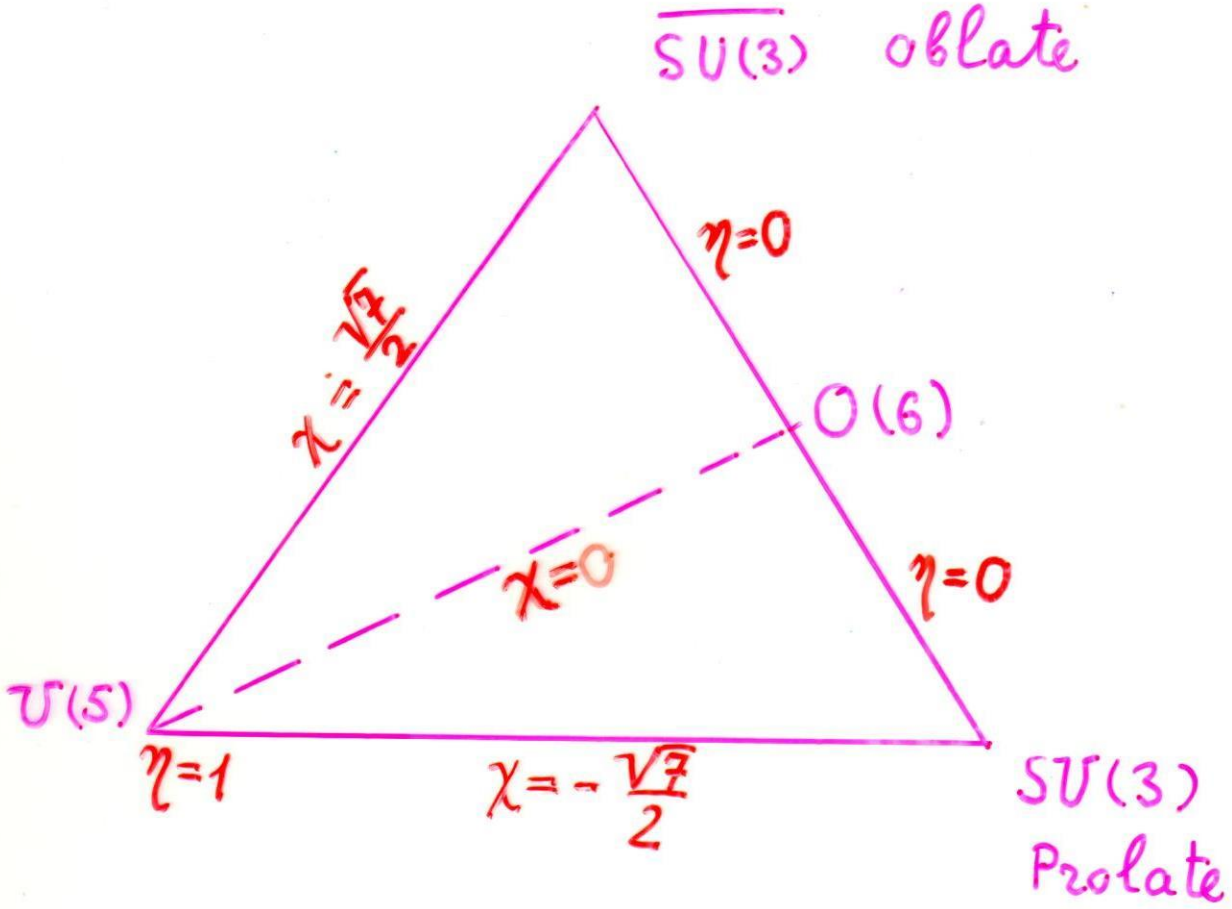
SU(3) oblate
η=0
χ = √2
O(6)
χ=0
η=0
U(5)
η=1
χ = -√2
SU(3)
Prolate

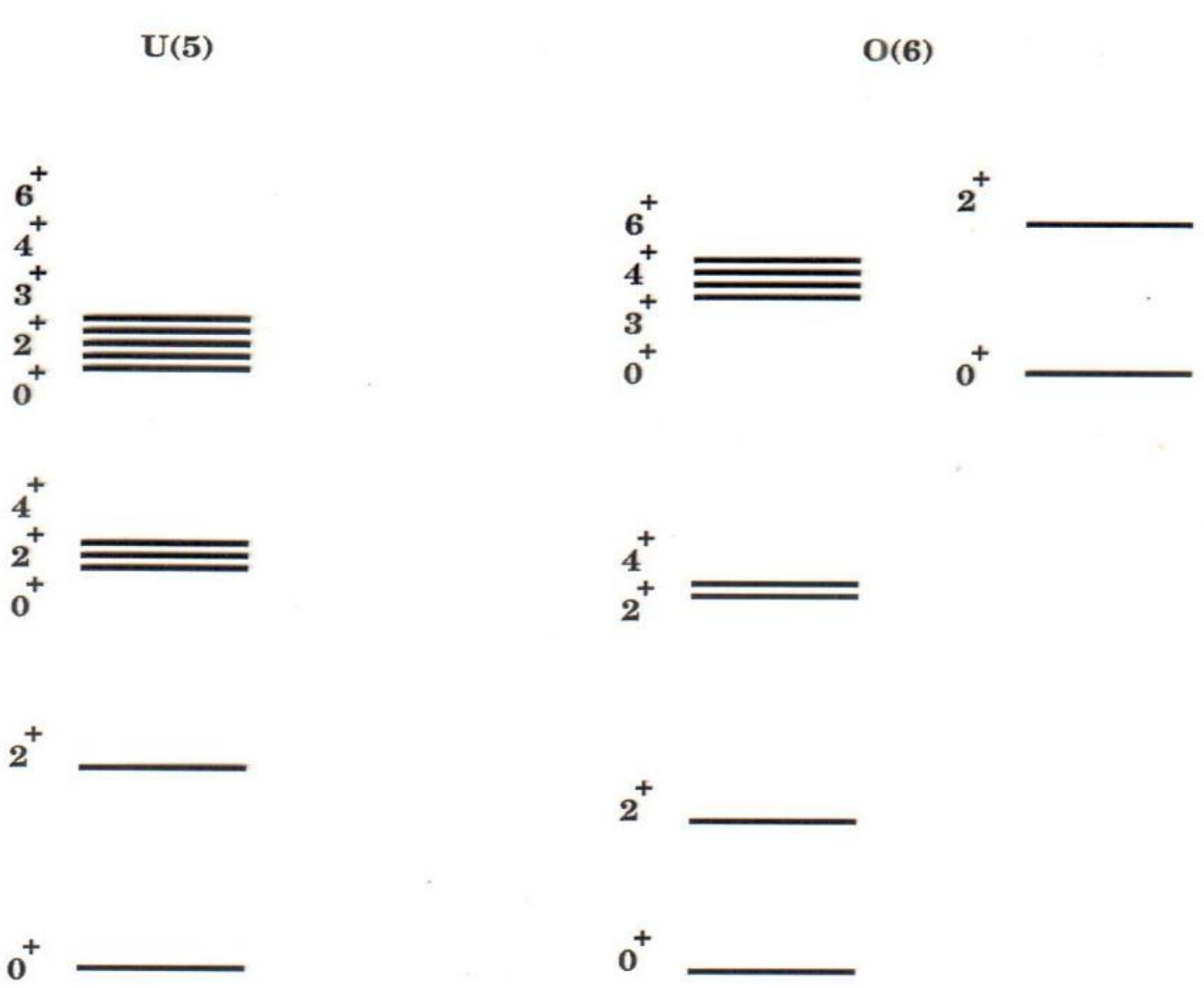
U(5)
O(6)
6+
4+
3+
2+
0+
4+
2+
0+
2+
0+
6+
4+
3+
0+
4+
2+
2+
0+
2+
0+

или два β-фонона ($K = 0$), или два γ-фонона ($K = 0, 4$), или один

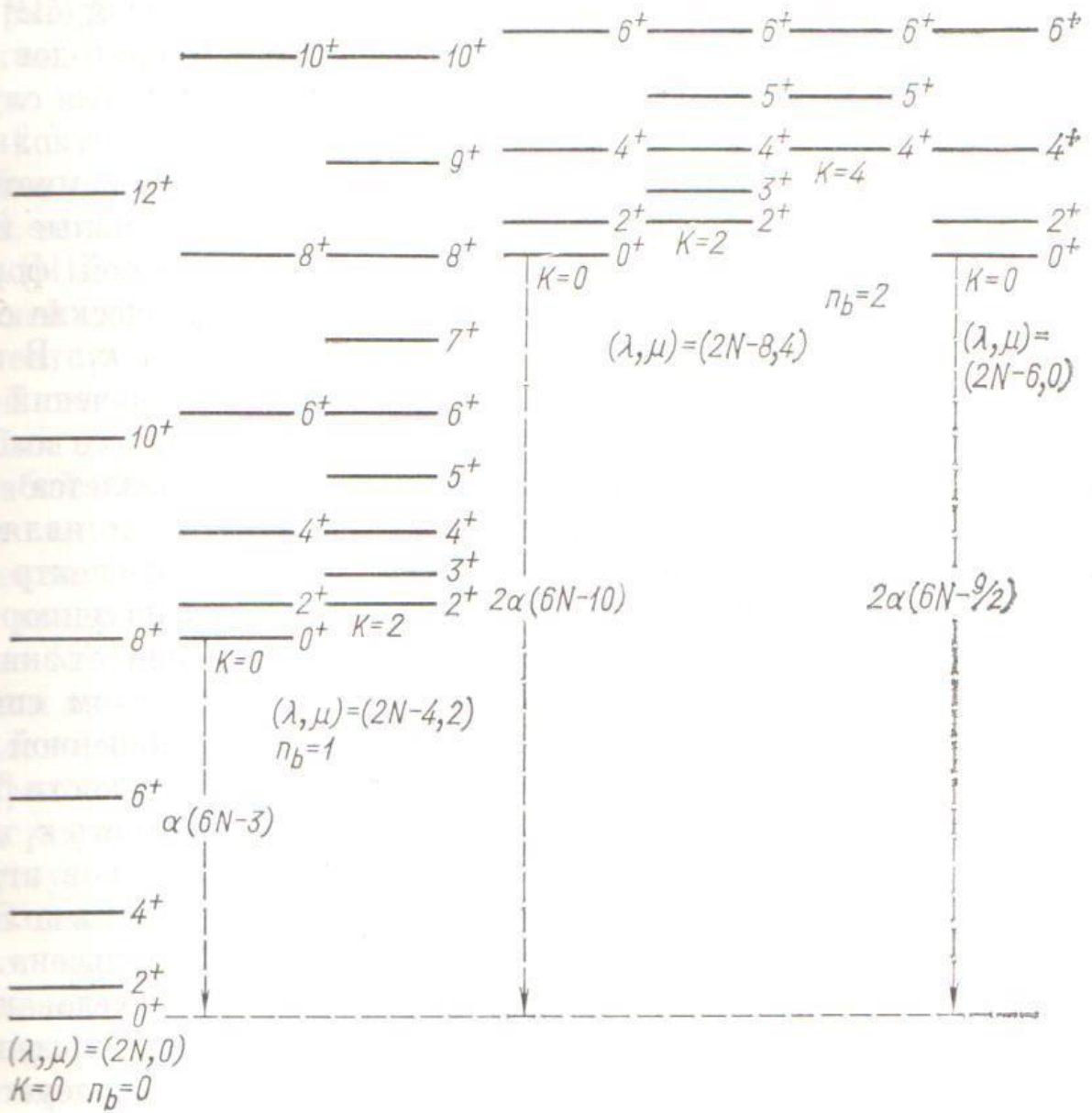

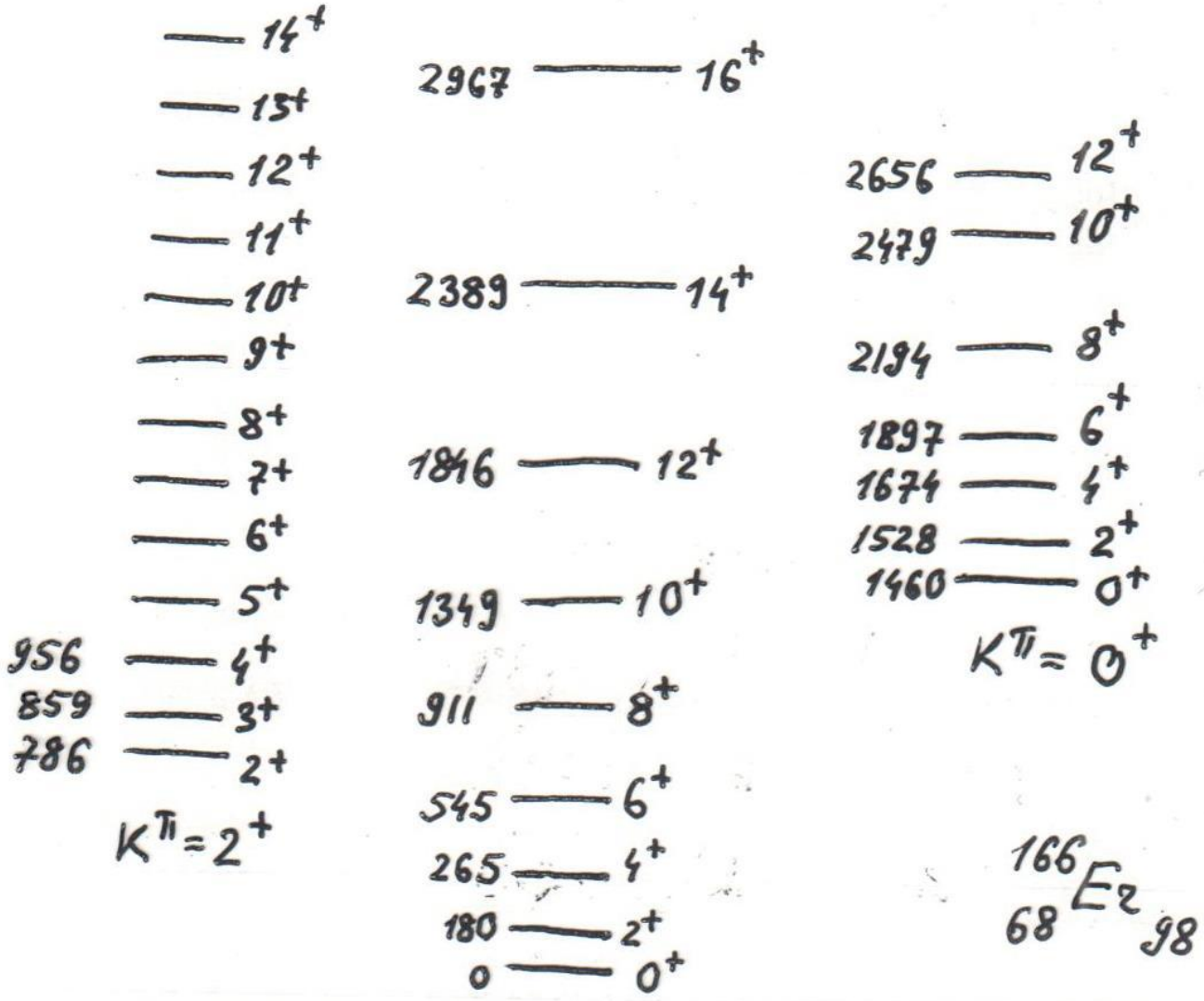
14+
15+
12+
11+
10+
9+
8+
7+
6+
5+
956 4+
859 3+
786 2+
K^π = 2+
2967 16+
2389 14+
1846 12+
1349 10+
911 8+
545 6+
265 4+
180 2+
0 0+
G.S.B.
2656 12+
2479 10+
2194 8+
1897 6+
1674 4+
1528 2+
1460 0+
K^π = 0+
166 68 Er 98

$$H = \sum_{k=1}^{A} \left(\frac{\bar{p}_k^2}{2m} + \frac{1}{2} m\omega^2 \bar{r}_k^2 \right)$$

$$x = \sqrt{\frac{\hbar}{2m\omega}} \left(b_x^+ + b_x \right)$$

$$\frac{d}{dx} = \sqrt{\frac{m\omega}{2\hbar}} \left(b_x - b_x^+ \right)$$

$$H = \hbar\omega \left(b_x^+ b_x + b_y^+ b_y + b_z^+ b_z + 3/2 \right)$$

$$\hat{n}_x \qquad \hat{n}_y \qquad \hat{n}_z$$

$$\hat{N} \equiv \hat{n}_x + \hat{n}_y + \hat{n}_z$$

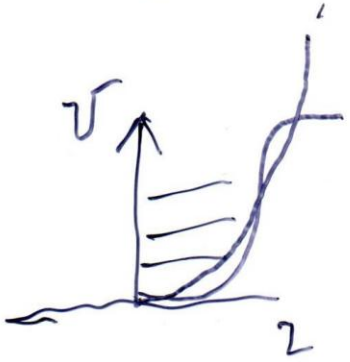

. . . . . .

	0	0	1
1	0	1	0
	1	0	0

0	0	0	0
N	n_x	n_y	n_z

$\alpha + \alpha \rightarrow {}^{8}Be$

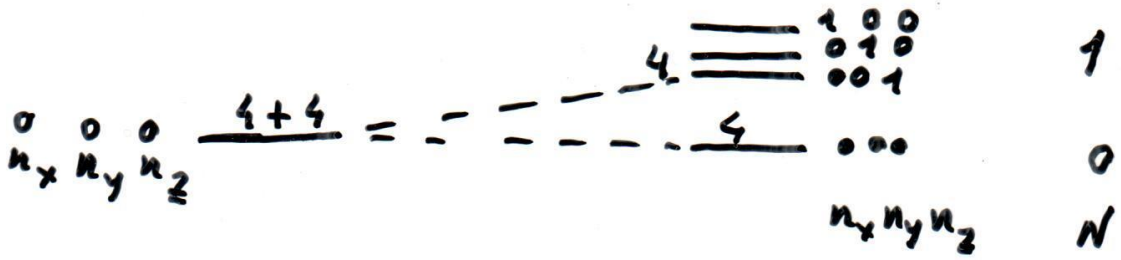

$\alpha + {}^{8}Be \rightarrow {}^{12}C$

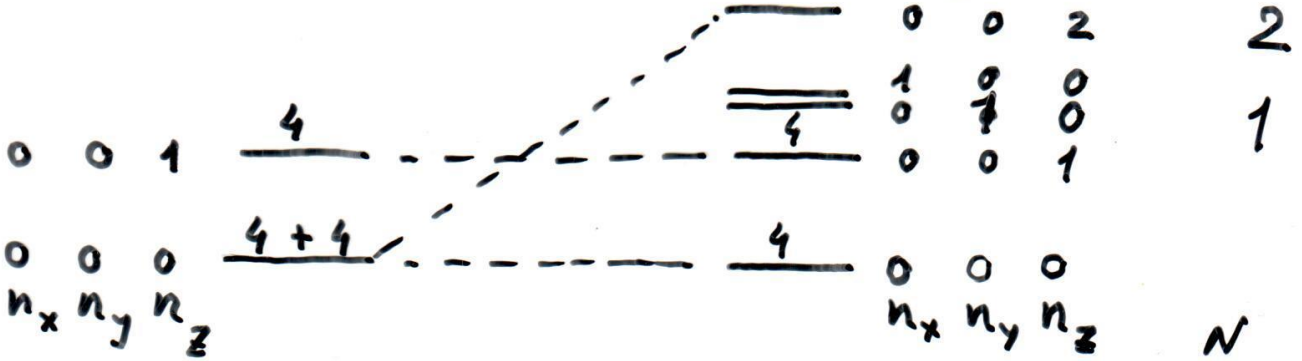

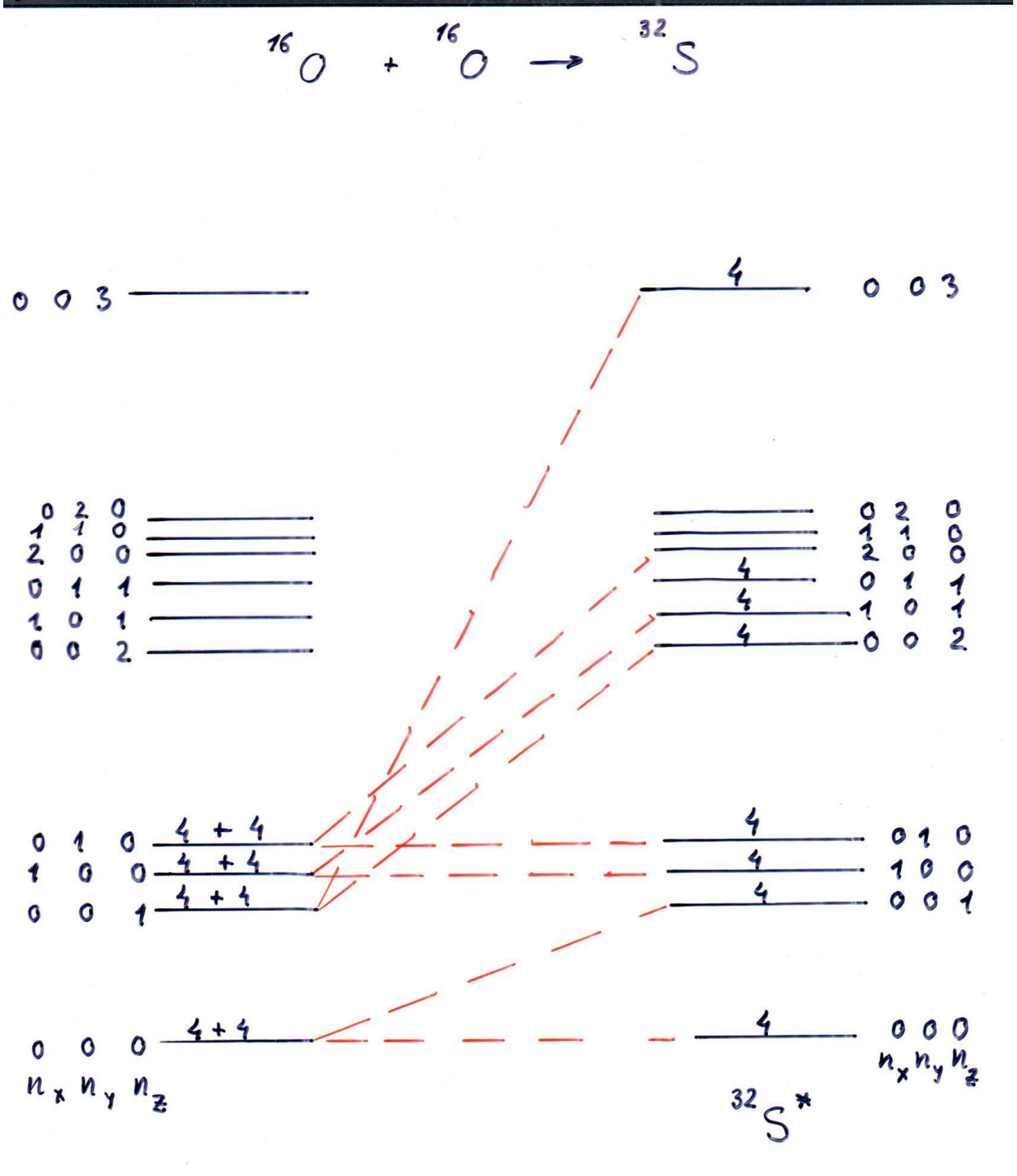
16O + 16O → 32S
0 0 3
4
0 0 3
0 2 0
1 1 0
2 0 0
0 1 1
1 0 1
0 0 2
4
4
4
0 2 0
1 1 0
2 0 0
0 1 1
1 0 1
0 0 2
0 1 0
1 0 0
0 0 1
4 + 4
4 + 4
4 + 4
4
4
4
0 1 0
1 0 0
0 0 1
0 0 0
4 + 4
4
0 0 0
nx ny nz
nx ny nz
32S*

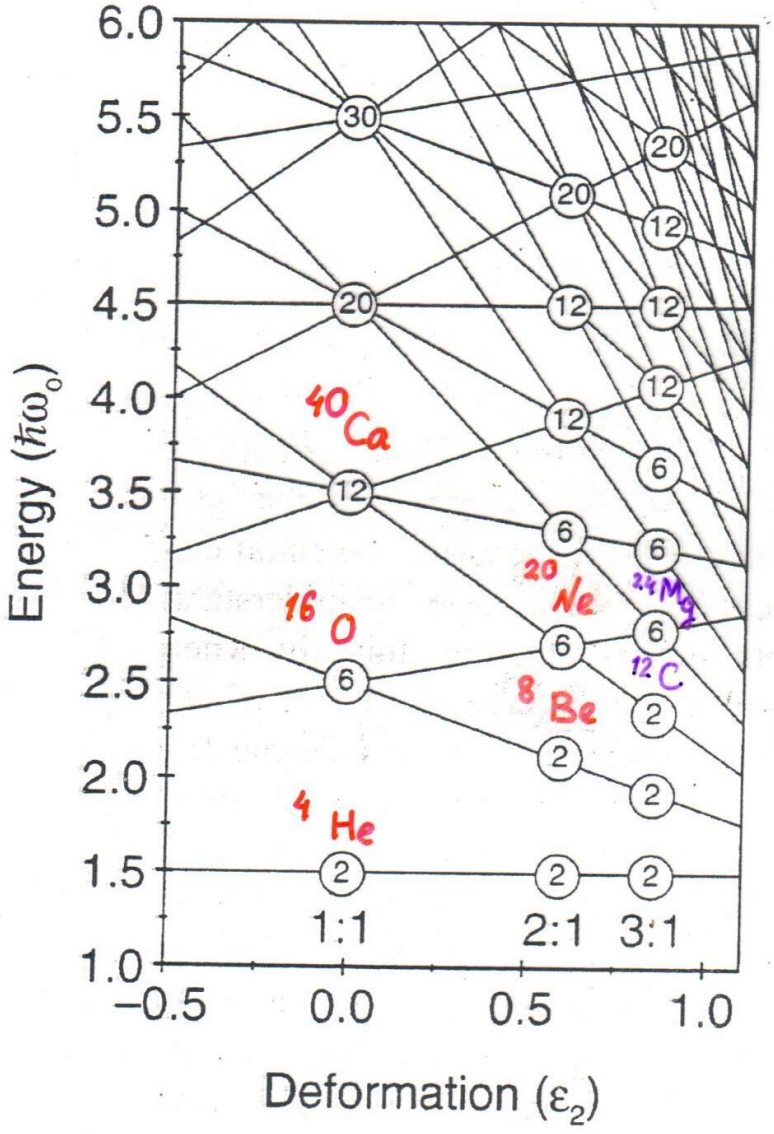

$^{8}Be \rightarrow {}^{4}He - {}^{4}He$

$^{20}Ne \rightarrow {}^{16}O - {}^{4}He$

$^{12}C \rightarrow {}^{4}He - {}^{4}He - {}^{4}He$

$^{24}Mg \rightarrow {}^{4}He - {}^{16}O - {}^{4}He$

The deformation process can be viewed as the division of the original spherical potential into a series of small potentials aligned along the deformation axis.

Figure 1. The deformed-harmonic oscillator energy levels plotted as a function of the quadrupole deformation (ϵ_2). The numbers shown inside the circles indicate the degeneracy of the levels for the various crossing points.

It is seen that the configuration reached from $^{16}O + ^{16}O$ is in fact the "ground state" of the superdeformed ^{32}S nucleus. Thus, the Harvey prescription provides the connection between wave functions associated with the highly deformed minima and cluster-type configurations into which deformed states is likely to decay.

It is possible to systematically associate cluster configurations with the w.f. of the superdeformed configurations. It can be observed that all the magic numbers at the deformation of $\omega_\perp : \omega_z = 2:1$ are the sums of pairs of spherical magic numbers

Magic numbers at $\omega_\perp : \omega_z = 2:1$	Spherical magic numbers	Cluster configurations
4	2 + 2	$\alpha - \alpha$
10	8 + 2	$^{16}O - \alpha$
16	8 + 8	$^{16}O - ^{16}O$
28	20 + 8	$^{40}Ca - ^{16}O$
40	20 + 20	$^{40}Ca - ^{40}Ca$

Cluster radioactivity

1982

Oxford

$$\frac{Ra(C)Pb}{Ra(\alpha)Rn} \approx 10^{-9}$$

$$^{223}_{88}Ra \rightarrow {}^{209}_{82}Pb + {}^{14}_{6}C,$$

$$^{228}_{90}Th \rightarrow {}^{208}_{82}Pb + {}^{20}_{8}O$$

$$^{235}_{92}U \rightarrow {}^{211}_{82}Pb + {}^{24}_{10}Ne$$

$$^{235}_{92}U \rightarrow {}^{207}_{80}Hg + {}^{28}_{12}Mg$$

$$^{240}_{94}Pu \rightarrow {}^{206}_{80}Hg + {}^{34}_{14}Si$$

Dinuclear model

$$\eta = \frac{A_1 - A_2}{A_1 + A_2}$$

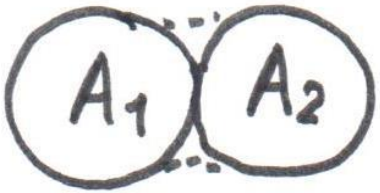

$|\eta| = 1$ if $A_1 = 0$ or $A_2 = 0$

$$|\eta_\alpha| = 1 - \frac{8}{A}$$

$$|\eta_{^8Be}| = 1 - \frac{16}{A}$$

$$H = -\frac{\hbar^2}{2}\frac{d}{d\eta}\frac{1}{B(\eta)}\frac{d}{d\eta} + U(\eta, I)$$

$$U(\eta, I) = B_1(\eta) + B_2(\eta)$$

$$+ V(R = R_m, \eta, I)$$

V is the nucleus - nucleus interaction potential

Several calculations performed for light and heavy nuclei have shown that configurations with large deformations and low-lying collective negative parity states are strongly related to clustering.

A direct consequence of the asymmetric cluster type structures is a presence of the rotational negative parity states with odd angular momenta together with positive parity states having even angular momenta. The negative parity states are shifted up with respect to the positive parity states due to the barrier penetration.

It was further shown that among different cluster configurations the only system which gives a significant contribution to the formation of the low-lying states is the α-cluster configuration

$$^{A}Z \rightarrow {}^{A-4}(Z-2) + {}^{4}He$$

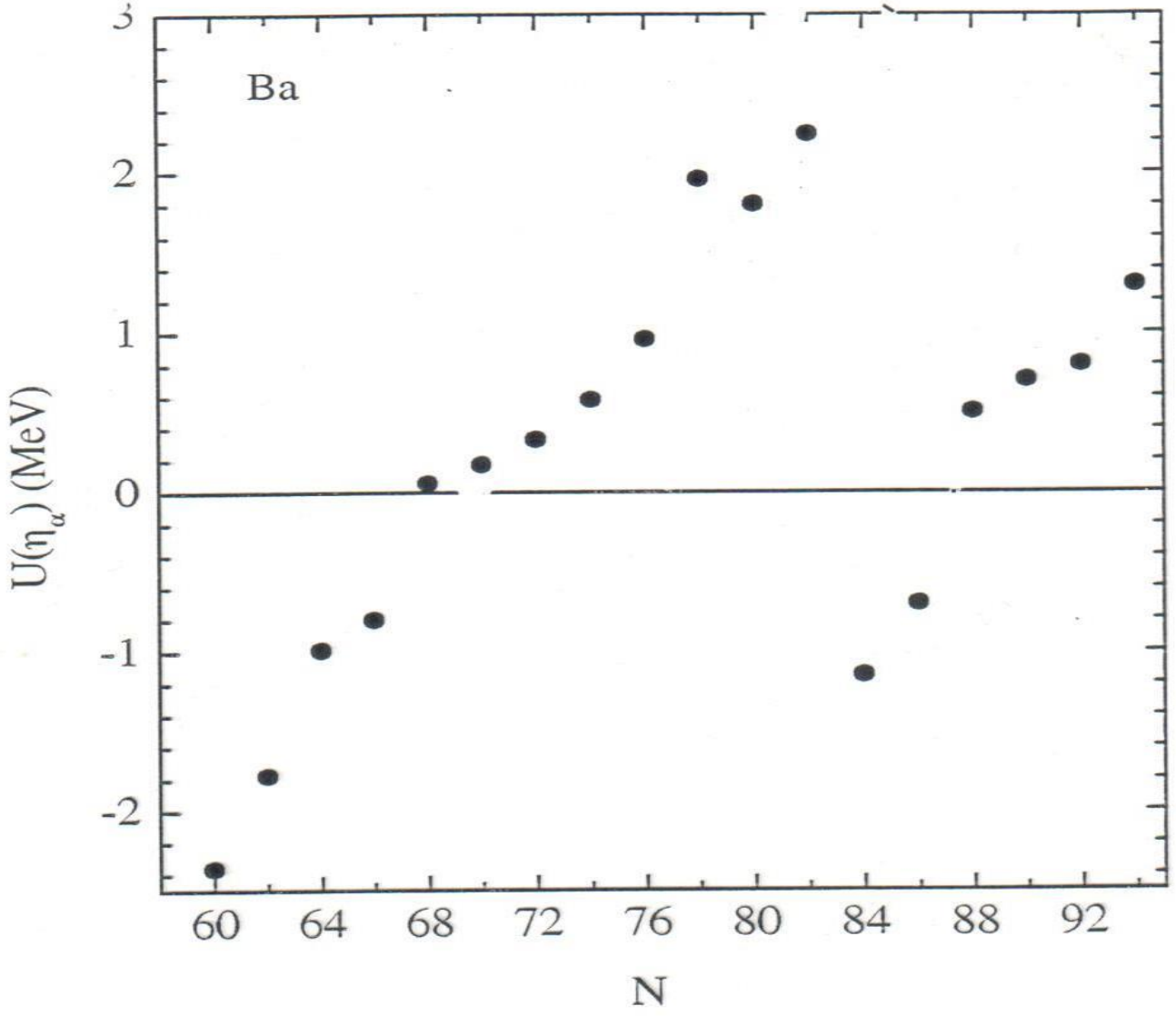
Ba
3
2
1
0
-1
-2
$U(\eta_\alpha)$ (MeV)
60
64
68
72
76
80
84
88
92
N

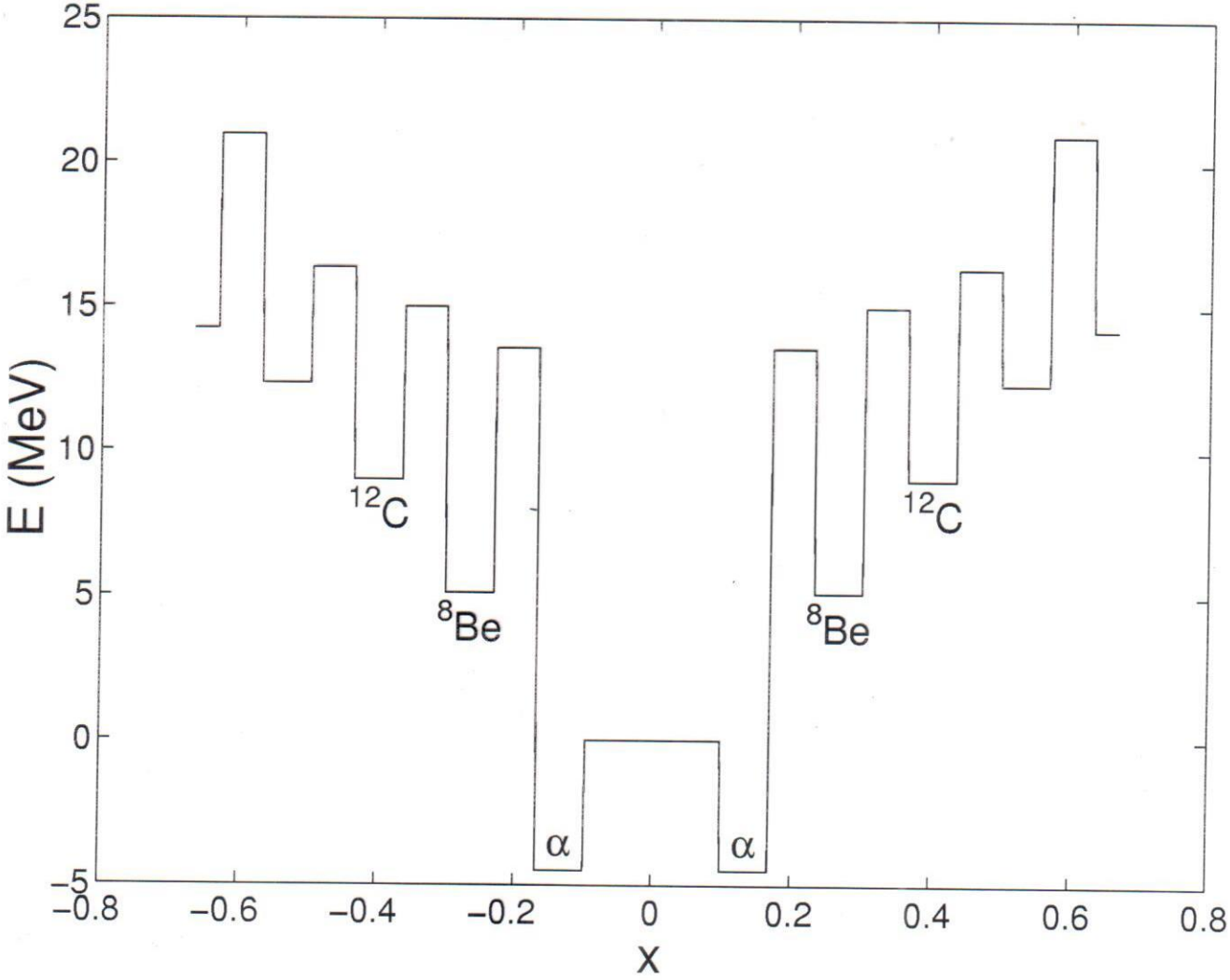
25
20
15
10
5
0
−5
E (MeV)
−0.8
−0.6
−0.4
−0.2
0
0.2
0.4
0.6
0.8
X
^{12}C
^{8}Be
α
α
^{8}Be
^{12}C

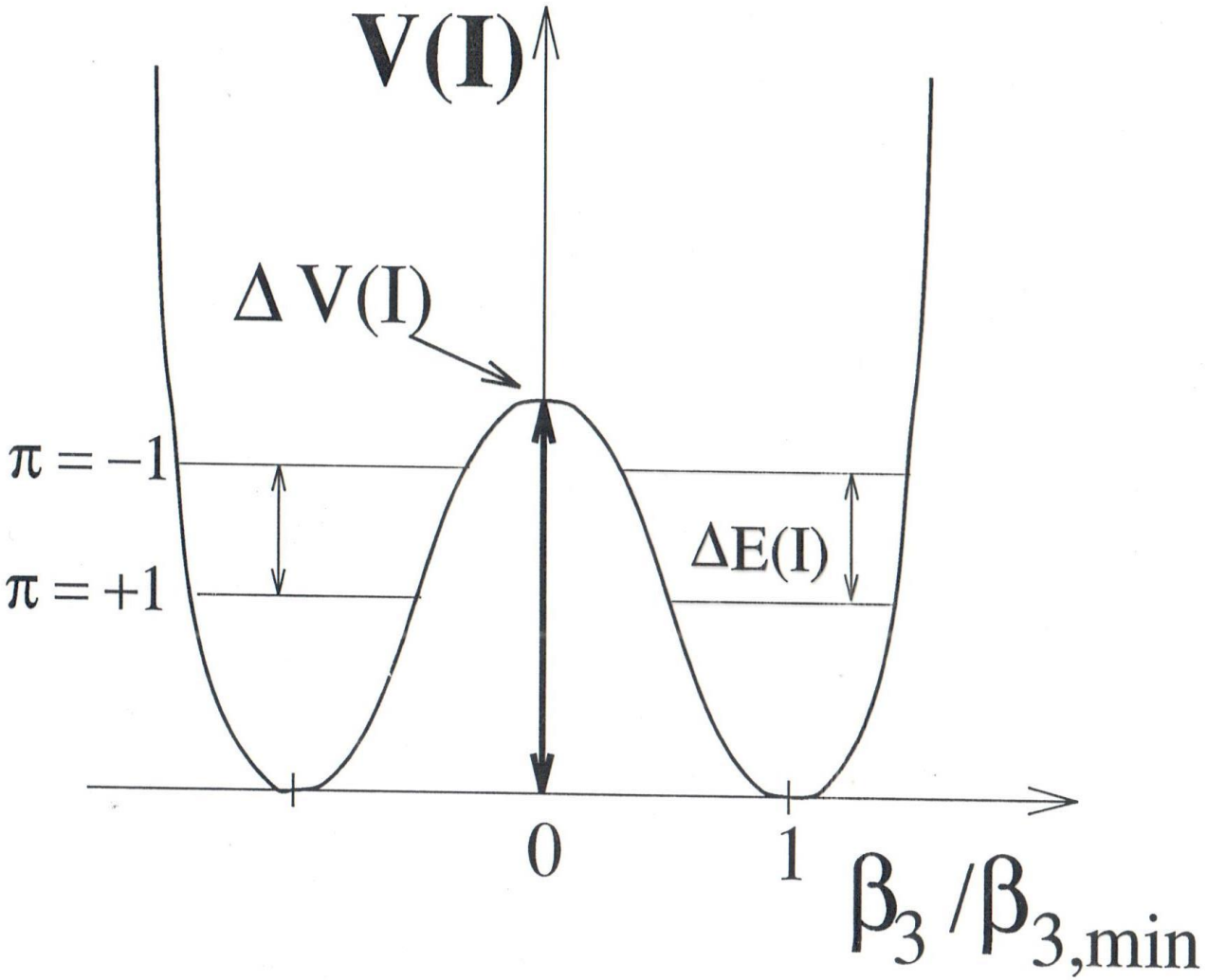
V(I)
Δ V(I)
π = −1
π = +1
ΔE(I)
0
1
β3 /β3,min

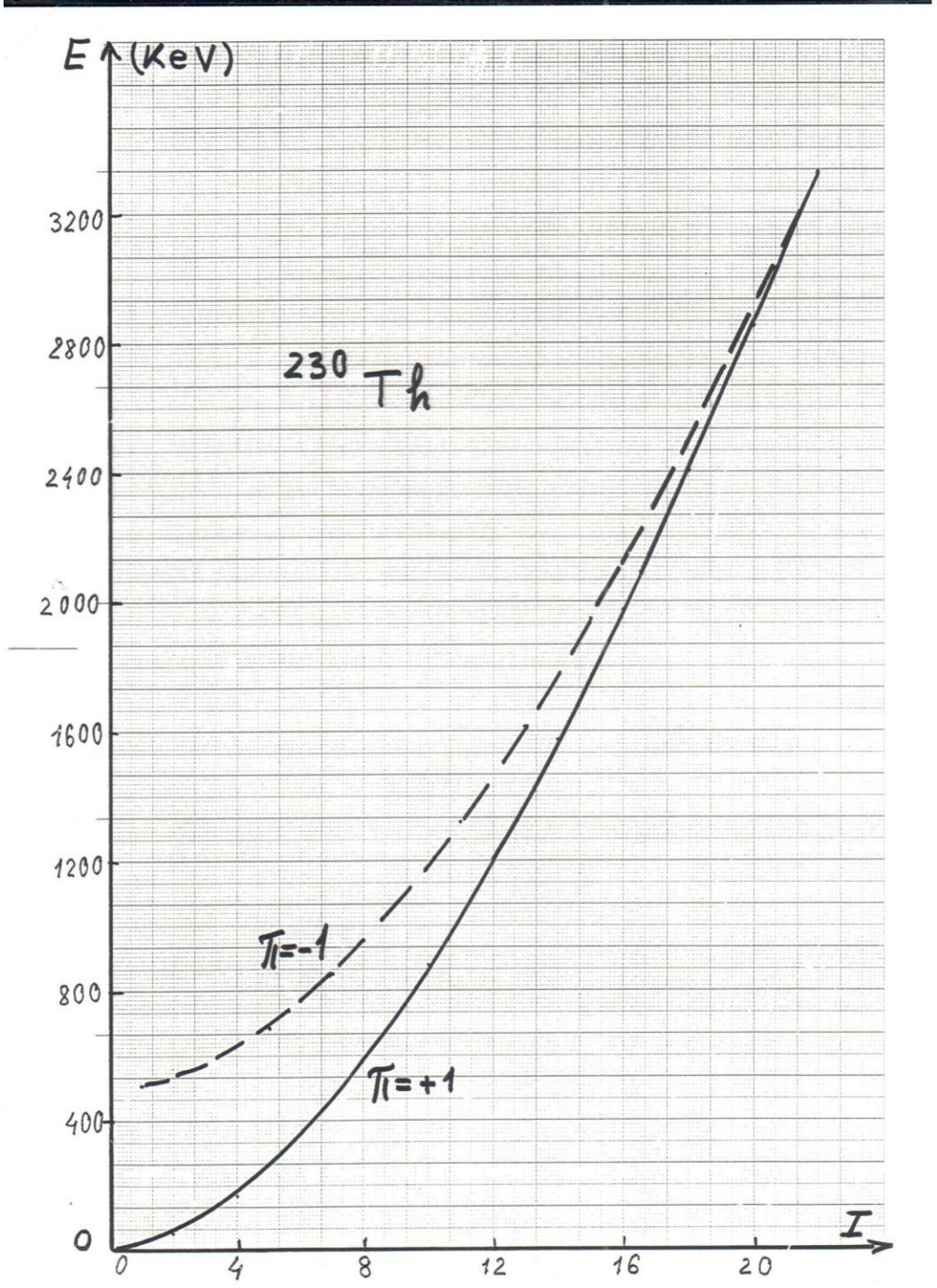
E (KeV)
3200
2800
230 Th
2400
2000
1600
1200
π=-1
800
π=+1
400
0
I
0
4
8
12
16
20

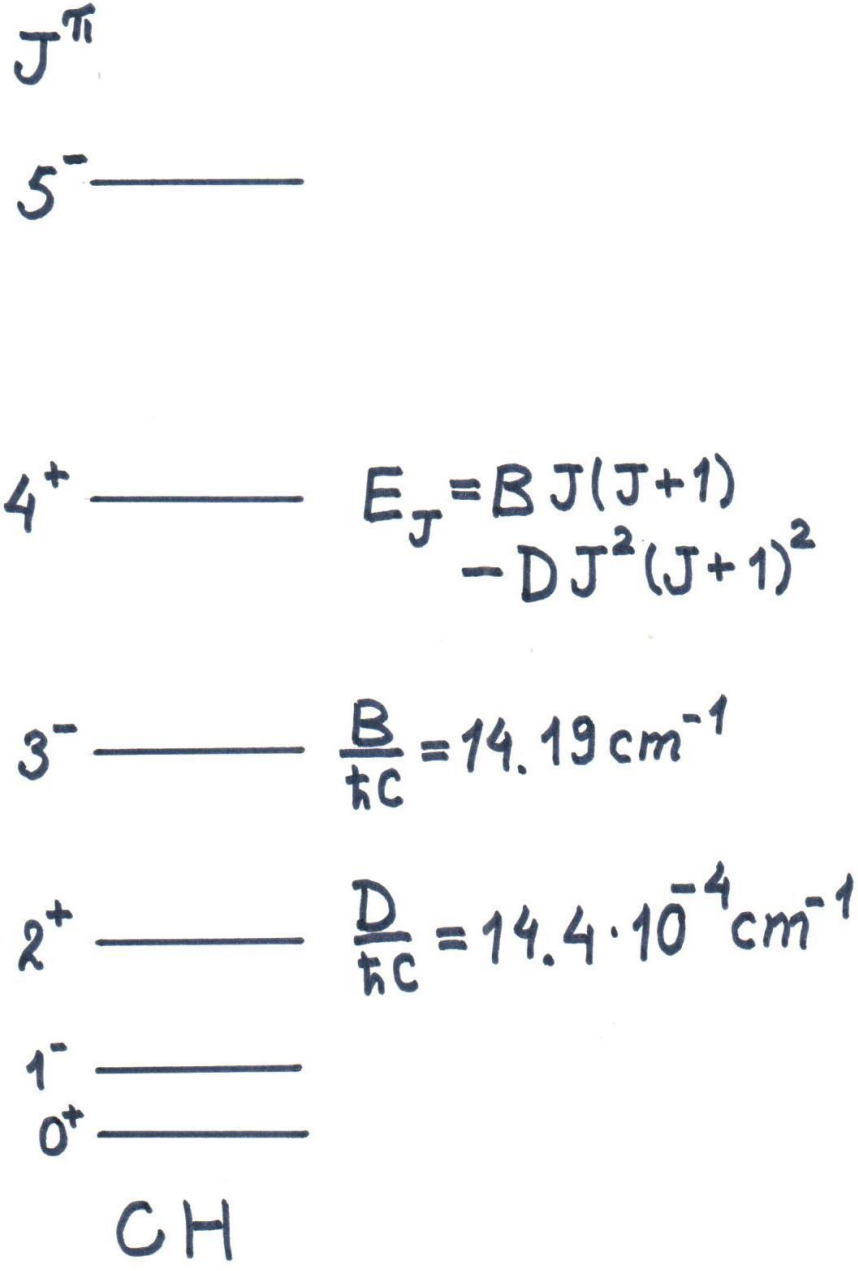
J^π
5^-
4^+
$E_J = B\,J(J+1) - D\,J^2(J+1)^2$
3^-
$\frac{B}{hc} = 14.19\ cm^{-1}$
2^+
$\frac{D}{hc} = 14.4 \cdot 10^{-4}\ cm^{-1}$
1^-
0^+
CH

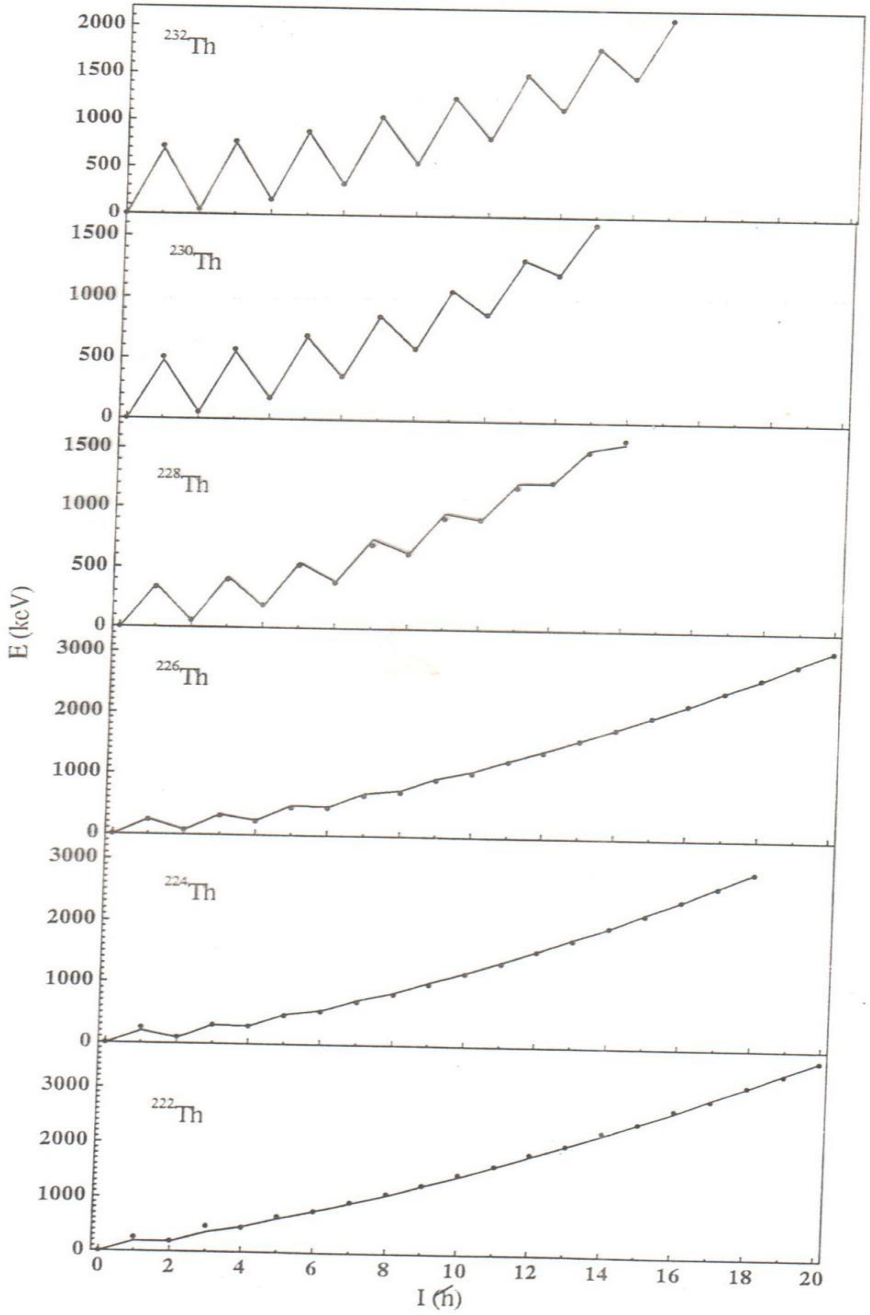
^{232}Th
^{230}Th
^{228}Th
^{226}Th
^{224}Th
^{222}Th
E (keV)
I (ħ)
0
500
1000
1500
2000
3000
0
2
4
6
8
10
12
14
16
18
20

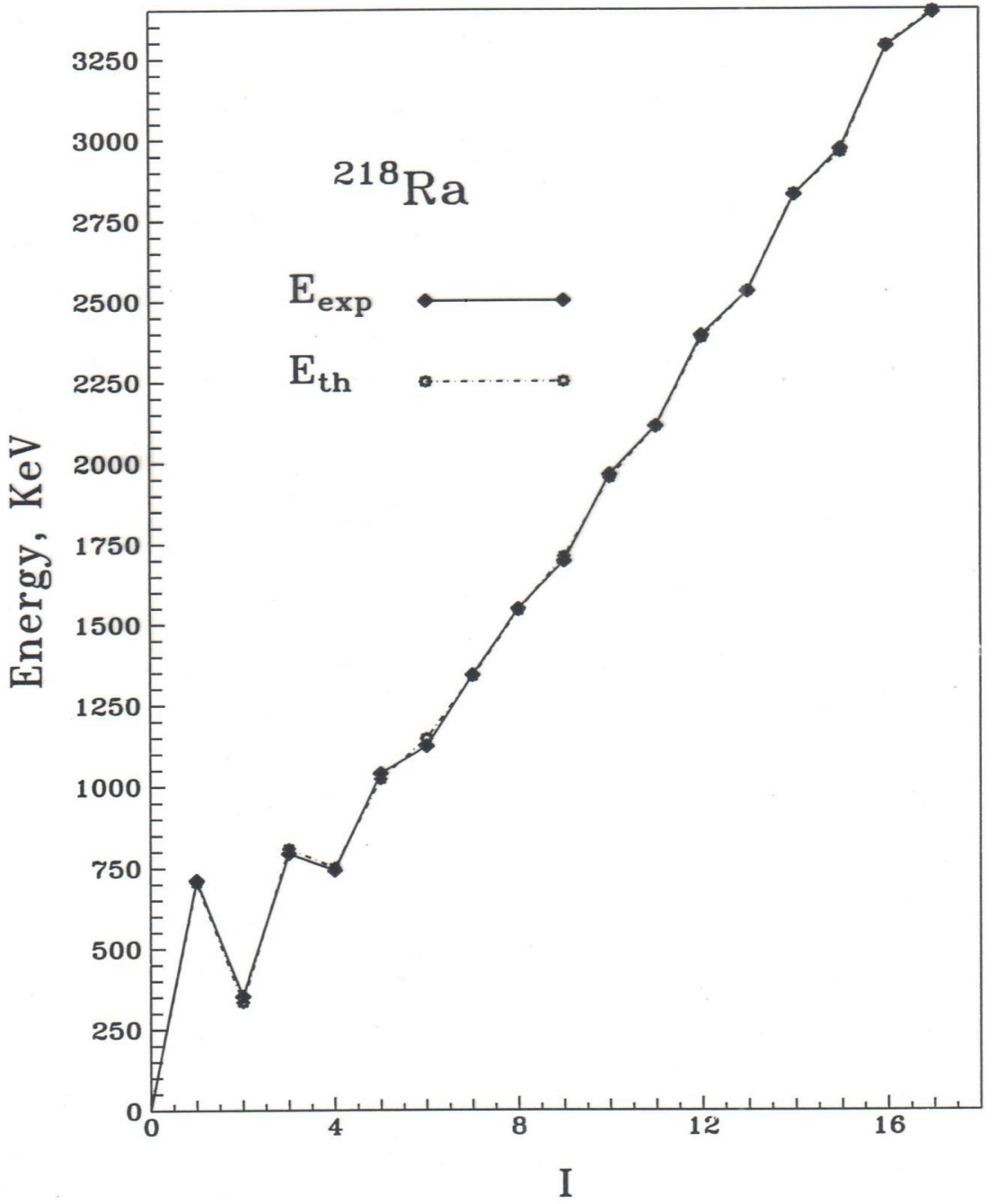
^{218}Ra
E_{exp}
E_{th}
Energy, KeV
I
0
250
500
750
1000
1250
1500
1750
2000
2250
2500
2750
3000
3250
0
4
8
12
16

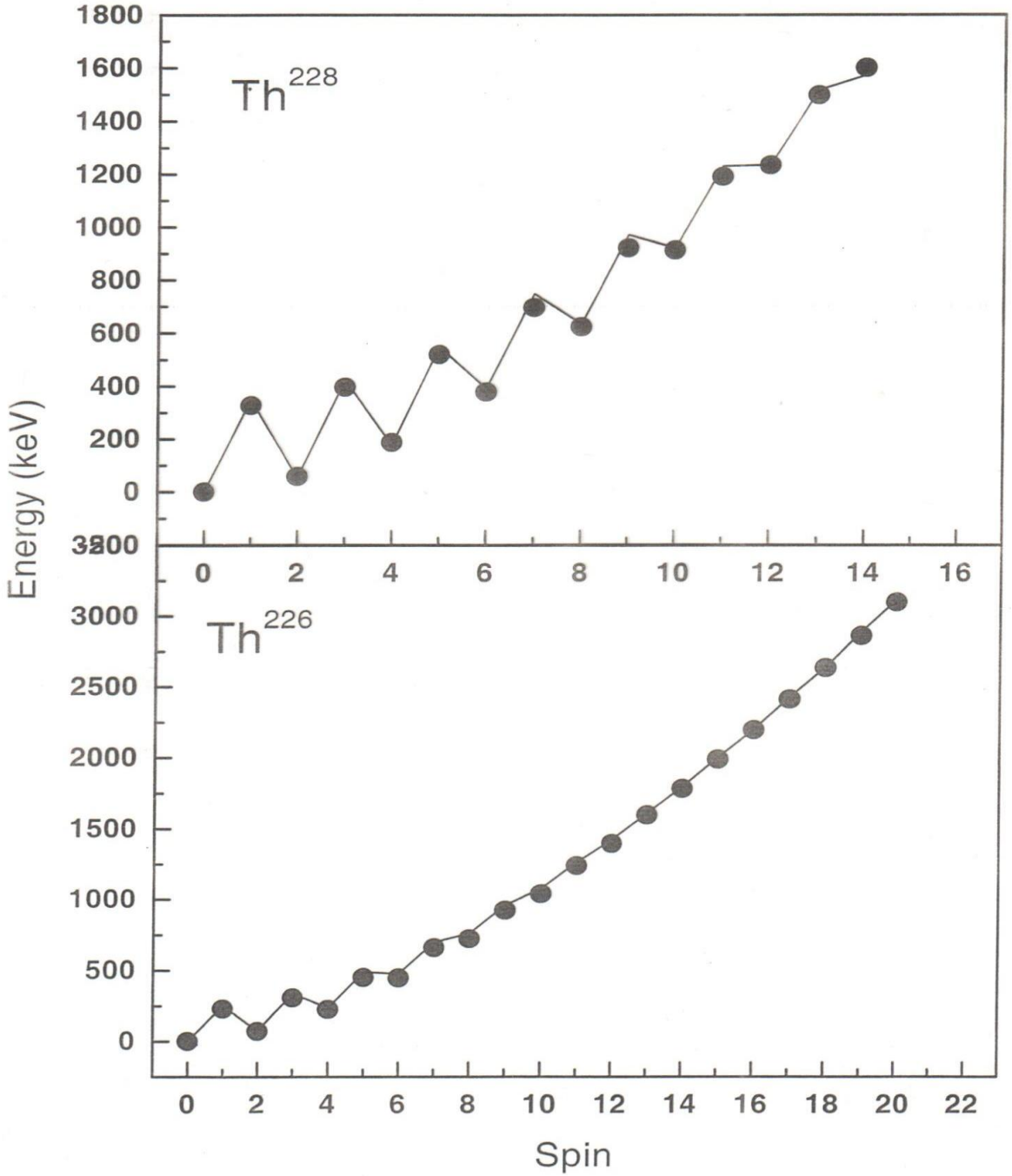
Th228
Th226
Energy (keV)
Spin
1800
1600
1400
1200
1000
800
600
400
200
0
3200
3000
2500
2000
1500
1000
500
0
0 2 4 6 8 10 12 14 16
0 2 4 6 8 10 12 14 16 18 20 22

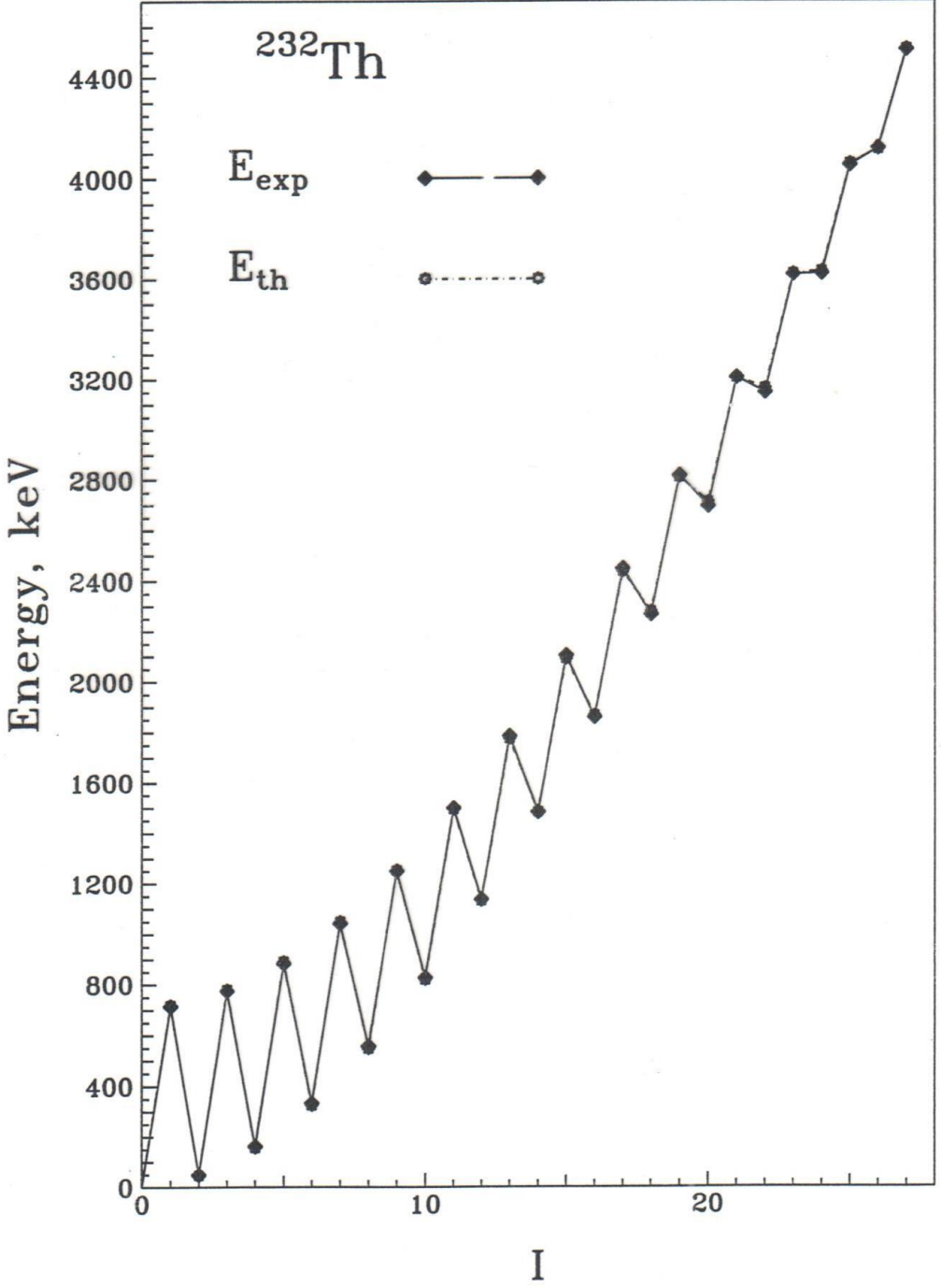
^{232}Th
E_{exp}
E_{th}
Energy, keV
0
400
800
1200
1600
2000
2400
2800
3200
3600
4000
4400
0
10
20
I

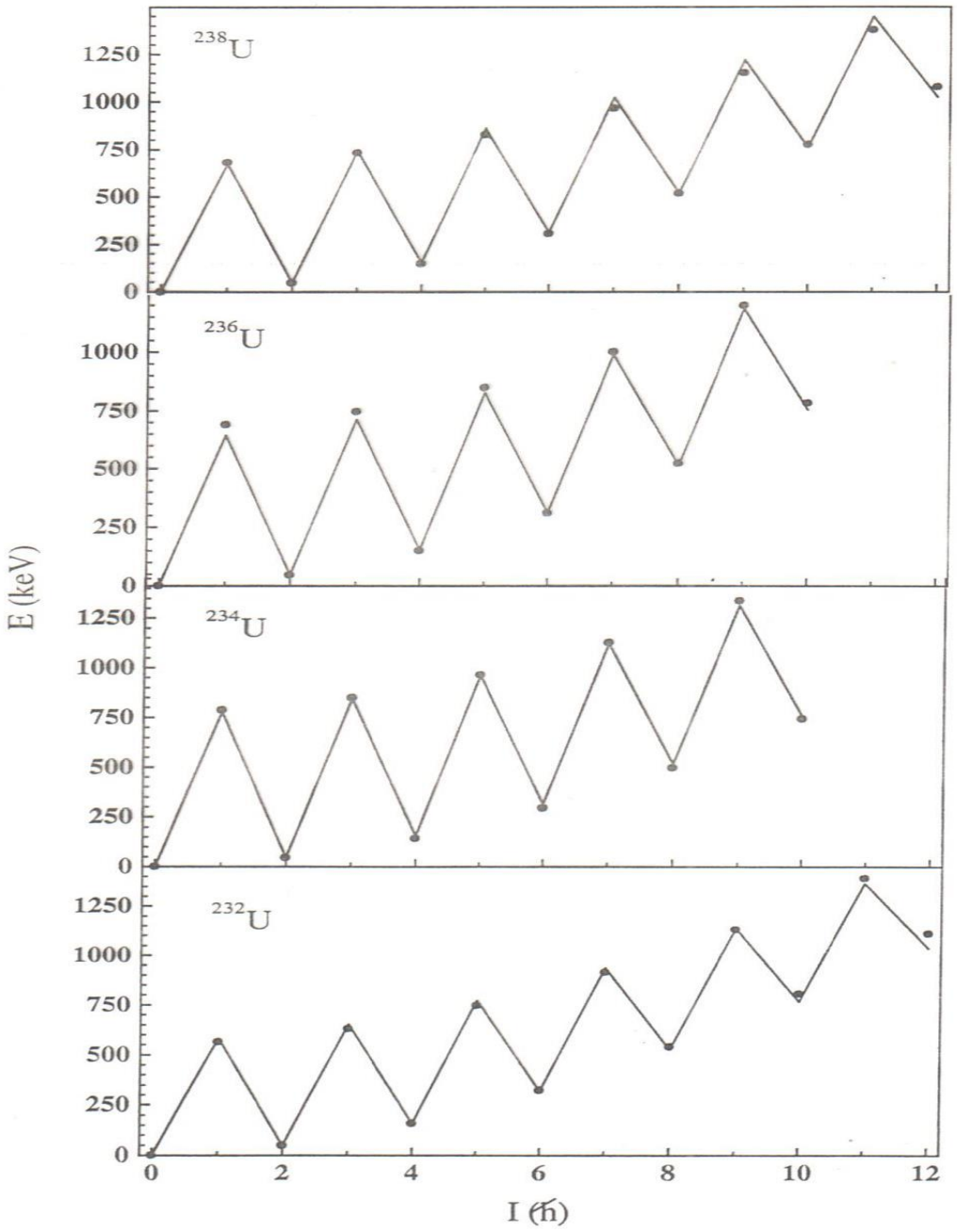

Fig.1

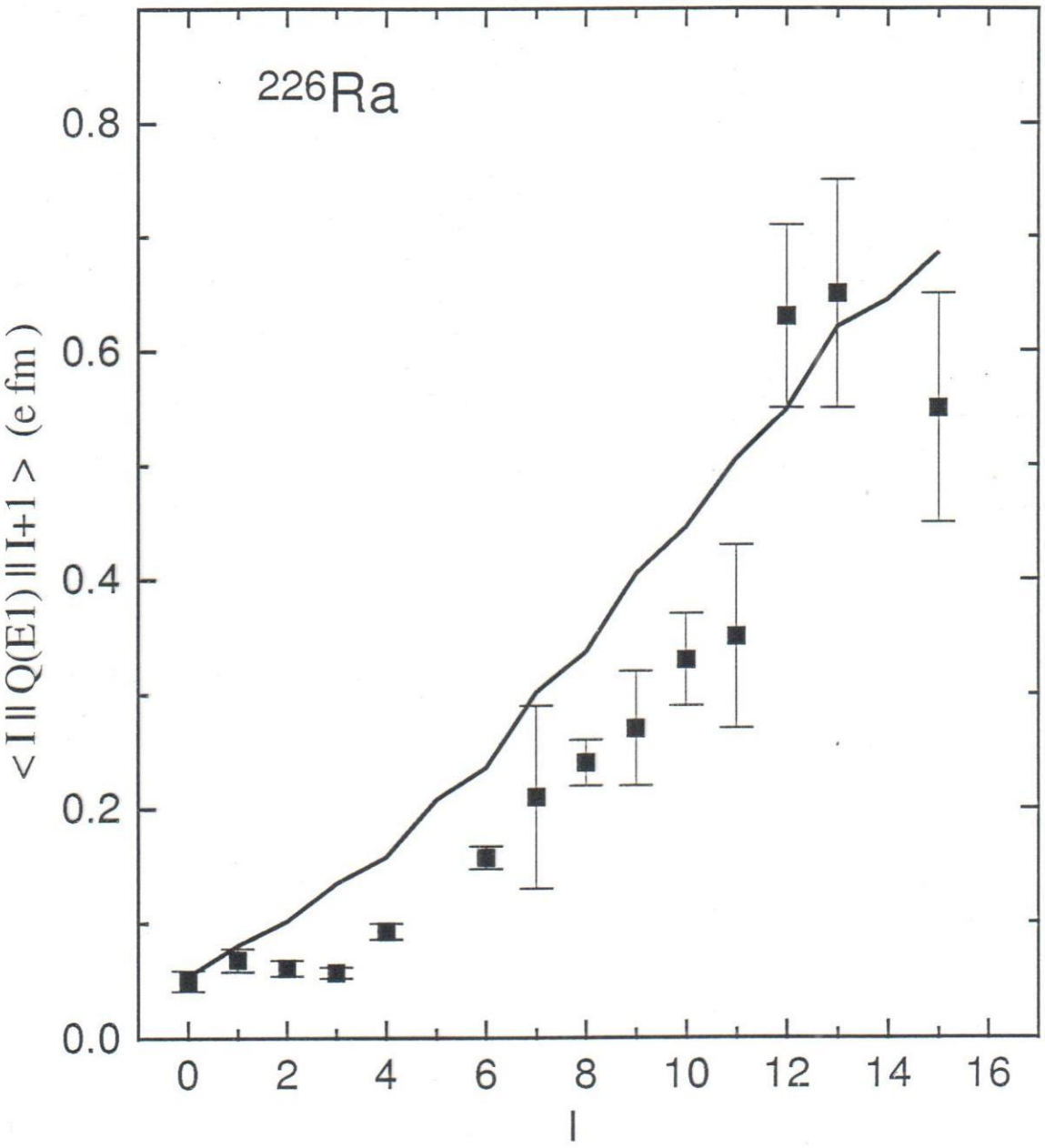
226Ra
0.0
0.2
0.4
0.6
0.8
0
2
4
6
8
10
12
14
16
I
< I ‖ Q(E1) ‖ I+1 > (e fm)

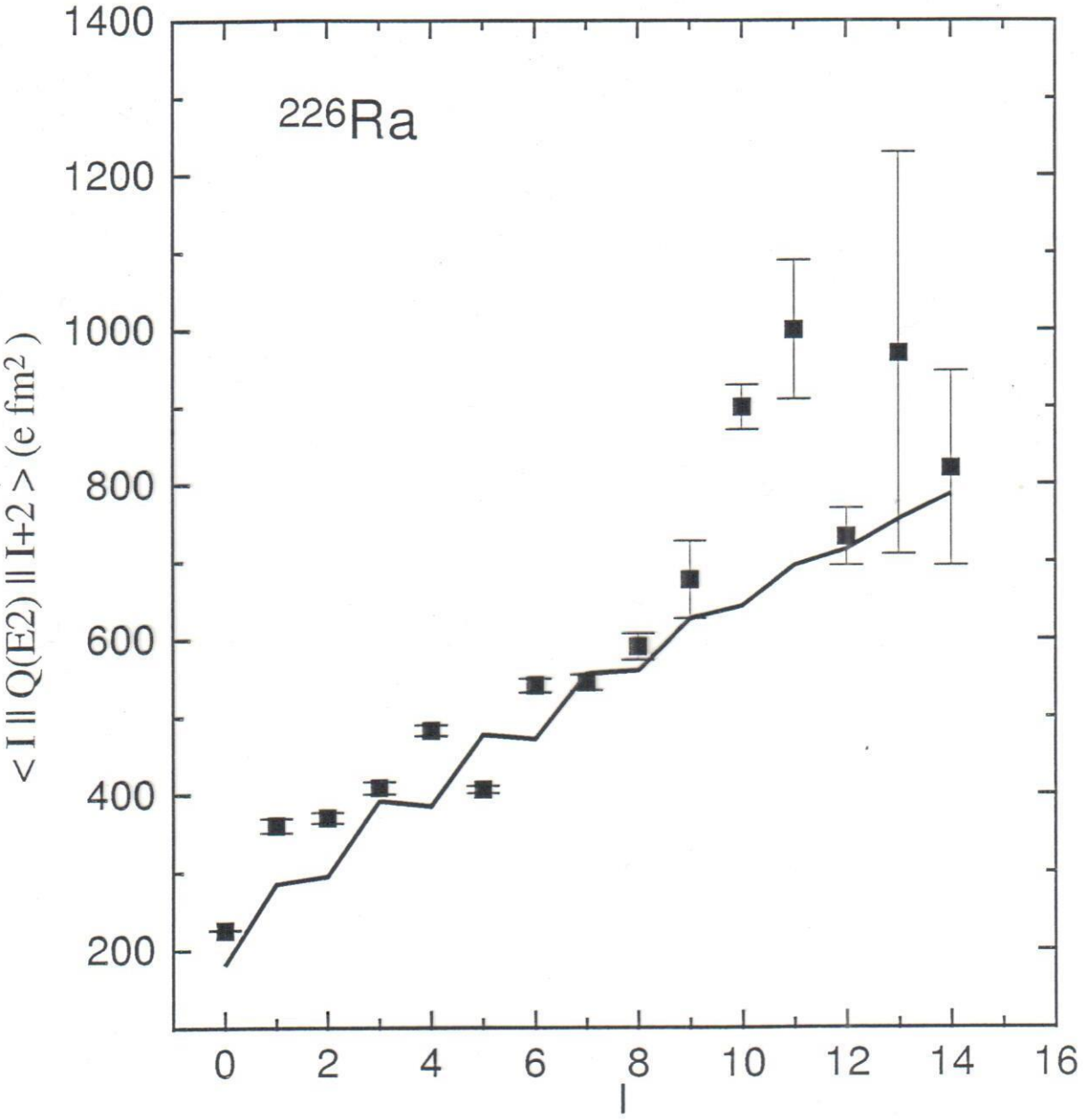
^{226}Ra
< I || Q(E2) || I+2 > (e fm^2)
I
1400
1200
1000
800
600
400
200
0
2
4
6
8
10
12
14
16

CONCLUSION

--The mass asymmetry degree of freedom play the main role in a description of an evolution of a dinuclear system formed in the entrance channel of the reactions leading to fusion or quasifission.

--The mass asymmetry mode also play an important role in a description of some nuclear structure phenomena, namely, the low-lying negative parity states and the super- and hyperdeformrd states.

Consider where our knowledge of physics was just before a discovery of nuclear physics. A leading physicist of that period Kelvin, in the year 1900 addressed the British Association of Science saying:

"There is nothing new to be discovered in physics now. All that remains is more and more precise measurements"

Where can we expect now the most interesting results?

--Nuclei far from stability

and

--At the borders with the other parts of physics

Nuclear and particle physics

Nuclei, which comprice most of the barionic matter in the universe, are made of slowly moving nucleons. One simply has to solve the Schrodinger equation for the A-nucleon system with the Hamiltonian having two-body, three-body and so on forces. Given the two-nucleon potential V_{ij} obtained from the analysis of the NN scattering data and adjusting a few parameters in the three-nucleon potential V_{ijk} the spectra of nuclei up to A=12 can be calculated with high accuracy.

However, in such a framework one can not explain why the 2N forces are so much stronger than the 3N ones. Furthermore, the connection to the fundamental theory of strong interaction, QCD, in which nucleons are not point-like particles but composite of quarks and gluons, is loose and it is difficulty to estimate the theoretical errors. The only ab-initio method that can deal with this without approximations is Lattice QCD (discrete Euclidean space-time lattice). However, calculations for nuclei are too difficult at present.

Over many decades a standard picture had evolved, in which nucleon-nucleon forces are described in terms of meson exchange.

Yukawa's pioneering work of 1935 laid to foundations of our understanding of the strong forces between the nucleons . A cornerstone of the development was the visionary of the inward-bound hierarchy of scales.

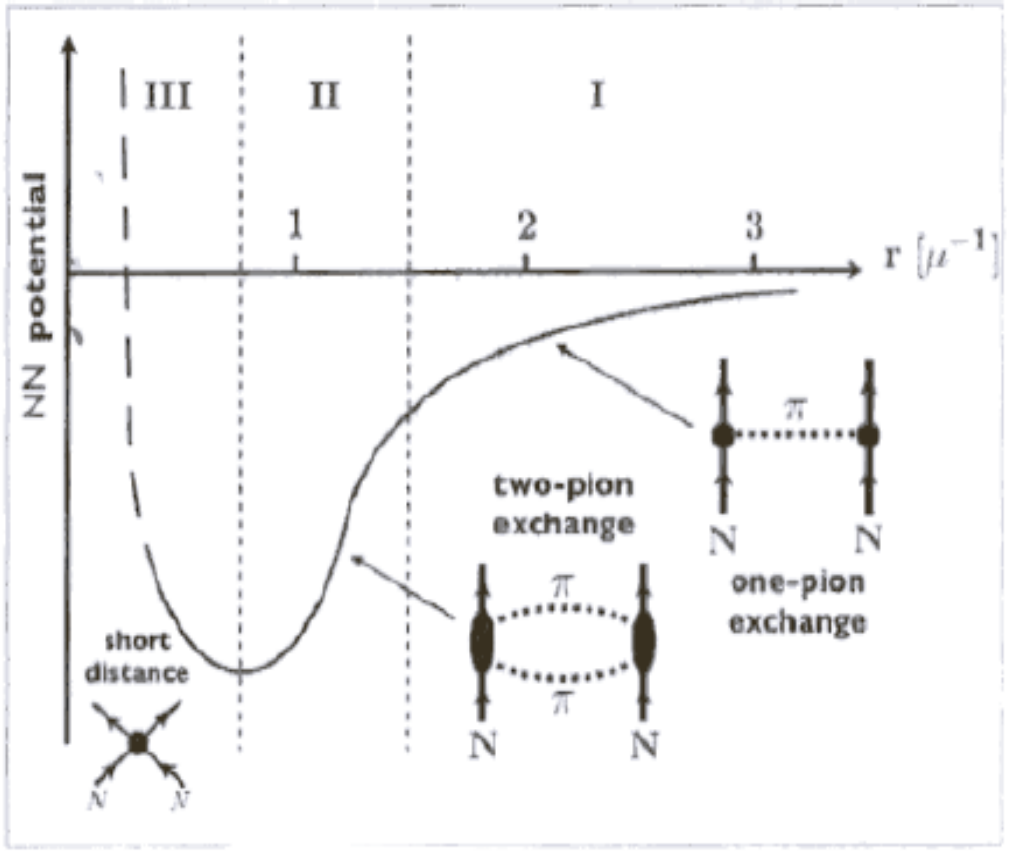

Fig. 2. Hierarchy of scales governing the nucleon-nucleon interaction (adapted from Taketani [5]). The distance r is given in units of the pion Compton wavelength, $\mu^{-1} \simeq 1.4$ fm.

QCD can be handled with the controlled approximation in the limit of low energies and momenta or long distances ($r>1$ fm) in which QCD is realized in the form of an effective field theory of weakly interacting bosons associated with the spontaneous symmetry breaking of chiral symmetry.

Low-energy QCD deals with system of light quarks. The mass gap in the spectrum of the lightests hadrons is a manifestation of a natural separation between light and heavy degrees of freedom.

The basic idea of the effective field theory is to introduce the light species as active degrees of freedom while the heavy particles are treated as almost static sources. In QCD the light degrees of freedom are identified with pions. In this theory pions together with nucleons form building blocks of a low-energy effective field theory.

Nuclear and Atomic physics

I) The lifetime of atomic nuclei can be affected by the electronic shells. Bound beta-decay, for instance, has been shown to produce particularly interesting effects and influences the lifetime of unstable levels in nuclei. The lifetime of the ^{187}Re isotope ground state changes from 42Gyr in the case of the neutral atom to 32.9yr for bare ions related to bound beta-decay.

Decay scheme of neutral atom

---------3/2-[512] 9.75 keV

$5/2^{+}[402]$ -------

β^{-} ↘2.7 keV

---------$1/2^{-}[501]$

^{187}Re ^{187}Os

Lifetime: $5 \cdot 10^{10}$ years

Deacay scheme of fully ionized ^{187}Re

$5/2^{+}[402]$ -------

$^{187}Re^{75+}$ β^{-} ↘≈ 73 keV

---------- $3/2^{-}$

----------$1/2^{-}$

^{187}Os

$T_{1/2}$≈ 45 days

Neutral pair 187Re-187Os has been considered because of the long half-life time as one of the most promising cosmological clocks. However, 187Re decay rate can be enhanced in stellar interiors.

The decay constants of radioactive nucleus undergoing orbital electron capture is proportional to the electron density at the nucleus $|\psi(0)|^2$. This fact seems to afford a possibility of altering the nuclear decay constant λ by acting on atomic electrons. In light nuclei it is possible to achieve by chemical means an alteration of $|\psi(0)|$ sufficiently large to affect in a measurable way the decay constant.

Year	Forms	$\Delta\lambda/\lambda$ (in 10^{-4})
1949	Be - BeO	1.5 (9)
1953	Be - BeO	1.3 (5)
	BeO - BeF_2	6.1 (6)
	Be - BeF_2	7.4 (5)
1970	BeO - BeF_2	11.3 (6)
1999	BeO - $Be(OH)_2$	- 149
	BeO - $Be^{+2}(OH_2)_4$	- 98

$e^- + p \rightarrow n + \nu_e$ ← more probable at low energies

$p \rightarrow n + e^+ + \nu_e$ ← has a larger probability at higher energies. Additional energy is needed to create positron.

If atom is ionized completely and decay energy is smaller than 511 keV (no β^+-decay) then radioactive nucleus becomes stable.

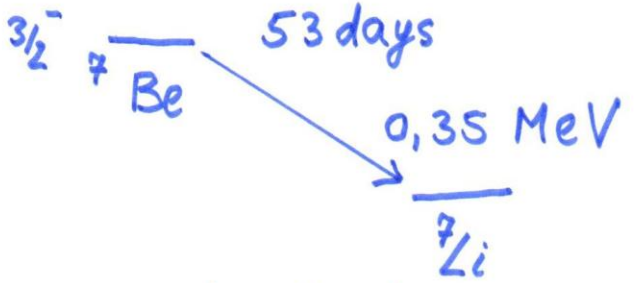

For neutral atom

$e^- + {}^7Be \rightarrow {}^7Li + \nu_e$, $T_{1/2} = 53$ days

However, ^7Be has been found in cosmic rays ($\sim 10^6$ years).

Nuclear decay by intrinsic conversion process.

This process is in a competition with γ-decay. Its probability increases with excitation energy decrease.

A partial ionization of atom decreases a probability of this process. A full ionization will stop it.

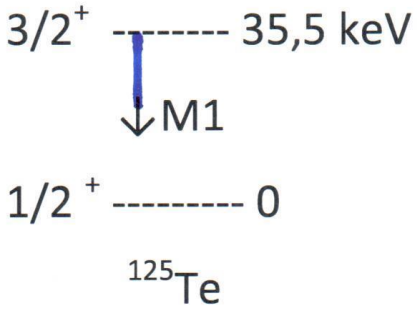

300%-640% increase of the life-time of the first excited state has been found for the ionized atoms of $^{125}Te^{47+}$ and $^{125}Te^{48+}$ correspondingly.

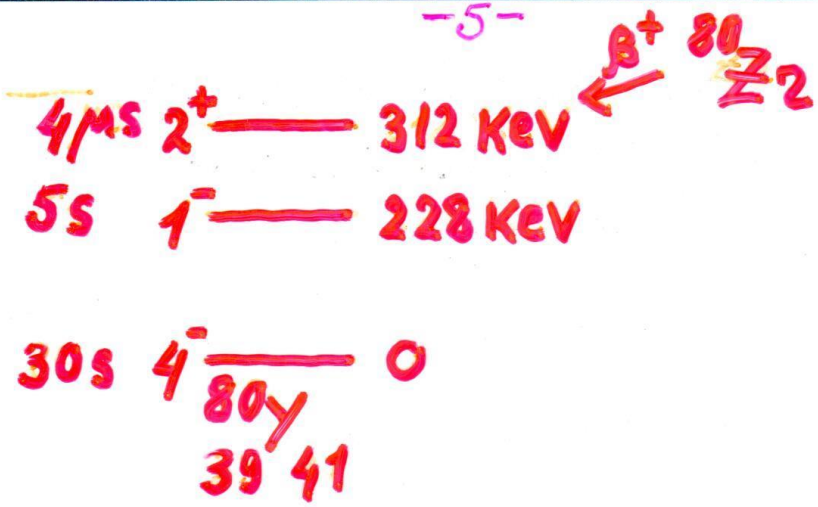

Nucleus	$T_{1/2}$, bare (s)	$T_{1/2}$, neutral (s)
^{80m}Y	6,8 ± 0,5	4,8 ± 0,3
^{151m}Er	19 (3)	0,58 (2)
^{149m}Dy	11 (1)	0,49 (2)
^{144m}Tb	12 (2)	4,25 (15)

In stellar plasma nuclei are expected to be fully ionized. Then the deexcitation of the isomeric states by emission of a conversion electron is impossible.

Neutral and ionized atoms and nuclear processes.

Ionozation of atom can delay or accelerate nuclear radioactive decay. Such situation can be observed in nuclear β-decay

$n \rightarrow p + e^- + \bar{\nu}_e$

Anemitted electron can leave atom or occupy an empty place in electron shell. In β-decay to the bound e^- state the energy is saved because e^- is bound. This decrease decay probability which is proportional to E^5. Moreover other decay channels can be open.

Experimentally β-decay of a fully ionized atom was observed for the first time in the case of ^{163}Dy. This nucleus is stable as a neutral atom, but as a fully stripped $^{163}Dy^{66+}$ ion it can decay into $^{163}Ho^{66+}$ by β_{bound} – decay into the K- and L- shells of a daughter atom.

Experiment has been done in GSI with a storage ring. $T_{1/2}^{\beta,\ bound} = 47 \pm 5$ days.

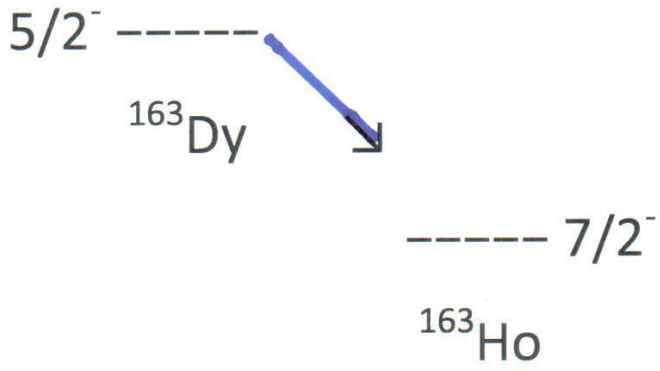

Production of the nuclear isomers.

In α-decay of ^{233}U the isomeric yield of ^{229}Th is around 10%. However, the isomeric state of ^{229}Th undergoes radioactive transition to the ground state with life-time (1-50)h which precludes collecting considerable amount of isomer.

A much more attractive way lies in the use of a pure ^{229}Th whose life-time in the ground state is around 7000 years.

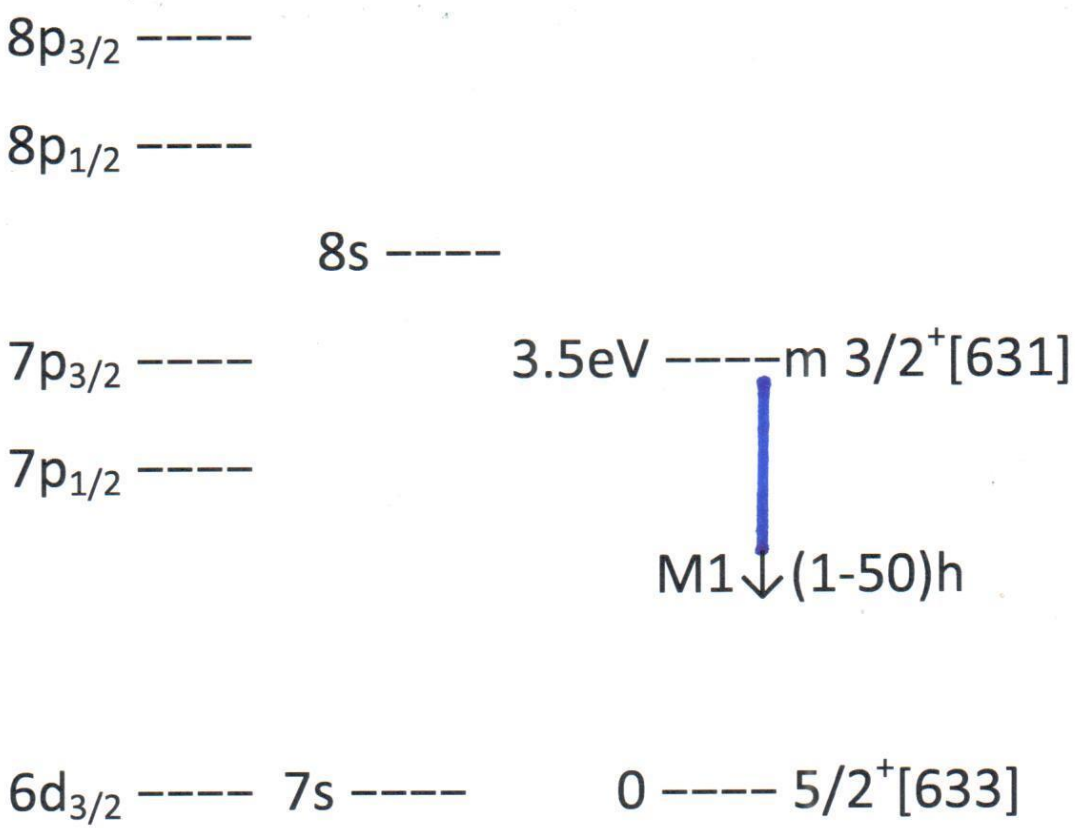

Electron configuration

The isomeric state can be populated by resonance laser radiation.

The Coulomb interaction between nucleus and electron shell mixes up the atomic 8s state with methastable nuclear isomer forming linear combination

$|A\rangle=\alpha|8s\rangle|gs\rangle+\beta|7s\rangle|m\rangle$

$|M\rangle=-\beta|8s\rangle|gs\rangle+\alpha|7s\rangle|m\rangle$

$\alpha\approx1,\ \beta=V/\Delta,\ \Delta=E(8s)-E(m)$

- The state $|A\rangle$ decay mainly by E1 transition to the $|7p\rangle$ state. For this reason populating state $|A\rangle$ would yield no isomer.
- The state $|M\rangle$ correlate with isomeric state.

- The electronic configuration $(7s)^2(6d_{3/2})^2$ corresponds to the ground state of the neutral Th atom.
- The Th^+ ion can be obtained by removing one of the loosely bound electrons 7s or $6d_{3/2}$. The states obtained are nearly degenerate $(7s)^2\,6d_{3/2}$ and $(7s)(6d_{3/2})^2$. The first is the ground state, the second is 0.03 eV higher.
- For the gs the electron transition chain is possible: 7s→8p→8s.
- Nuclear excitation occurs in a conclusive 8p→8s transition.
- The estimated probability of population is $6.4 \cdot 10^{-8}$.

Possible influence on fusion reactions

- Molecules are usually treated as purely Coulomb systems, while the strong interaction between their nuclear constituents is assumed to play negligible role. However, any Coulomb molecular level lying above the lower threshold of nuclear subsystem is embedded in the continuum spectrum of the nuclear part of the total Hamiltonian. The coupling between molecular and nuclear channels turns this level into a resonance.

- Due to the wide Coulomb barrier between the nuclei and a short range character of the nuclear interaction, this coupling and thus the width of the resonance, which determine the fusion probability of the nuclear constituents of the molecule, is in general extremely small.
- The situation may be rather different if a nuclear subsystem has a sufficiently narrow threshold resonance. Among the examples, can be even customary subsystems like $pp^{16}O$ and $p^{17}O$, i.e. the nuclear constituents of the water molecule H_2O and Hydroxyl ion OH-.

The best known example of such a phenomena is the muon catalyzed fusion of deuteron and triton in (dtμ) molecule, where the near threshold nuclear resonance $^{5}He(3/2^{+})$ plays a decisive role

Conclusion

- Nuclear theory is not derived from the first principle.
- Experiment → interpretation. New ideas → experiment.
- Shell model can be considered as a basis.